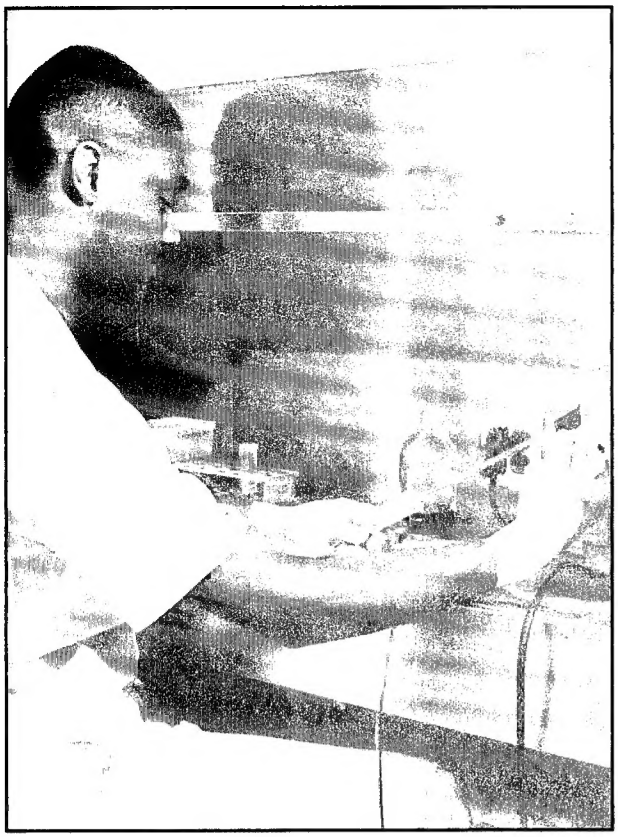

Fourth Quarter
1994

AFRRI Reports

Armed Forces Radiobiology Research Institute

8901 Wisconsin Avenue • Bethesda, Maryland 20889-5603

On the cover: *Air Force MSgt Kyle Sample, an AFRRI research laboratory technician, performs titration, which allows him to determine cell count, a means of measuring the effects of ionizing radiation. The effort is part of a project to develop treatments for radiation-induced gastrointestinal injury.*

REPORT DOCUMENTATION PAGE

Form Approved
OMB No. 0704-0188

1. AGENCY USE ONLY *(Leave blank)*	2. REPORT DATE	3. REPORT TYPE AND DATES COVERED
	February 1995	Reprints

4. TITLE AND SUBTITLE

AFRRI Reports, Fourth Quarter 1994

5. FUNDING NUMBERS

PE: NWED QAXM

6. AUTHOR(S)

7. PERFORMING ORGANIZATION NAME(S) AND ADDRESS(ES)

Armed Forces Radiobiology Research Institute
8901 Wisconsin Avenue
Bethesda, MD 20889-5603

8. PERFORMING ORGANIZATION REPORT NUMBER

SR94-22 - SR94-27

9 SPONSORING/MONITORING AGENCY NAME(S) AND ADDRESS(ES)

Uniformed Services University of the Health Sciences
4301 Jones Bridge Road
Bethesda, MD 20814-4799

10. SPONSORING/MONITORING AGENCY REPORT NUMBER

11 SUPPLEMENTARY NOTES

12a. DISTRIBUTION/AVAILABILITY STATEMENT

Approved for public release; distribution unlimited.

12b. DISTRIBUTION CODE

13. ABSTRACT *(Maximum 200 words)*

This volume contains AFRRI Scientific Reports SR94-22 through SR94-27 for October-December 1994.

14. SUBJECT TERMS

15. NUMBER OF PAGES
57

16. PRICE CODE

17. SECURITY CLASSIFICATION OF REPORT	18. SECURITY CLASSIFICATION OF THIS PAGE	19. SECURITY CLASSIFICATION OF ABSTRACT	20. LIMITATION OF ABSTRACT
UNCLASSIFIED	UNCLASSIFIED	UNCLASSIFIED	UL

CLASSIFIED BY:

DECLASSIFY ON:

CONTENTS

Scientific Reports

This and other AFRRI publications are available to qualified users from the Defense Technical Information Center, Cameron Station, Building 5, Attention: BCR, Alexandria, VA 22304-6145; telephone (703) 274-7633. Others may contact the National Technical Information Service, 5285 Port Royal Road, Springfield, VA 22161; telephone (703) 487-4650. AFRRI publications are also available from university libraries and other libraries associated with the U.S. government's Depository Library System.

INT. J. RADIAT. BIOL., 1994, VOL. 65, NO. 5, 559–569

Application of the constant exposure time technique to transformation experiments with fission neutrons: failure to demonstrate dose-rate dependence

E. K. BALCER-KUBICZEK*†, G. H. HARRISON†, B. A. TORRES‡ and W. A. McCREADY†

(Received 25 August 1993; revision received 15 November 1993; accepted 17 November 1993)

Abstract. A direct comparison of the effectiveness of fission neutrons at high (11·0–31·3 cGy/min) or several low dose-rates (0·14–3·2 cGy/min) was carried out under identical conditions. Monolayers of exponentially growing C3H/10T½ cells were exposed at 37°C to reactor-produced neutrons (fluence-mean energy $E_n = 0{\cdot}68$ MeV, $\leqslant 5\%$ γ component, frequency mean linear energy $y_F = 21$ keV/μm, dose mean lineal energy $y_D = 42$ keV/μm in an 8-μm spherical cavity). Survival or transformation induction were studied at five doses from 10·5 to 94 cGy. In low dose-rate irradiations, these doses were protracted over 0·5, 1, 3 or 4·5 h, resulting in 17 different dose-rates. Up to six experiments were performed at each of five exposure times. Concurrently with transformation we studied cell proliferation in control versus cells irradiated at 40 cGy (acute and a 4·5-h protraction) and found no evidence of a shift in the cell cycle distribution among these cells. At a given dose and dose-rate, the effect of dose protraction on survival or transformation was assessed by the dose-rate modifying factor (DRMF), defined as the low:high dose-rate effect ratio at the same dose. Survival or transformation induction curves were nearly linear with initial slopes, respectively, of about $6{\cdot}5 \times 10^{-3}$ or $6{\cdot}2 \times 10^{-6}$ cGy^{-1}. Consistent with dose–response curves, DRMFs were independent of the dose and dose-rate. The mean values of the DRMF with their uncertainties and 99% confidence intervals, based on measurements in individual doses and dose-rates for survival or transformation were, respectively: $1{\cdot}01 \pm 0{\cdot}03$ (0·92, 1·09) or $0{\cdot}98 \pm 0{\cdot}04$ (0·83, 1·08) indicating a similar precision in determining DRMF for survival or transformation, and no dose or dose-rate influence on these end points.

1. Introduction

Numerous theoretical and experimental studies have been conducted with the objective of improving our knowledge of dose–response relationships for radiation carcinogenesis at high dose-rate or protracted doses of medium and high linear energy transfer (LET) radiations. Among these studies several neutron fields, including that at the Armed Forces Radiobiology Research Institute (AFRRI) TRIGA reactor, have been used to irradiate C3H/10T½ cells. Exposure of these cells to putative carcinogens, including ionizing radiation, may convert a cell with normal growth and morphologic characteristics to one with the characteristics of a tumour cell, a process termed neoplastic transformation. It is well established experimentally in the C3H/10½ system that high-LET radiations have greater biological effectiveness than low LET radiations. However, the effects of protracted or split-dose exposures continue to be a subject of controversy; for the literature background on dose protraction studies with low and high LET radiations, see Balcer-Kubiczek and Harrison 1991c, Brenner and Hall 1990, 1992, Elkind 1991 and Cao *et al.* 1992. In the case of fission neutrons, the need for additional transformation measurements at doses $\leqslant 0{\cdot}5$ Gy and dose-rates $\leqslant 0{\cdot}5$ cGy/min has been identified (Brenner and Hall 1990, 1992, Hall 1991, Redpath *et al.* 1991).

All the previous dose-rate experiments with C3H/10T½ cells, including our transformation studies with TRIGA neutrons (Balcer-Kubiczek *et al.* 1988, 1991, Balcer-Kubiczek and Harrison 1991a), used a constant dose-rate approach in which the total dose is proportional to the exposure time. Consequently, different irradiation times are needed to accumulate different doses, a procedure which makes the analysis of the protracted data conceptually complicated especially when intervals of enhanced sensitivity within the cell cycle, the division delay, repair or similar kinetic and time- or dose-dependent phenomena, singly or in combination, are suspected to affect the induction process (Rossi and Kellerer 1986, Brenner and Hall 1990, 1992, Elkind 1991, Hall 1991, Cao *et al.* 1992, Watt 1992).

The objective of the present series was to re-evaluate the effect of fission neutron dose-protraction on neoplastic transformation of C3H/10T½ cells by using a constant exposure time approach in which dose-rates are proportional to the total dose (Kellerer

*Author for correspondence.
†Department of Radiation Oncology, University of Maryland School of Medicine, Baltimore, MD 21201, USA
‡Armed Forces Radiobiology Research Institute, Bethesda, MD, USA.

and Rossi 1972). Consequently, different doses are accumulated over the same exposure time. An additional advantage of the constant exposure time technique is that contributions of the total dose and dose-rate can be separated, so consequently questions of time-, dose- and/or dose-rate-dependent windowed responses can be addressed directly by a suitable choice of doses and exposure durations (Sykes and Watts 1989). In our present experiments, total doses of about 10, 25, 40, 60 and 90 cGy were protracted over $\tau = 0{\cdot}5$, 1, 3 or 4·5 h, resulting in 17 dose-rates from 0·14 to 3·2 cGy/min. Our previous constant exposure time experiments with X-rays showed that a moderate protraction ($\tau \leqslant 5$ h) of doses in the dose range from 25 cGy to 4 Gy, can produce a significant, statistically discernable reduction of cell killing and transformation in the C3H/10T½ assay (Balcer-Kubiczek *et al.* 1987).

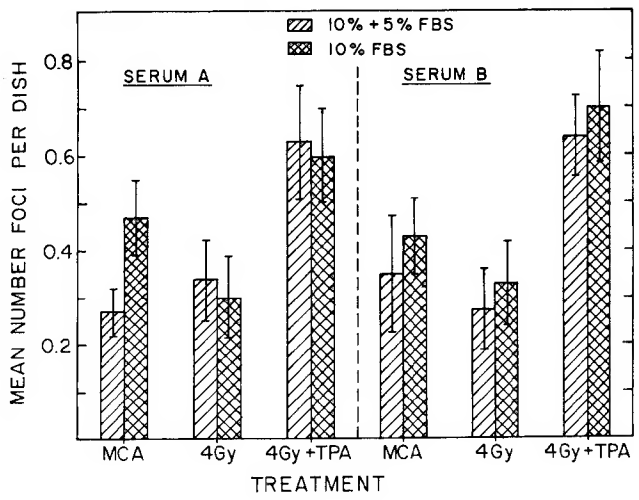

Figure 1. Comparison of transformation induction in C3H/10T½ cells by X-rays or chemicals with carcinogenic activity (methylcholanthrene, MCA; 12-*O*-tetradecanoyl phorbol-13-acetate, TPA) to demonstrate the effect of serum quality and concentration on transformation or clonogenic responses (data not shown). Other abbreviations have the following meaning: 10% + 5% FBS, indicates a protocol with the first four media changes performed using medium containing 10% of foetal bovine serum (FBS), and the remaining three media changes performed using a 5%-serum content; 10% FBS, high-serum medium-change protocol.

2. Materials and methods

2.1. *Cell culture and media*

C3H/10T½ cells from the line established by Reznikoff *et al.* (1973a, b) were maintained as described previously (Balcer-Kubiczek *et al.* 1988, Balcer-Kubiczek and Harrison 1990, 1991a–c) in conformity with published guidelines for this assay (IARC/NCI/EPA Working Group 1985). Our quality control of experiments with C3H/10T½ cells is described in the reports cited above. New batches or lots of serum are routinely prescreened using procedures and criteria summarized in the IARC/NCI/EPA Working Group (1985) report. Serum lots are characterized as being suitable for the transformation assay by ascertaining compliance with survival and transformation expectations after 4 Gy X-rays, after 4 Gy X-rays with post exposure to 0·1 μg TPA/ml, or after 2·5 μg MCA/ml. Results for two lots, matched with respect to the concentration of 11 natural serum components, tested for use in the present study are shown in Figure 1; a single lot, denoted serum B in Figure 1, was used in the experiments reported here.

2.2. *Transformation and survival assays*

Cells in passage 10 were used for experimentation. Before neutron irradiation, cells were plated in several 25-cm^2 flasks at 5×10^4 cells per flask. Experiments were performed 2 days later to ensure that treated cells were in exponential growth phase (see §2·3). Except for neutron irradiation, flasks were kept in horizontal position at all times to facilitate attachment/reattachment of mitotic cells. A hypersensitivity of these cells to transformation was suggested (Elkind 1991, Brenner and Hall 1992, Cao *et al.* 1992). Temperature was maintained at 36–37°C, including during neutron irradiation. Cells were transported to the reactor in a 20-litre thermally insulated container, similar to that described previously (Balcer-Kubiczek *et al.* 1988, Balcer-Kubiczek and Harrison 1991c). At the reactor site, cell temperature before and after neutron irradiation was controlled by immersing culture flasks filled with warm medium in a constant-temperature water bath.

Each experimental run included a high dose-rate exposure group and, in most cases, more than one low dose-rate exposure group at the same dose. Neutron irradiations were arranged such that low dose-rate exposures always preceded high dose-rate exposure. Consequently, cultures that received low dose-rate irradiations were incubated in a horizontal position for up to 5 h before transporting them from Bethesda to our cell culture laboratory in Baltimore. There, cells were removed from flasks by trypsiniza-

Table 1. Pooled data from constant exposure time experiments with TRIGA fission neutrons

Mean dose $\pm\sigma$ (cGy)	Mean exposure time $\pm\sigma$ (min)	Mean dose rate $\pm\sigma$ (cGy/min)	$SF\pm\sigma$	N	Y	X	P	$X/N\pm\sigma$ (10^{-2})	$TR\pm\sigma$ (10^{-4})
10·68±0·74	0·94±0·08	11·35±0·77	0·994±0·059	692	671	23	280	3·3±0·7	1·10±0·24
26·22±1·32	2·37±0·15	11·06±0·46	0·780±0·176	365	342	24	297	6·6±1·3	2·19±0·46
41·47±1·60	1·39±0·08	30·02±2·34	0·538±0·063	191	165	30	334	15·7±0·9	4·15±0·86
62·28±1·84	5·68±0·37	11·01±0·78	0·431±0·100	513	453	65	259	12·7±1·6	5·68±0·37
91·30±4·45	2·92±0·13	31·29±1·28	0·266±0·057	333	249	89	303	26·7±2·8	9·58±1·05
10·23±0·21	29·87±0·19	0·34±0·01	0·947±0·083	293	283	10	278	3·4±1·1	1·25±0·39
25·38±1·75	29·34±1·09	0·87±0·06	0·804±0·198	272	248	24	346	8·8±1·8	2·67±0·55
40·20±0·35	28·16±2·30	1·44±0·11	0·527±0·075	359	332	27	298	7·5±1·5	2·63±0·51
61·43±2·17	30·10±0·07	2·04±0·08	0·546±0·067	187	159	29	245	15·5±3·9	6·62±1·27
91·95±1·85	28·84±1·16	3·19±0·06	0·260±0·097	76	52	24	371	31·6±6·5	10·24±2·10
10·50±0·61	57·56±2·18	0·18±0·01	0·948±0·087	311	302	10	256	3·2±1·0	1·15±0·38
26·20±1·25	57·83±2·18	0·45±0·01	0·733±0·175	228	211	18	289	7·9±1·9	2·68±0·65
41·50±1·38	61·48±2·55	0·68±0·04	0·585±0·050	264	234	33	291	12·5±2·2	4·15±0·76
60·50±0·50	59·15±0·00	1·02±0·01	0·499±0·119	79	67	12	333	15·2±4·4	4·95±1·43
90·00±0·00	62·53±2·15	1·44±0·05	0·341±0·051	100	67	33	360	33·0±5·6	11·13±1·95
25·92±1·30	179·3±6·6	0·14±0·01	0·806±0·145	239	224	17	307	7·1±1·7	2·11±0·54
40·53±0·91	186·4±4·8	0·22±0·01	0·491±0·072	221	199	31	312	14·0±2·5	3·37±0·72
61·34±1·37	178·3±1·0	0·34±0·01	0·408±0·053	125	111	17	234	13·6±3·3	5·08±1·36
90·32±0·27	180·6±4·3	0·50±0·01	0·232±0·093	362	291	77	246	21·3±2·4	8·86±1·05
40·40±0·60	251·8±3·8	0·16±0·00	0·661±0·079	218	203	19	263	8·7±2·0	2·71±0·70
59·95±0·05	258·8±2·8	0·23±0·00	0·432±0·008	185	158	32	280	17·3±3·1	5·63±1·09
90·45±0·90	271·5±3·7	0·33±0·01	0·250±0·022	353	279	80	299	22·7±2·5	7·86±0·92

SF, surviving fraction, plating efficiency of control was 55%; *N*, *X*, *Y*, *P*, total number of dishes, number of transformants of type 2 or 3 (Reznikoff *et al.* 1973b, IARC/NCI/EPA Working Group 1985), number of dishes without transformants, number of cells per dish corrected for plating efficiency of unirradiated cells, or surviving fraction and plating efficiency of irradiated cells; X/N, transformation rate per dish (IARC/NCI/EPA Working Group 1985) and its standard error, σ (Hieber *et al.* 1987); *TR*, transformation rate per survivor (Han and Elkind 1979) and its standard error, σ (Balcer-Kubiczek *et al.* 1987).

tion, counted, diluted, and plated at concentrations estimated to result in either 250 viable cells per dish for the transformation assay, or 50 viable cells per dish for the cell survival assay. As in previous studies the growth medium was renewed at weekly intervals (2 weeks for survival assay and 8 weeks for transformation assay). However, in the present experiments, medium with serum content reduced from 10 to 5% was used in the last three medium changes. As shown in Figure 1, this modified medium-change protocol has no effect on transformation frequency.

Cell survival was determined by colony formation, while neoplastically transformed foci were identified according to published criteria (Reznikoff *et al.* 1973a, b, IARC/NCI/EPA Working Group 1985). The end point of transformants per surviving cell was calculated by the null method of Han and Elkind (1979) with uncertainties determined according to our modified analysis (Balcer-Kubiczek *et al.* 1987). In addition, we determined the mean number of transformants per dish as recommended by IARC/NCI/EPA (1985) with uncertainties calculated according to published methods (Hieber *et al.* 1987).

2.3. *Proliferation studies of irradiated and control cells*

Concurrently with several of the above studies, experiments were performed to compare proliferation of cells taken to and from the reactor facility (90 and 40 cGy, acute or a 4·5-h protraction) with those continuously maintained in our laboratory. Up to four cultures per condition per experiment, established as described above for transformation assay, were used to establish growth curves and to perform flow cytometry measurement of the DNA content. Growth curves were initiated by plating 500 cells per 100-mm dish. Cell counts were obtained every 12 h for a period of 2 weeks. The results, summarized in Table 2, showed no difference in growth rates and in the cell cycle distributions between travelled and non-travelled cultures.

Table 2. Proliferation parameters of C3H/10T½ cells used in reported studies

Parameter†	Travelled cells	Laboratory control	40 cGy (brief)	40 CGy (4·5 h)
Cell cycle distribution (%)				
G_2/M	12	10	14	12
G_2	69	74	70	68
S	19	16	16	20
Doubling time (h)	18·8±0·3	19·2±0·2	nd	nd

†Cells were processed immediately after return from the reactor facility. nd, Not done.

2.4. *Dosimetry and irradiation*

Experiments were performed at the Armed Forces Radiobiology Research Institute (AFRRI) TRIGA Reactor Facility with fission neutron field optimized for low dose-rate studies. The technical descriptions of the neutron source and of the exposure facility were published previously (Moore and Elsasser 1986, Balcer-Kubiczek *et al.* 1988, Redpath *et al.* 1991). The mean fluence-weighted neutron energy for this configuration is 0·68 MeV (Goodman 1985).

Since our previous experiments, the lead shielding arrangement around the point of cellular exposure was redesigned to reduce the turnover time for samples from the previous 45 min to about 1 min, and reduce the γ contamination by fully enclosing samples with 5-cm lead shielding and by increasing the source-to-target distance, measured from the central axis of the reactor core, from 1 to 2 m, thus providing favourable conditions for the multiple protracted exposures required in the present study. The latter modification, suggested by one of us (G.H.H.), permits achieving dose-rates of $<0{\cdot}5$ cGy/min at correspondingly higher reactor power, leading to an improved neutron-to-total dose ratio.

Dosimetric measurements were performed at the plane of cellular exposure prior to each of our 19 experimental runs using the paired ionization chamber technique (ICRU 1976, AAPM 1980, Goodman 1985, Zeman *et al.* 1988). A tissue-equivalent (TE)-wall, methane-based TE-gas filled 0·5-cm^3 Exradin chamber was used to measure γ and neutron events, whereas a 0·5-cm^3 magnesium-wall, argon-filled chamber was used to measure the γ events in the neutron-plus-γ field. From the measurements made by the paired chambers, the portions of neutrons and γ in the mixed field could be determined. For the present irradiations, the ratio of neutron to total dose was 0·95±1·4% at all dose-rates. The instrumental uncertainties for dose and dose-rate determinations were ±3·1 and 3·6%, respectively.

Recently, the radiation quality of the TRIGA-reactor neutron field has been characterized in terms of microdosimetric spectra (H. Gerstenberg, manuscript in preparation). The spectrum was calculated from a TRIGA neutron spectrum based on both measurements and calculations (Verbinski *et al.* 1981a, b). Briefly, the mean values of lineal energy based on measured spectra using 1- or 8-μm diameter detectors, respectively, are: $y_F = 38{\cdot}9$ keV/μm and $y_D = 70{\cdot}5$ keV/μm, or $y_F = 21{\cdot}1$ keV/μm and $y_D = 41{\cdot}5$ keV/μm.

2.5. *Statistical analysis*

At the total doses used in this study the survival level were >20%. Accordingly, a linear–quadratic equation $-\ln S = \alpha \cdot d + \beta \cdot d^2$ was appropriate to analyse survival data. In the case of transformation data, several radiobiologically realistic relationships were tried, such as:

$$T = a + b \cdot d \quad (1)$$

$$T = a + b \cdot d + c \cdot d^2 \quad (2)$$

$$T = b \cdot d + c \cdot d^2, \quad (3)$$

where T is the incidence of transformation, d the dose, a, b and c are regression coefficients for the induction of neoplastic transformation. The calculated best-fit curves were compared using several goodness-of-fit criteria. The coefficient of determination was used to estimate the fraction of the total variance accounted by a model, and the model selection criterion (Akaike 1976) was used to evaluate least-squares fittings to competing models. Calculations were performed using commercial software (PSI-Plot, Poly Software Inc., 1993).

Quantitative comparison of dose–response curves for cell transformation from our five protraction protocols was performed by multiple-regression analysis. We used this procedure to test specifically whether the high dose-rate regression line and protracted irradiation regression lines could have come from populations with the same regression coefficients (Kleinbaum *et al.* 1988, Peixoto 1993). Commercial software (MathCAD version 2·5, MathSoft, Inc., 1989) was used for interactive programming of F-value calculations from transformation data sets in Table 1 (see Appendix).

In addition, the effect of dose protraction on survival or transformation was assessed by the dose-

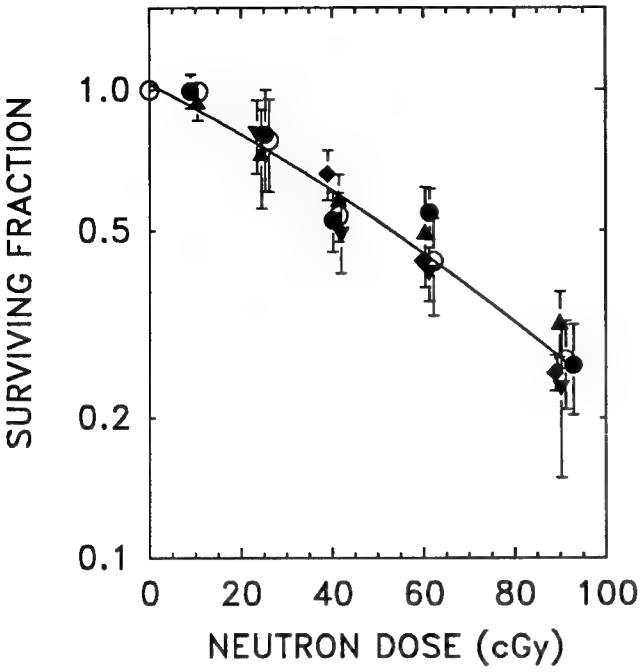

Figure 2. Survival of C3H/10T½ cells after irradiation with AFRRI TRIGA neutrons. Symbols correspond to the following patterns of exposure: ○, acute; and ●, $\tau=0{\cdot}5$ h; ▲, $\tau=1$ h; ▼, $\tau=3$ h; and ◆, $\tau=4{\cdot}5$ h; τ denotes irradiation times with the actual values listed in Table 1.

rate modifying factors (DRMF), defined as the low : high dose-rate effect ratio at the same dose. Standard formulas were used to calculate the uncertainties in DRMF estimates shown in Figures 4 and 5. The DRMF for survival or transformation were analysed by linear regression to determine whether or not they were independent of dose and dose-rate. The actual equations were:

$$DRMF = a + b \cdot d \qquad (4)$$

$$DRMF = a + b \cdot \delta \qquad (5)$$

where d the dose, δ the dose rate, a, b are regression coefficients in Table 3. The t-values obtained from data analysis by the above equations (4) and (5) were compared with the tabulated values, as described in the Appendix. Required calculations were performed using commercial software (MathCAD version 2·5, MathSoft, Inc., 1989).

3. Results

As shown in Table 1 and Figure 2, there were no significant effects of temporal dose distributions on cell survival. The shape of the curve was close to exponential with a linear coefficient $\alpha = (6{\cdot}48 \pm 1{\cdot}46) \times 10^{-3}\,\mathrm{cGy}^{-1}$ and a quadratic coefficient $\beta = (1{\cdot}03 \pm 0{\cdot}25) \times 10^{-4}\,\mathrm{cGy}^{-2}$. These results are in good agreement with observations from related experiments with high-LET radiations reported earlier by us (Balcer-Kubiczek *et al.* 1991, 1993, Balcer-Kubiczek and Harrison 1991a) as well as others (Han and Elkind 1979, Hill *et al.* 1982, Hieber *et al.* 1987, Saran *et al.* 1991, Goodhead *et al.* 1992, Komatsu *et al.* 1993).

As in the earlier studies with cycling or stationary cultures of C3H/10T½ cells and TRIGA neutrons (Balcer-Kubiczek *et al.* 1988, and references cited above), the dose–response curve for transformation induction was well represented by two- or three-parameter models, given by the equations (1), (2) or (3), whether exposure-time groups were considered separately or pooled. However, the amount of data in each dose response set was too small to assert any model conclusively by the usual curve fitting. Multiple-regression analysis of all the transformation data in Table 1 showed $F = 1{\cdot}59$, whereas $F_{0{\cdot}95}(4, 16) = 3{\cdot}01$ and $F_{0{\cdot}99}(4, 16) = 5{\cdot}24$ are

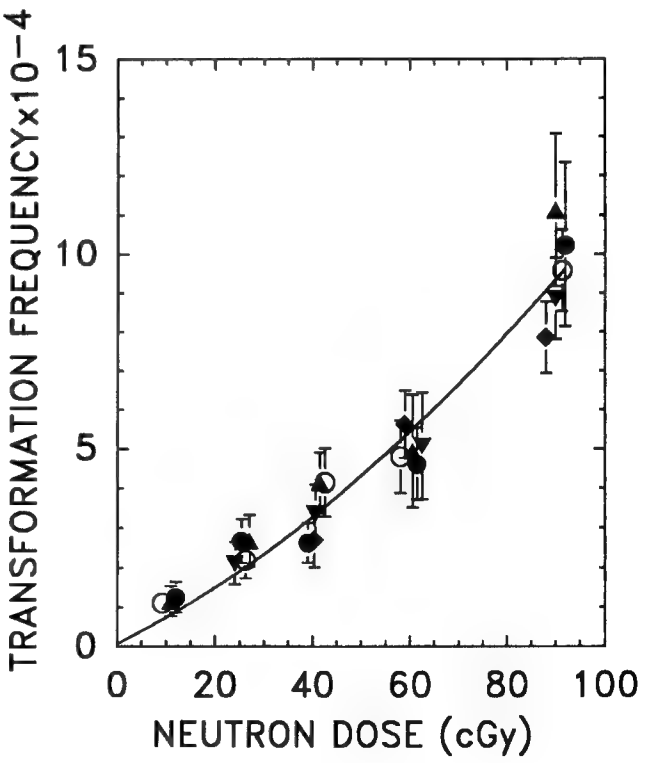

Figure 3. Neoplastic transformation of C3H/10T½ cells after irradiation with AFRRI TRIGA neutrons. Symbols correspond to the following patterns of exposure: ○, acute; ●, $\tau=0{\cdot}5$; ▲, $\tau=1$ h; ▼, $\tau=3$ h; and ◆, $\tau=4{\cdot}5$ h; τ denotes irradiation times with the actual values listed in Table 1.

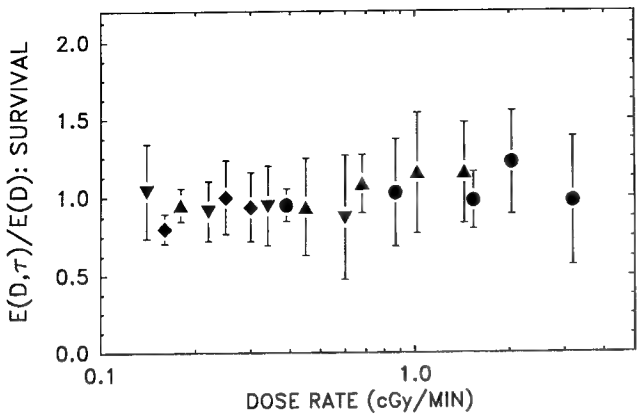

Figure 4. Dose-rate modifying factors for survival of C3H/10T½ cells plotted as a function of AFRRI TRIGA neutrons dose rate. Symbols correspond to the following patterns of exposure: ●, $\tau = 0{\cdot}5$ h; ▲, $\tau = 1$ h; ▼, $\tau = 3$ h; and ◆, $\tau = 4{\cdot}5$ h; denotes irradiation times with the actual values listed in Table 1.

required for differences among the means to be significant at the 5 and 1% levels, respectively. Thus, we concluded that the five dose–response curves were satisfactorily homogeneous, and, consequently, that at a given dose there was no dependence of transformation response on dose protraction.

Accordingly, we were able to pool the data from our five exposure time groups in determining dose dependencies in transformation induction. For the models (1)–(3), the goodness-of-fit measures had similar values: coefficients of determination 0·93–0·95, model selection criteria 2·5–2·8, correlation coefficients 0·94–0·95. Predictably, the numerical

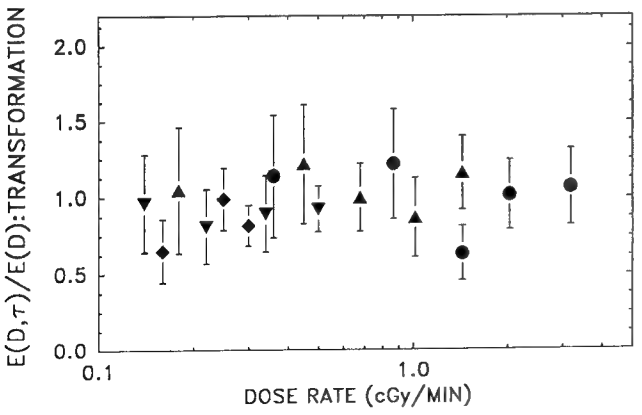

Figure 5. Dose-rate modifying factors for the induction of neoplastic transformation of C3H/10T½ cells plotted as a function of AFRRI TRIGA neutrons dose rate. Symbols correspond to the following patterns of exposure: ●, $\tau = 0{\cdot}5$ h; ▲, $\tau = 1$ h; ▼, $\tau = 3$ h; and ◆, $\tau = 4{\cdot}5$ h; denotes irradiation times with the actual values listed in Table 1.

Table 3. Linear regression coefficients and the test of independence for dose rate modifying factors (DRMF)

	a	b†	t
Survival			
DRMF versus dose	0·955	0·001	0·23
DRMF versus dose-rate	0·975	0·071	0·60
Transformation			
DRMF versus dose	0·961	-7×10^{-4}	0·18
DRMF versus dose-rate	1·014	0·052	0·45

a, intercept; b, slope; t value defined in Appendix.

†The unit to be used with factor b is: for the dose–response relationships (cGy^{-1}) and for the dose-rate–response relationships (min/cGy). Dose-rate modifying factors calculated from the data on survival or transformation (Table 1) are plotted, respectively, in Figures 4 or 5 as a function of dose-rate.

values of regression coefficients depended on the model. Our best estimate of the initial slope based on the pooled data is $5{\cdot}0$–$7{\cdot}5 \times 10^{-6}\,cGy^{-1}$, and the mean weighted by the reciprocal of the variance is $6{\cdot}2 \times 10^{-6}\,cGy^{-1}$. The solid line in Figure 3 represents the best fit to the linear–quadratic equation (3), with the numerical solution $b = (7{\cdot}5 \pm 2{\cdot}4) \times 10^{-6}$ cGy^{-1}, and $c = (2{\cdot}4 \pm 1{\cdot}9)\ 10^{-8}\,cGy^{-2}$. Thus, if the statistical analysis is restricted to the initial part of transformation induction curve (<60 cGy) a linear fit is an adequate representation, since the contribution from the quadratic term is $<10\%$.

To further confirm the above findings, dose-rate modifying factors for survival or transformation, shown in Figures 4 or 5, were tested for dependence on dose and dose-rate by the equations (4) and (5). Specifically, the dependence of DRMF on dose provides qualitative information about the basic form of dose–response curve obtained for different dose protraction patterns, relative to the basic form of dose–response curve obtained from a high dose-rate exposure at the same dose. The results of the numerical curve fitting of our four data sets to a straight line with the intercept a and the slope b (cGy^{-1} or min/cGy) are shown in Table 3. The last column in Table 3 lists t-values of about 0·2 for dependence of DRMFs on the dose and of about 0·5 for dependence of DRMFs on dose-rate. At $\alpha = 0{\cdot}05$, the critical $t_{0{\cdot}025}(15) = 2{\cdot}131$ and at $\alpha = 0{\cdot}01$, $t_{0{\cdot}005}(15) = 2{\cdot}947$. Therefore, we are required to conclude that, at the 5 or 1% levels of significance, the DRMFs were independent of both the dose-rate and dose; that is, the basic forms of dose–response curves are the same. Intuitively, the same conclusion can be reached by observing that both the intercepts and the mean values of DRMFs are close to unity; for survival and transformation they were respectively: 1·01 (0·92, 1·09) and 0·98 (0·83, 1·08), where

the numbers in brackets are 99% confidence limits. By inspecting Figures 4 and 5, an additional observation can be made that the quality of the transformation data can be quite good, comparable with the quality of survival data. Thus, the scatter in transformation data sets should not be relied upon in justifying a wide range of model-based speculations (Brenner and Hall 1990, 1992, Hall 1991).

4. Discussion

In this report cell survival and the induction of neoplastic transformation were studied after fission neutron irradiations at up to five exposure durations per dose. Such an experimental design, the first reported for high-LET radiation studies, permitted direct examination of the dose-rate influence on these end points at multiple dose rates. The dose-rate range included single values of dose rate $\leqslant 0{\cdot}5$ cGy/min previously studied in this and other laboratories using the constant dose-rate approach. The reference acute irradiations were performed concurrently with protracted irradiations at the same dose. Identical protocols were used in all irradiations, including media composition, age and proliferative state of cultures, initial plating densities and the numbers of dishes, thus providing statistically acceptable conditions for testing the null hypothesis that, at the same dose, there was no difference in the effectiveness of fission neutrons due to differences in the temporal pattern of exposure.

Technical limitations in the present study precluded investigations of neutron doses of < 10 cGy, a limitation that also applies to most (Hill *et al.* 1982, 1984, Balcer-Kubiczek *et al.* 1988, Coggle 1988, Miller *et al.* 1990, 1993, Hill and Zhu 1991, Miller and Hall 1991, Saran *et al.* 1991) but not all *in vivo* and *in vitro* studies of radiation carcinogenesis (Ullrich 1984, Balcer-Kubiczek and Harrison 1991a). Nevertheless, two interesting and potentially important results emerged from the present investigations. First, we confirmed that the dose–response curves for survival and transformation at doses < 1 Gy are best described by a linear equation or, possibly, a linear–quadratic equation with a weak positive quadratic term. Similar to previous results with exponential or plateau cultures of C3H/10T½ cells and TRIGA neutrons (Balcer-Kubiczek and Harrison 1991a) as well as with some other neutron sources (Coggle 1988, Saran *et al.* 1991, Komatsu *et al.* 1993), we did not observe 'supralinearity' in the dose–response curve for transformation, often associated with the so-called 'inverse dose-rate effect' reported for γ-, X-rays (Borek and Hall 1974, Miller and Hall 1978, Little 1979, Hall and Miller 1981) and fission neutrons (Hill *et al.* 1982, Ullrich 1984). Indeed, models by Rossi (1981), Rossi and Kellerer (1986), Burch and Chesters (1986), Brenner and Hall (1990) and Elkind (1991) show, either directly or by implication, that the enhancement of an effect due to protraction may occur in a dose range where a dose–response curve has a fine structure such, for example, has a locally negative (convex) curvature; 'bending down' segments of response curves after brief and/or protracted exposures to low and high LET radiations were reported for neoplastic transformation, animal carcinogenesis and, more recently, for mutation induction, but not cell survival or mortality (Miller and Hall 1978, 1991, Little 1979, Hall and Miller 1981, Hill *et al.* 1982, Ullrich 1984, Bettega *et al.* 1992, Tauchi *et al.* 1993). Thus, our second important result that, at a given dose, survival or transformation did not vary with a temporal pattern of exposure, can be seen as a direct consequence of the first result, just discussed above, that dose–response curves for neutrons are linear < 1 Gy. Similar conclusions were published by Coggle (1988) based on the analysis of rodent carcinogenesis data.

Recently, several interpretations of locally complex dose–response curves and the inverse dose-rate effect have been proposed (Rossi and Kellerer 1986, Dennis and Dennis 1988, Sykes and Watt 1989, Brenner and Hall 1990, Elkind 1991, Watt 1992). Most of these models are an extension of an idea (Oftedal 1968) that there is a time period in the cell cycle during which cells are more susceptible to transformation (or mutation; Tauchi *et al.* 1993) than at other times. A corollary is that for exponentially growing cultures with the same distribution of cells throughout the cell cycle at the beginning of exposure, different distributions and, therefore, different fractions of the hypersensitive cells are expected at the end of protracted versus brief exposures. At present, there is no agreement among the models as to a duration (Rossi and Kellerer 1986, Brenner and Hall 1990, Elkind 1991, Harrison and Balcer-Kubiczek 1992, Watt 1992) or a specific location of the sensitive period within the cell cycle (Brenner and Hall 1990, Elkind 1991, Cao *et al.* 1992, Komatsu *et al.* 1993, Miller *et al.* 1993, Tauchi *et al.* 1993), but periods of sensitivity lasting from a few seconds or less to about 1 or 2 h can be inferred, as discussed below. Although the present study was concerned with investigation of dose-rate effects of fission neutrons rather than with testing the biophysical models cited above, our measurements of the cell cycle distributions of control and irradiated cells (Table 2) argue directly against the validity of these notions. Independently, quantitatively similar results and conclu-

sions, based on experiments with fission neutrons (Saran *et al.* 1993) and with monoenergetic neutrons of several different energies (0·5, 1·0 and 6·0 MeV) (Pazzaglia *et al.* 1993), were recently reported for control and neutron-irradiated C3H/10T½ cells.

In experimental investigations of dose-rate or dose-fractionation effects, it is important to ascertain whether the variability of a response can be attributed to a pattern of exposure and not merely the scatter of data. Figures 4 and 5 show enhancements (and reductions) of less than a factor of 2 at several dose-rates, such as are reported by some investigators as the inverse dose-rate effect. However, in contrast with our present report, these other constant dose-rate studies were limited to, at best, two dose-rates (Hill *et al.* 1982, Hill and Zhu 1991, Miller and Hall 1991, Redpath *et al.* 1991) and/or a narrow range of doses, including measurements at a single dose (Ullrich 1984, Hill and Zhu 1991, Miller *et al.* 1991, 1993, Redpath *et al.* 1991); consequently, these results do not lend themselves to rigorous analysis by conventional statistical methods such as presented here, nor to the analysis by multiparameter models, such as those proposed for transformation data by Burch and Chesters (1986), Rossi and Kellerer (1986) or Brenner and Hall (1990).

We examined the latter model analytically (Harrison and Balcer-Kubiczek 1992) with the intention of applying the model to our transformation data for TRIGA neutrons (Balcer-Kubiczek *et al.* 1988, 1991, Balcer-Kubiczek and Harrison 1991a, and this report) and found a lack of a single-valued solution for the duration of the postulated transformation-susceptible portion of the cell cycle for neutrons (Figures 1 and 2; Harrison and Balcer-Kubiczek 1992); this is in contrast with conclusions published by these authors that the model predicts a single sensitivity period of $1{\cdot}02 \pm 0{\cdot}25$ h. Our subsequent examination of the mathematical determination of model input parameters from experimental data (Balcer-Kubiczek and Harrison 1992) revealed an additional caveat, that the prediction of the inverse dose-rate for transformation by neutrons requires an unrealistically low value of frequency mean lineal energy, such as, $y_F = 1$ keV/μm (in an 8-μm diameter cavity) for fission neutrons. As shown here, this assumption is out of line for TRIGA neutrons with $y_F = 21{\cdot}2$ keV/μm. In the case of other neutron sources, for JANUS neutrons $y_F = 42$ keV/μm, and for 6-MeV monoenergetic neutrons $y_F = 18{\cdot}7$ keV/μm in an 8-μm site, which is similar to y_F for TRIGA neutrons (H. Gerstenberg, manuscript in preparation), whereas $y_F = 1$ or $15{\cdot}7$ keV/μm were, respectively, assumed in the model calculations (Brenner and Hall 1990); thus, depending on neutron source, the model input variable y_F was *underestimated* by up to a factor of 40, so it follows that the magnitude of the inverse dose-rate for these sources was *overestimated* by correspondingly similar factors. Applied to our present data, this means that, based on the Brenner and Hall model, no enhancement can be expected in exponentially growing cultures of C3H/10T½ cells even at dose rates $< 0{\cdot}5$ cGy/min in the dose range examined. To further illustrate the impact of the higher y_F on this model, we note that no dose-rate effect can be predicted to occur in neutron doses and dose-rates relevant to radiation protection. Specifically, to use the example in Brenner and Hall (1990), no enhancement for fission neutrons can be expected at 0·5 cGy and a dose-rate $= 10^{-6}$ cGy/min. In fact, we calculated that in order to obtain the two-fold transformation enhancement for fission neutrons at this dose-rate, the total dose would have to be 50 cGy. Assuming a quality factor of 10, this corresponds to the dose which is 100 times the annual effective occupational dose permitted by current US standards.

In summary, it seems reasonable to conclude from the present direct comparisons of cell survival, transformation and age distributions of control and irradiated cells, as well as by examining assumptions in biophysical models of the inverse dose-rate effect, that there is no real, in a statistical sense, modification of these end points by extending the duration of fission neutron exposure or, equivalently, by lowering the fission neutron dose-rate.

Acknowledgements

We are very grateful to Dr P. David Wilson, Department of Epidemiology and Preventive Medicine at UMAB for suggesting application of multiple-regression methods for analysis of transformation data, and to Dr Josè Ordonez, University of Maryland Cancer Center, for performing flow cytometry and for donating reagents needed to perform these measurements. We thank Miss Yang Xu for her assistance with the transformation studies and Miss Debra Dixon for her excellent help in the preparation of this manuscript. We thank the Armed Forces Radiobiology Research Institute for interest in our work. We are grateful to Dr E. J. Ainsworth, Scientific Director, C. B. Galley, Captain, US Navy, MSC and E. G. Daxon, Lieutenant Colonel, US Army, MSC, for donating beam time and dosimetry support and to the numerous AFRRI staff members for collaboration. This work was partially supported by the USPHS Grant CA 50629 from the National Cancer Institute.

Appendix

The following methods are independent of any model assumptions for error calculation of surviving fractions, transformation frequency or derived qualities.

A1. *Test of independence*

One criterion of independence is that the mean DRMF is the same for each value of dose or dose-rate, which in the case of linear regression, requires that the slope equals 0. To test for independence of DRMF, we calculated:

$$t=\frac{(b-0)\cdot S_x\sqrt{n-1}}{S_{y\cdot x}},$$

where b is the slope, n the number of observations, and S_x and $S_{y\cdot x}$ have the usual meaning (Dixon and Masey 1957), and compared its value with the t-distribution. The null hypothesis: $b=0$ can be rejected at the α-level of significance, and the two variables are said to be dependent, if $t<t_{1/2\cdot\alpha}(n-2)$ or if $t>t_{1-1/2\cdot\alpha}(n-2)$.

A2. *Multiple-regression analysis*

This section will provide explicit formulas and mathematical procedures used in the multiple-regression analysis of transformation data graphed in Figure 3. They are also suitable for a similar analysis of any results, if the assumption can be made that all the curves have a coinciding intercept; in the present case, this is a reasonable expectation since the intercept, by definition, is the spontaneous transformation frequency.

We consider our exposure-time groups, $i(i=0, 1, 2, 3, 4)$, where $i=0$ denotes an arbitrary reference group, chosen here to be the high dose-rate group, and separate independent variables $x_k(k=1, 2, 3, 4)$, such that $x_k=1$, if group k, and $=0$ otherwise. The multiple-regression equation or

'full' model: $T=a+d\cdot b_0+x_1\cdot d\cdot b_1+\cdots+x_4\cdot d\cdot b_4$

has six independent multiple-regression coefficients to be found. A regression coefficient such as b_1, denotes the regression coefficient of T on variable x_1 that one would expect to obtain if other variables in the 'full' model equation x_2, x_3 and x_4 had been held constant experimentally. Thus, the 'full' model for group 1: $T=a+d\cdot b_0+x_1\cdot d\cdot b_1$, for group 2: $T=a+d\cdot b_0+x_2\cdot d\cdot b_2$, etc. The null-hypothesis is,

$$H_0: b_1=b_2=b_3=b_4=0,$$

and, accordingly:

$$H_0 \text{ model: } T=a+d\cdot b_0.$$

It should be noted that the above equation doses not imply that the actual relationship between transformation frequency and the dose is linear, but rather than a linear approximation explains a significant amount of variability in T over the range of d values, which is true in the case of our data.

The procedure compares the calculated F to the $F_\alpha(\mu_1,\mu_2)$ distribution with the appropriate numbers of degrees of freedom; the symbols have the following definitions: $\mu_1=(n-2)-(n-6)$, $\mu_2=n-6$ are degrees of freedom in the numerator and denominator, respectively, $\alpha=$ the cumulative probability, $n=$ the number of observations in all groups, and

$$F=\frac{[SSE(H_0 \text{ model})-SSE \text{ ('full' model)}]/\mu_1}{SSE \text{ ('full' model)}/\mu_2},$$

where $SSE=$ sum of squared sampling errors, defined just below.

Let $t_{ij}=$ observed transformation response of ith group at jth dose, and $d_j=j$th dose.

For H_0 model: $SSE=\Sigma[t_{ij}-(a+d_j\cdot b_0)]^2$,

where summation is performed over groups, $i(=0, 1, \ldots, 4)$ and data points in the combined set, $j(=1, \ldots, 22$ for our data set; Table 1).

For 'full' model: $SSE=\mathbf{T}^{\mathrm{T}}\cdot\mathbf{T}-\mathbf{T}^{\mathrm{T}}\cdot\mathbf{X}\cdot\boldsymbol{\beta}$,

where the matrix $\mathbf{X}$ is defined below, $\mathbf{T}$ denotes a vector constructed from t_{ij} values, and β denotes a vector constructed from multiple-regression coefficients found by solving the following matrix equation:

$$\begin{bmatrix} t_{0,1} \\ t_{0,2} \\ t_{1,1} \\ \cdot \\ \cdot \\ \cdot \\ t_{4,1} \\ t_{4,2} \\ t_{4,3} \end{bmatrix} \equiv \begin{bmatrix} 1 & d_1 & 0 & 0 & 0 & 0 \\ 1 & d_2 & 0 & 0 & 0 & 0 \\ 1 & d_6 & 1 & 0 & 0 & 0 \\ \cdot & \cdot & \cdot & \cdot & \cdot & \cdot \\ \cdot & \cdot & \cdot & \cdot & \cdot & \cdot \\ \cdot & \cdot & \cdot & \cdot & \cdot & \cdot \\ 1 & d_{20} & 0 & 0 & 0 & 1 \\ 1 & d_{21} & 0 & 0 & 0 & 1 \\ 1 & d_{22} & 0 & 0 & 0 & 1 \end{bmatrix} \begin{bmatrix} a \\ b_0 \\ b_1 \\ b_2 \\ b_3 \\ b_4 \end{bmatrix}$$

$\mathbf{T}$ $\mathbf{X}$ $\boldsymbol{\beta}$

This equation has the solution:

$$\boldsymbol{\beta} = (\mathbf{X}^{\mathrm{T}} \cdot \mathbf{X})^{-1} (\mathbf{X}^{\mathrm{T}} \cdot \mathbf{T})$$

which is then used to determine *SSE* for 'full' model and, finally *F*. For the present data: $b_0 = -0{\cdot}433$, $b_1 = 0{\cdot}103$, $b_2 = 0{\cdot}222$, $b_3 = -0{\cdot}363$, $b_4 = 0{\cdot}354$, and $b_5 = -0{\cdot}981$. The sign change in multiple-regression coefficients indicates that both up and down adjustments in groups 1 ($\tau = 0{\cdot}5$ h), 2 ($\tau = 1$ h), 3 ($\tau = 3$ h), 4 ($\tau = 4{\cdot}5$ h) are required, consistent with small *F*-values which, in turn, corresponds to a high probability that the same curve holds for the data.

References

AAPM, 1980, Protocol for neutron beam dosimetry. Report No. 7 (New York, American Association of Physicists in Medicine, American Institute of Physics).

Akaike, H., 1976, An information criterion. *Mathematical Science*, **1,** 5–9.

Balcer-Kubiczek, E. K. and Harrison, G. H., 1991a, Lack of dose-rate modification (0·0049 versus 0·12 Gy/min) of fission-neutron-induced neoplastic transformation in C3H/10T½ cells. *International Journal of Radiation Biology*, **59,** 1017–1026.

Balcer-Kubiczek, E. K. and Harrison, G. H., 1991b, Neoplastic transformation of C3H/10T½ cells following exposure to 120-Hz modulated 2·45-GHz microwaves and phorbol ester tumor promoter. *Radiation Research*, **126,** 65–71.

Balcer-Kubiczek, E. K. and Harrison, G. H., 1991c, '*Inter silvas Academi quaerere verum*': reply to Letter to the Editor by M. M. Elkind. *International Journal of Radiation Biology*, **59,** 1477–1482.

Balcer-Kubiczek, E. K. and Harrison, G. H., 1992, AFRRI-neutron transformation results viz. current models (Poster P-24-9). 40th Annual Meeting of the Radiation Research Society, Salt Lake City, UT, USA, 14–18 March.

Balcer-Kubiczek, E. K. and Harrison, G. H. and Hei, T. K., 1991, Neutron dose-rate experiments at the AFRRI nuclear reactor. *Radiation Research*, **128,** S65–70.

Balcer-Kubiczek, E. K. and Harrison, G. H. and Thompson, B. W., 1987, Repair time for oncogenic transformation in C3H/10T½ cells subjected to protracted X-irradiation. *International Journal of Radiation Biology*, **51,** 219–226.

Balcer-Kubiczek, E. K. and Harrison, G. H., Zeman, G. H., Mattson, P. J. and Kunska, A., 1988, Lack of inverse dose-rate effect on fission neutron induced transformation of C3H/10T½ cells. *International Journal of Radiation Biology*, **54,** 531–536.

Balcer-Kubiczek, E. K., Hill, C. K., Harrison, G. H. and Blakely, W. F., 1993, Effects of WR-1065 and WR-151326 on survival and neoplastic transformation in C3H/10T½ cells exposed to TRIGA or JANUS fission neutrons. *International Journal of Radiation Biology*, **63,** 37–46.

Bettega, D., Calzolari, G., Noris Chiorda, G. and Tallone-Lombardi, L., 1992, Transformation of C3H/10T½ cells with 4·3 MeV α particles at low doses: effects of single and fractionated doses. *Radiation Research*, **131,** 66 71.

Borek, C. and Hall, E. J., 1974, Effect of split doses of X-rays on neoplastic transformation of single cells. *Nature*, **252,** 499 501.

Brenner, D. J. and Hall, E. J., 1990, Inverse dose-rate effect for oncogenic transformation by neutrons and charged particles: a plausible interpretation consistent with published data. *International Journal of Radiation Biology*, **58,** 745–758.

Brenner, D. J. and Hall, E. J., 1992, Commentary 2 to Cox and Little: Radiation-induced oncogenic transformation: the interplay between dose, dose protraction, and radiation quality. *Advances in Radiation Biology*, **16,** 167–179.

Burch, P. R. J. and Chesters, M. E., 1986, Neoplastic transformation of cells *in vitro* at low and high dose rates of fission neutrons: an interpretationn. *International Journal of Radiation Biology*, **49,** 495–500.

Cao, J., Wells, R. L. and Elkind, M. M., 1992, Enhanced sensitivity to neoplastic transformation by ^{137}Cs γ-rays of cells in the G_2/M-phase age interval. *International Journal of Radiation Biology*, **62,** 191–199.

Goggle, J. E., 1988, Lung tumour induction in mice after X-rays and neutrons. *International Journal of Radiation Biology*, **53,** 585–598.

Dennis, J. A. and Dennis, L. A., 1988, Neutron dose relationships at low doses. *Radiation and Environmental Biophysics*, **27,** 91–101.

Dixon, W. J. and Massey, F. J., 1957, *Introduction to Statistical Analysis* (New York, McGraw-Hill), chapter 11.

Elkind, M. M., 1991, Enhanced transformation due to protracted exposures of fission-spectrum neutrons: a biophysical model. *International Journal of Radiation Biology*, **59,** 1471–1476.

Goodhead, D. T., Belli, M., Mill, A. J., Bance, D. A., Allen, L. A., Hall, S. C., Ianzani, F., Simone, G., Stevens, D. L., Stretch, A., Tabocchini, M. A. and Wilkinson, R. E., 1992, Direct comparison between protons and alpha-particles of the same LET. I. Irradiation methods and inactivation of asynchronous V79, HeLa and C3H/10T½ cells. *International Journal of Radiation Biology*, **61,** 611–624.

Goodman, L. J., 1985, A practical guide to ionization chamber dosimetry at the AFRRI reactor. AFRRI Contract Report CR85-1 (Bethesda, MD, Armed Forces Radiobiology Research Institute).

Hall, E. J., 1991, Weiss Lecture: The dose rate factor in radiation biology. *International Journal of Radiation Biology*, **59,** 595–610.

Hall, E. J. and Miller, R. C., 1981, The how and the why in *in vitro* oncogenic transformation. *Radiation Research*, **87,** 208–223.

Han, A. and Elkind, M. M., 1979, Transformation of mouse C3H/10T½ cells by single and fractionated doses of X-rays and fission spectrum neutrons. *Cancer Research*, **39,** 123–130.

Harrison, G. H. and Balcer-Kubiczek, E. K., 1992, Ambiguity of the Brenner–Hall model. *International Journal of Radiation Biology*, **61,** 139–142.

Hieber, L., Ponsel, G., Roos, H., Fenn, S., Fromke, E. and Kellerer, A. M., 1987, Absence of a dose rate effect in the transformation of C3H/10T½ cells by α-particles. *International Journal of Radiation Biology*, **52,** 859–869.

Hill, C. K., Buonoguro, F. M., Myers, C. P., Han, A. and Elkind, M. M., 1982, Fission-spectrum neutrons at

reduced dose rate enhance neoplastic transformation. *Nature*, **298,** 67–68.

Hill, C. K., Han, A. and Elkind, M. M., 1984, Fission-spectrum neutrons at low dose rate enhance neoplastic transformation in the linear, low dose region (0–10cGy). *International Journal of Radiation Biology*, **46,** 11–14.

Hill, C. K. and Zhu, L., 1991, Energy and dose-rate dependence of neoplastic transformation and mutations induced in mammalian cells by fast neutrons. *Radiation Research*, **124,** S48–S52.

IARC/NCI/EPA Working Group, 1985, Cellular and molecular mechanisms of cell transformation and standardization of transformation assays of established cell lines for prediction of carcinogenic chemicals: overview and recommended protocols. *Cancer Research*, **45,** 2395–2399.

ICRU, 1976, Neutron dosimetry for biology and medicine. Report No. 26, (Washington, DC, International Commission on Radiation Units and Measurements).

Kellerer, A. M. and Rossi, H. H., 1972, The theory of dual radiation action. *Current Topics in Radiation Research Quarterly*, **8,** 85–158.

Kleinbaum, D. G., Kupper, L. L. and Muller, K. E., 1988, *Applied Regression Analysis and Other Multivariate Methods* (Boston, PWS-Kent).

Komatsu, K., Sawada, S., Takeoka, S., Kodama, S. and Okumura, Y., 1993, Dose-rate effects of neutrons and gamma rays on the induction of mutation and oncogenic transformation in plateau-phase mouse m5S cells. *International Journal of Radiation Biology*, **52,** 859–869.

Little, J. B., 1979, Quantitiative studies of radiation transformation with A31-11 mouse BALB3/3T3 cell line. *Cancer Research*, **39,** 1474–1480.

Miller, R. C. and Hall, E. J., 1978, X-ray dose fractionation and oncogenic transformation in cultured mouse embryo cells. *Nature*, **272,** 58–60.

Miller, R. C., Brenner, D. J., Randers-Pehrson, G., Marino, S. A. and Hall, E. J., 1990, The effects of the temporal distribution of dose on oncogenic transformation by neutrons and charged particles of intermediate LET. *Radiation Research*, **124,** S62–68.

Miller, R. C. and Hall, E. J., 1991, Oncogenic transformation of C3H/10T½ cells by acute and protracted exposures to monoenergetic neutrons. *Radiation Research*, **128,** S60–64.

Miller, R. C., Randers-Pehrson, G., Hieber, L., Marino, S. A., Richards, M. and Hall, E. J., 1993, The inverse dose-rate effect for oncogenic transformation is dependent on linear energy transfer. *Radiation Research*, **133,** 360–364.

Moore, M. L. and Elsasser, S., 1986, The TRIGA Reactor Facility at the Armed Forces Radiobiology Research Institute: a simplified technical desctription. AFRRI Technical Report TR86-1 (Bethesda, MD, Armed Forces Radiobiology Research Institute).

Oftedal, P., 1968, A theoretical study of mutant yield and cell killing after treatment of heterogeneous cell populations. *Hereditas*, **60,** 177–210.

Pazzaglia, S., Priset, L., Saran, A., Robessi, S., Coppola, M., Di Majo, V., Broerse, J. J., Zotelief, H. and Covelli, V., 1993, Neutron-induced neoplastic transformation of C3H/10T½ cells (Poster 17). International Symposium on Molecular Mechanisms of Radiation and Carcinogen-induced Cell Transformation. Mackinac Island, MI, USA, 19–23 September.

Peixoto, J. L., 1993, Incorrect F-formulas in regression analysis. *American Statistician*, **47,** 194–197.

Redpath, J. L., Sun, C. and Blackely, W. F., 1991, Effect of fission-neutron dose rate on the induction of a tumor-associated antigen in human cell hybrids (HeLa × skin fibroblasts). *Radiation Research*, **128,** S71–74.

Reznikoff, C. A., Bertrham, J. S., Brankow, D. W. and Heidelberger, C., 1973b, Quantitative and qualitative studies of chemical transformation of cloned line of C3H mouse embryo cells sensitive to postconfluence inhibition of cell division. *Cancer Research*, **33,** 3239–3249.

Reznikoff, C. A., Brankow, D. W. and Heidelberger, C., 1973a, Establishment and characterization of a cloned line of C3H mouse embryo cells sensitive to postconfluence inhibition of cell division. *Cancer Research*, **33,** 3231–3238.

Rossi, H. H., 1981, Consideration on the time factor in radiobiology. *Radiation and Environmental Biophysics*, **18,** 1–9.

Rossi, H. H. and Kellerer, A. M., 1986, The dose-rate dependence of oncogenic transformation by neutrons may be due to variation of response during the cell cycle. *International Journal of Radiation Biology*, **50,** 353–361.

Saran, A., Pazzaglia, S., Pariset, L., Rebessi, S., Coppola, M., Di Majo, V. and Covelli, V., 1993, Cell-cycle dependence of C3H/10T½ cell transformation by fission-spectrum neutrons and X-rays (Poster P-17-4). 41st Annual Meeting of the Radiation Research Society, Dallas TX, USA, 20–25 March.

Saran, A., Pazzaglia, S., Coppola, M., Rebessi, S., Di Majo, V., Garavini, M. and Covelli, V., 1991, Absence of dose-fractionation effect on neoplastic transformation induced by fission-spectrum neutrons in C3H/10T½ cells. *Radiation Research*, **126,** 343–348.

Sykes, C. E. and Watt, D. E., 1989, Interpretation of the increase in the frequency of neoplastic transformations observed for some ionising radiations at low dose rates. *International Journal of Radition Biology*, **55,** 925–942.

Tauchi, H., Nakamura, N. and Sawada, S., 1993, Cell cycle dependence for the induction of 6-thioquanine-resistant mutations: G_2/M stage is distinctively sensitive to ^{252}Cf neutrons but not to ^{60}Co γ-rays. *International Journal of Radiation Biology*, **63,** 475–481.

Ullrich, R. L., 1984, Tumor induction in BALB/c mice after fractionated or protracted exposures to fission-spectrum neutrons. *Radiation Research*, **97,** 587–597.

Verbinski, V. V., Ferlick, K., Cassapakis, C. C., Daxon, E. and Hagan, W. K., 1981a, Radiation field characterization for the AFRRI TRIGA reactor. Report No. 5793F-1, Vol. 1 (Washington, DC, Defense Nuclear Agency).

Verbinski, V. V., Ferlick, K., Cassapakis, C. C., Daxon, E. and Hagan, W. K., 1981b, Calculation of the neutron and gamma-ray environment in and around for the AFRRI TRIGA reactor. Report No. 5793F-2, Vol. 2 (Washington, DC, Defense Nuclear Agency).

Watt, D. E., 1992, Comment on mechanism of radiation effects with special reference to transformation. Letter to Editor. International Journal of Radiation Biology, **61,** 263–267.

Zeman, G. H., Dooley, M., Eagleson, D. M., Goodman, L., Schwartz, R. B., Eisenhauer, C. M. and McDonald, J. C., 1988, Intercomparison of neutron dosimetry techniques at the AFRRI TRIGA reactor. *Radiation Protection Dosimetry*, **23,** 317–320.

Ionizing Radiation Increases Endothelial and Epithelial Cell Production of Influenza Virus and Leukocyte Adherence[1]

Margaret Colden-Stanfield,* John F. Kalinich,† and Elaine K. Gallin[2]*

Departments of *Physiology and †Radiation Biochemistry, Armed Forces Radiobiology Research Institute, Bethesda, MD 20889

To characterize the effect of ^{60}Co gamma radiation on cell-cell and pathogen-cell interactions, the adherence of undifferentiated HL-60 cells to HUVEC monolayers was tested in the absence and presence of LPS or influenza virus type A. Basal HL-60 cell adherence to uninfected HUVEC monolayers (3.0 ± 1.6%, n = 30) was not altered when HUVECs were exposed to 1- to 10-Gy gamma irradiation 4 to 72 h before the adhesion assay. LPS treatment of HUVEC monolayers (0.5 μg/ml, 4 h) produced a 6.9-fold increase in adherence that was not altered by previous irradiation. However, when HUVEC monolayers were subjected to 1–10 Gy 41 h before influenza virus infection (10^6 pfu/ml) for 7 h, virus-induced adherence was enhanced in a dose-dependent manner. Increased virus hemagglutinin (HA) protein expression mediated the radiation-induced adherence for the following reasons: 1) HA Ag increases paralleled increases in leukocyte adherence. 2) Northern blot analysis demonstrated a time-dependent increase in mRNA HA levels. 3) Anti-HA blocked HL-60 cell adherence to irradiated and virus-infected HUVEC monolayers. These changes were associated with an increased virus titer yield and virus-induced HUVEC killing. In contrast, cytotoxicity produced by vesicular stomatitis virus, which unlike influenza virus replicates cytoplasmically, was not altered by radiation in HUVECs. In related studies, the canine kidney epithelial (MDCK) cell line showed a similar increased influenza virus production after gamma radiation, indicating that the radiation-induced increase in production of influenza virus is not cell-specific and probably involves a nuclear mechanism. *The Journal of Immunology,* 1994, 153: 5222.

Increased susceptibility to bacterial and viral infections is common after exposure to therapeutic doses of ionizing radiation. Oral ulcerations caused by herpes simplex reactivation are associated with head and neck radiation (1–2), and both herpes (3–4) and cytomegalovirus (5) infections occur after total body irradiation. Although it is often assumed that the increased susceptibility to infections after radiation is primarily a result of radiation-induced leukopenia (6), other radiation-induced changes may contribute to the increased incidence of infection. For example, radiation-induced damage to epithelial and endothelial cells can enhance leukocyte-cell interactions leading to further breakdown of anatomical barriers and pathogen infiltration. An in vivo radiation study has reported an increased vascular permeability associated with enhanced leukocyte "sticking" and infiltration within hours of irradiation (7). Similarly, in vitro studies have demonstrated that production of leukocyte chemoattractants (8) and neutrophil adhesion to bovine aortic endothelial cells are increased 4 h after exposure to 5-Gy gamma radiation (9).

Virus infection in the absence of radiation exposure promotes leukocyte-cell interactions and can lead to breakdown of both epithelial and endothelial cell barriers (10). In vitro studies of cultured endothelial cells have demonstrated that infection by a variety of viruses, including herpes simplex virus, cytomegalovirus, adenovirus, or influenza virus enhances the interaction between leukocytes and endothelial cells (11–15). Although Etingin et al. (13) have demonstrated an indirect role of viral glycoprotein C in the herpes simplex virus-induced monocyte adherence, we have shown that influenza virus glycoprotein, hemagglutinin (HA),[3] directly mediates leukocyte adherence to influenza virus-infected endothelial cells (15). The experiments presented in this paper examined whether exposure

Received for publication June 14, 1994. Accepted for publication August 24, 1994.

The costs of publication of this article were defrayed in part by the payment of page charges. This article must therefore be hereby marked *advertisement* in accordance with 18 U.S.C. Section 1734 solely to indicate this fact.

[1] This work was supported by the Armed Forces Radiobiology Research Institute, Defense Nuclear Agency, under work unit 00020.

[2] Address correspondence and reprint requests to Dr. Elaine K. Gallin, Department of Physiology, Armed Forces Radiobiology Research Institute, 8901 Wisconsin Avenue, Bethesda, MD 20889–5603.

[3] Abbreviations used in this paper: HA, hemagglutinin; VSV, vesicular stomatitis virus; pfu, plaque-forming unit; BAEC, bovine aortic endothelial cell.

0022-1767/94/$02.00

of endothelial cells to ionizing radiation affects their subsequent susceptibility to virus infection and virus-induced leukocyte adherence. We demonstrate that, although adherence to endothelial cell monolayers was unchanged 4 to 72 h after gamma irradiation (1 to 10 Gy), exposure of endothelial cells to ionizing radiation before influenza virus infection augmented the virus-induced adherence. Furthermore, increased virus titer and augmented virus-induced cell killing after irradiation indicate that radiation increases the susceptibility of endothelial cells to influenza virus infection. Similar results were also noted in Madin-Darby canine kidney (MDCK) epithelial cells, suggesting that radiation exposure increases the sensitivity of a variety of cell types to influenza virus infection.

Materials and Methods

Cell culture

Isolation, harvest, and identification of HUVECs have been previously described by Colden-Stanfield et al. (15). HUVECs were seeded in collagen-coated culture vessels with complete MCDB107 culture medium (American Biorganics, Inc., Niagara Falls, NY) containing 10% heat-inactivated FBS (HyClone Laboratories, Inc., Logan, UT), 100 U/ml penicillin, 100 μg/ml streptomycin, 2 mM glutamine (all from Life Technologies Inc., Grand Island, NY), 100 μg/ml heparin (Sigma Chemical Co., St. Louis, MO), and 50 μg/ml endothelial cell growth supplement (H-Neurext, Upstate Biotechnology, Inc., Lake Placid, NY). Experimental data were obtained from HUVECs in their second to sixth passages, which were 1 to 2 days postconfluent.

Human HL-60 promyelocytic leukemia cells (23rd to 27th passage; American Type Culture Collection (ATCC), Rockville, MD) were predominantly used in the undifferentiated state to assess leukocyte-endothelial cell adherence. The cell line was grown in suspension with RPMI 1640 medium (Life Technologies, Inc.) containing 10% heat-inactivated FBS, 100 U/ml penicillin, 100 μg/ml streptomycin, 200 μg/ml neomycin, and 2 mM glutamine. Some experiments were repeated with HL-60 cells differentiated to neutrophil-like cells (dibutyryl cAMP 500 μM for 48 h; Ref. 16) and freshly isolated human neutrophils to corroborate our results with undifferentiated HL-60 cells.

The MDCK epithelial cell line (ATCC) was used as a positive control in several experiments because it is well established that these cells are infected by influenza and vesicular stomatitis viruses (VSV) (17–18). MDCK cells were grown in DMEM medium (Life Technologies, Inc.) containing 10% heat-inactivated FBS, 100 U/ml penicillin, 100 μg/ml streptomycin, 2 mM glutamine, and 5 mM glucose. Experimental data was obtained from confluent MDCK monolayers in their 27th to 30th passage.

Radiation protocol

Confluent HUVEC monolayers were grown in complete medium in 96- or 24-well plates (Corning Co., Corning, NY). The plates containing the HUVEC monolayers were uniformly irradiated, to total doses of 1 to 10 Gy at a dose rate of 1 Gy/min, in a bilateral gamma radiation field at the Armed Forces Radiobiology Research Institute ^{60}Co facility (19). HUVEC monolayers transported to the cobalt facility, but not irradiated, served as control, sham-irradiated monolayers. Cultures were incubated at 37°C for 4, 7, 24, 48, or 72 h in a 5% CO_2-humidified incubator. Dosimetry measurements were performed in accordance with the American Association of Physicists in Medicine protocol for the determination of absorbed dose from high energy photon and electron beams (20).

Virus preparation and infection

The WSN (H1N1) strain of influenza virus type A was grown in the MDCK cell line as previously reported (21). Stock virus was titered at 4×10^8 plaque forming units/ml (pfu/ml) in MDCK cells, and stored in liquid nitrogen until needed. Endothelial cells were infected by adding influenza virus (at a multiplicity of infection of 1 pfu per cell, 10^6 pfu/ml, unless otherwise stated) in complete MCDB107 to HUVEC monolayers. After 1 h of adsorption at 37°C in a 5% CO_2-humidified incubator, the medium was aspirated and rinsed once before fresh complete MCDB107 was added to each well.

VSV (Mudd-Summers strain, Indiana serotype) was kindly provided to us by Mark Akeson, National Institute of Mental Health, Bethesda, MD, and stored frozen (−70°C) at a titer ≈10^9 pfu/ml. HUVEC monolayers were infected by adding VSV (2×10^6 pfu/ml) in complete MCDB107 in the presence of DEAE-dextran (100 μg/ml), which enhances VSV infectivity (22), for 30 min in a 37°C incubator. After the adsorption period, HUVEC monolayers were washed once to remove unbound virus and refed with complete medium. Successful VSV infection was confirmed by ELISA analysis of VSV G surface protein expression 5 h after infection, monitored by using anti-G mAb as described by Lefrancois and Lyles (23).

Adhesion assay

HUVECs (30×10^4 cells/well) were seeded in collagen-coated 24-well plates 24 to 48 h before the confluent monolayers were either sham- or gamma irradiated. At various times after irradiation, some HUVEC monolayers were influenza virus-infected for 7 h before ^{51}Cr-labeled HL-60 cells (0.5×10^6 cells/well) suspended in DMEM/5% FBS were added to the HUVEC monolayers for 30 min at 37°C in a 5% CO_2-humidified incubator. Unbound HL-60 cells were aspirated, and the HUVEC monolayers were washed five times with assay medium before the remaining adherent cells were lysed with 1 N NH_4OH. The lysate and a second wash with NH_4OH were transferred to vials for subsequent radioanalysis with the use of an LKB 1282 COMPUGAMMA Counter CS (LKB Wallac, Turku, Finland). The percentage of HL-60 cell adherence was calculated as:

$$\% \text{ adherence} = (\text{cpm test HL-60 cells}) - (\text{cpm } NH_4OH) \div (\text{cpm total HL-60 cells}) - (\text{cpm } NH_4OH) \times 100 \quad (1)$$

mAb

Murine mAb H17-L19 (IgG1), which blocks the RBC binding site on the globular head of the viral glycoprotein HA, was produced from a hybridoma provided by Dr. W. Gerhard (Wistar Institute, Philadelphia, PA). Control murine mAb, W6/32 (IgG_{2a}; Accurate Chemical & Scientific Corporation, Westbury, NY), which recognizes an HLA-A, -B, -C determinant constitutively expressed on HUVECs, was used as a nonrelevant binding Ab.

Detection of cell surface Ags

As we have previously described (15), surface Ag expression was measured by using an ELISA. Uninfected or influenza virus-infected HUVEC monolayers that had been previously exposed to sham radiation or gamma radiation were paraformaldehyde-fixed and then incubated with PBS/1% BSA for 30 min at room temperature to block nonspecific binding. Each subsequent step of the ELISA was conducted at room temperature with three washes of PBS/1% BSA between steps. The fixed monolayers were incubated in turn with a saturating concentration of anti-HA or anti-HLA and a peroxidase-conjugated goat anti-mouse IgG (Sigma Chemical Co.) for 1 h. *O*-phenylenediamine (0.4 mg/ml)/0.012% hydrogen peroxide in a 0.05/0.025 M phosphate/citrate buffer, pH 5.0, was added to each well. Color development was stopped with 3 M H_2SO_4 at 20 min, and the OD was read at 492 nm wavelength on a Titertek ELISA plate reader (ICN Biomedical, Costa Mesa, CA). The degree of specific Ag expression was calculated by subtracting nonspecific binding of the secondary Ab from all test values.

RNA isolation and Northern blot analysis

At 0, 24, or 48 h after sham or 10-Gy irradiation, HUVEC monolayers were mock- or influenza virus-infected for 24 h. Total RNA was isolated from the six groups of HUVEC monolayers by using a single step procedure (24) at 1, 2, or 3 days after irradiation. Northern analysis, with the use of a dot blot vacuum technique (25), was conducted. Filters were

prehybridized overnight at 42°C in 0.25 M Na_2HPO_4 (pH 7.2), 1 mM EDTA, 20% SDS, and 5% BSA (26). The cDNA probe for the HA gene (a gift from Dr. Mary-Jane Gething, Howard Hughes Medical Institute, University of Texas Southwestern Medical Center at Dallas, Dallas, TX) was digested, purified, and radiolabeled by nick translation with [^{35}S]dATP. The nitrocellulose filters were hybridized overnight at 42°C with 2.5 ng/ml nick translated HA cDNA in prehybridization buffer. Filters were washed twice for 15 min each time at room temperature in 1X SSC/0.1% SDS, then twice for 15 min each at room temperature in 0.25X SSC/0.1% SDS before exposure to x-ray film. The films were scanned with a Molecular Dynamics Laser Densitometer (Sunnyvale, CA) with density volumes calculated using the associated ImageQuant software. Data were normalized to β-actin mRNA levels.

Virus titration assay

To determine the effect of gamma radiation on influenza virus production, we performed a HA assay (27) with virus progeny harvested from sham or 10 Gy-irradiated, infected HUVEC monolayers. Twenty-four hours after HUVEC monolayers were sham or 10 Gy-irradiated, they were infected with influenza virus (1.5×10^7 pfu total). At 24 h postinfection the monolayers were subjected to three freeze/thaw cycles to release all virus into the culture medium. After an ultracentrifugation step, serial dilutions of the virus progeny (100 μl) were incubated with 100 μl of human Type O RBCs in a 96-well U-bottom plate for 45 min at room temperature. Virus-RBC complexes settle in the form of a lattice, whereas unbound RBCs settle to the bottom of the well as a compact pellet.

Assessment of cell viability

Cell viability was assessed by using the ability of live cells to hydrolyze the membrane permeable probe (calcein-AM) to a fluorescent product (calcein) (Molecular Probes, Inc., Eugene, OR). HUVEC monolayers plated in 96-well plates that had been sham or 10 Gy-irradiated were infected with either influenza virus or VSV for 24 h. At various times postirradiation, endothelial cell monolayers were rinsed with PBS (without calcium and magnesium) before calcein-AM (1 μM) was added to each well. After a 30-min incubation at room temperature, the fluorescence was monitored (485 nm excitation/530 nm emission) on a CytoFluor 2350 fluorescence plate reader (Millipore, Marlborough, MA). The following formula was used to calculate percentage of viable cells:

$$\%\ \text{cell viability} = \text{experimental signal} - \text{minimum signal} \div \text{maximum signal} - \text{minimum signal} \times 100 \quad (2)$$

where the minimum signal is the calcein signal from dead cells (saponin-treated 50 μg) and the maximum signal is the calcein signal from control cells.

Data analysis

To test the effects of gamma radiation on HL-60 cell adherence, surface Ag expression, and virus-induced cell killing, the Student's *t*-test and, in some instances, a Mann-Whitney statistical analysis, was used with significance set at $p \leq 0.05$.

Results

Exposure to ^{60}Co gamma radiation does not alter basal leukocyte adherence to endothelial cell monolayers

The dose-response of HL-60 cell adherence to HUVEC monolayers was determined 48 h after gamma irradiation of HUVEC monolayers. Basal undifferentiated HL-60 cell adherence to sham-irradiated HUVEC monolayers was 3.0 ± 1.6% (mean ± SEM, $n = 30$; Fig. 1, *A* and *B*, △, ▲). Previous exposure of endothelial cells to single gamma radiation doses up to 10 Gy did not alter basal HL-60 cell adherence (Fig. 1*A*). There was no effect of radiation on adherence as early as 4 h and as late as 3 days after radiation exposure of HUVEC monolayers (Fig. 1*B*).

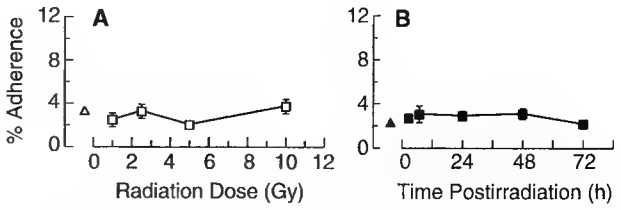

FIGURE 1. (*A*) Dose-response of basal HL-60 cell adherence to HUVEC monolayers 48 h after gamma irradiation and (*B*) time course of basal HL-60 cell adherence to 10 Gy-gamma irradiated HUVEC monolayers. Each point represents the mean ± SEM of six replicates in a representative experiment of three separate experiments. △, ▲ denote leukocyte adherence to sham-irradiated HUVEC monolayers. In this graph and all subsequent graphs, error bars are omitted when smaller than the size of the symbol.

These results contrast with those of Dunn et al. (9) who reported an increase in human neutrophil adherence 4 h after exposing bovine aortic endothelial cells to 5-Gy gamma radiation. Thus, to directly compare our results to those of Dunn et al. (9) and to determine whether these observations extended to related cell types, we assessed the adherence of undifferentiated HL-60 cells, neutrophil-like, cAMP-differentiated HL-60 cells or human neutrophils to irradiated bovine aortic endothelial cell (BAEC) monolayers as well as to HUVEC monolayers (Table I). Similar to our data on HUVEC monolayers, undifferentiated HL-60 cell adherence to bovine endothelial cell monolayers was unaffected by gamma irradiation. Furthermore, although there was an increase in the basal adherence of both cAMP-differentiated HL-60 cells and human neutrophils to HUVECs compared with undifferentiated HL-60 cells, radiation exposure of the HUVEC monolayers had no effect on basal levels of adherence. A similar lack of effect of radiation was noted in studies on BAECs. Additionally, increasing the radiation dose to 10 Gy failed to change basal undifferentiated HL-60 cell, cAMP-differentiated HL-60 cell, and neutrophil adherence to HUVEC monolayers (data not shown).

Gamma radiation does not affect LPS-induced leukocyte adherence but enhances influenza virus-induced leukocyte adherence to endothelial cell monolayers

Exposing HUVEC monolayers to LPS, a well known promoter of leukocyte adherence (28–29), produced a 6.9-fold increase in HL60 cell adherence that was not affected by previous gamma irradiation (Table II). ELISA analysis of the endothelial adhesion molecules, E-selectin and ICAM-1, which mediate the LPS-induced adherence, revealed no change in Ag expression after irradiation (data

Table I. *Percentage of leukocytes adhering to γ-irradiated endothelial cell monolayers*[a]

Cells	BAEC Monolayers			HUVEC Monolayers		
	Sham, 0 Gy	5 Gy 4 h pi[b]	5 Gy 48 h pi	Sham, 0 Gy	5 Gy 4 h pi	5 Gy 48 h pi
Undifferentiated HL-60s	3.52 ± 0.32 (4)	4.21 ± 0.38 (4)	4.28 ± 0.37 (2)	2.04 ± 0.25 (4)	2.40 ± 0.37 (2)	2.00 ± 0.33 (4)
cAMP-differentiated HL-60s	3.72 ± 0.30 (2)	5.35 ± 0.65 (2)	5.38 ± 0.64 (2)	6.82 ± 0.96 (2)	5.74 ± 0.35 (2)	7.24 ± 0.96 (2)
Human PMNs	4.09 ± 0.20 (2)	4.30 ± 0.23 (2)	3.98 ± 0.53 (2)	14.97 ± 0.78 (1)	13.69 ± 0.59 (1)	15.11 ± 0.92 (1)

[a] Values are means ± SEM. The number of separate experiments each with six replicates is in parentheses. Adherence of ^{51}Cr-labeled undifferentiated or cAMP-differentiated HL-60 cells or freshly isolated human neutrophils to sham- or 5 Gy-irradiated BAEC or HUVEC cell monolayers was measured as described in the *Materials and Methods* section.

[b] pi denotes postirradiation.

Table II. *Percentage of undifferentiated HL-60 adherence to HUVEC monolayers*[a]

Treatment	0 Gy, Control	10 Gy
Control	3.24 ± 0.30 (8)	3.73 ± 0.67 (8)
LPS treated	22.21 ± 0.92 (2)*	22.56 ± 0.58 (2)*
Influenza infected	59.72 ± 0.61 (8)*	80.21 ± 0.92 (8)*†

[a] Values are mean ± SEM. The number of separate experiments each with six replicates is in parentheses. Control, LPS-treated (0.5 μg/ml, 4 h)- or virus-infected (10^6 pfu/ml, 7 h) HUVEC monolayers were exposed to sham or 10-Gy irradiation 48 h before the adhesion assay was performed.

* signifies a statistical difference ($p \leq 0.05$) compared to the corresponding control group.

† denotes a statistical difference compared with the sham-irradiated, influenza-infected group.

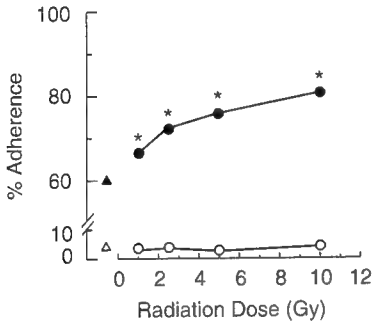

FIGURE 2. Dose response of HL-60 cell adherence to uninfected (○) or influenza virus-infected (●, 7 h postinfection) HUVEC monolayers 48 after gamma irradiation of the endothelial cells. △ and ▲ signify adherence to sham-irradiated mock-infected and influenza virus-infected HUVEC monolayers, respectively. Each point represents the mean ± SEM of six replicates in a representative experiment of three separate experiments. *denotes a statistical significance between the infected, sham-irradiated HUVEC group and the infected, irradiated HUVEC monolayers.

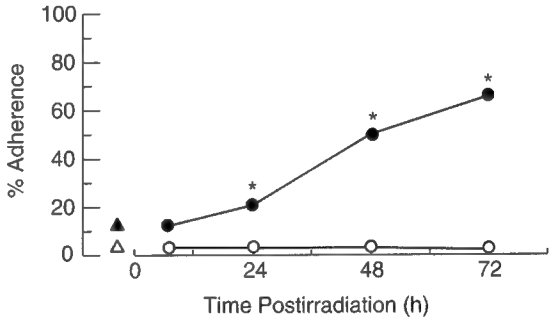

FIGURE 3. Time course of HL-60 adherence to uninfected (○) or influenza virus-infected (●, 7 h postinfection) HUVEC monolayers after gamma irradiation. HL-60 cell adherence to HUVEC monolayers was monitored at various times after 10-Gy irradiation. △ and ▲ signify adherence to sham-irradiated mock-infected and influenza virus-infected HUVEC monolayers, respectively. Each point is the mean ± SEM of six replicates in a representative experiment of three separate experiments. * denotes a statistical significance between the infected, sham-irradiated HUVEC group and the infected, irradiated HUVEC monolayers.

not shown). However, ionizing radiation had a profound effect on HL-60 cell adherence to HUVEC monolayers subsequent to influenza virus infection (Table II). We have previously demonstrated that influenza virus infection of HUVEC monolayers produces a time- and concentration-dependent increase in HL-60 cell adherence (15) (Fig. 2, ▲). Irradiation of HUVEC monolayers 48 h before the adhesion assay produced a dose-dependent augmentation of influenza virus-induced HL-60 cell adherence (Fig. 2). A single 10-Gy dose produced a 34.3% enhancement of virus-induced HL-60 cell adherence. At 24 h, 10 Gy significantly enhanced virus-induced adherence by 17.9% (data not shown), but lower radiation doses had no effect on virus-induced adherence.

In related studies, we altered the time after 10-Gy irradiation that HUVECs were infected with virus and then monitored HL-60 cell adherence 7 h after viral infection (Fig. 3). Control studies on irradiated, uninfected HUVECs (Fig. 3, ○) indicated that there was no increase in HL-60 adherence up to 72 h postirradiation. On the other hand, there was a time-dependent increase in the effects of gamma radiation on leukocyte adherence to virus-infected HUVEC monolayers. Infection of sham-irradiated HUVECs with a low virus titer (10^5 pfu/ml) increased adherence to 12% (Fig. 3, ▲). This virus-induced HL-60 cell adherence was enhanced 1.8-, 4.3-, and 5.6-fold at 24, 48, and 72 h, respectively, after gamma irradiation (Fig. 3). It is noteworthy that, even at 3 days after irradiating the HUVEC monolayers, leukocyte adherence had not reached a plateau. The ability of radiation to enhance, to a similar degree, the virus-induced leukocyte adherence was confirmed with cAMP-differentiated HL-60 cells and human neutrophils (data not shown).

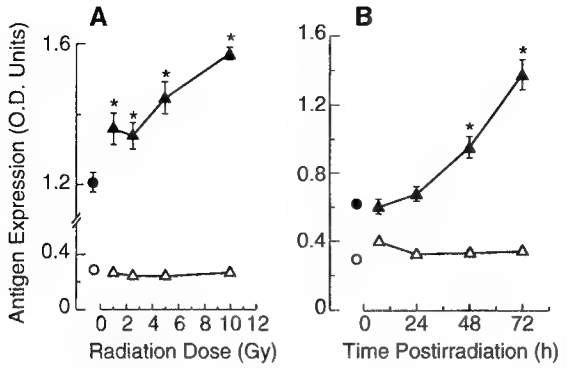

FIGURE 4. (*A*) Dose response and (*B*) time course of influenza virus HA surface Ag expression on uninfected (△) or virus-infected (▲, 7 h postinfection) HUVEC monolayers. (*A*) Forty-one hours after HUVEC monolayers were gamma irradiated, they were infected with influenza virus for 7 h, fixed, and HA Ag expression was quantitated by using H17-L19 (anti-HA) in the ELISA assay described in *Materials and Methods*. (*B*) At 0, 17, 41, or 65 h after HUVEC monolayers were 10 Gy irradiated, they were influenza virus-infected for 7 h before HA Ag expression was quantitated. ○ and ● signify HA Ag expression on sham-irradiated, uninfected, and virus-infected HUVEC monolayers, respectively. Each point is the mean ± SEM of quadruplicate wells in a representative experiment of two separate experiments. * denotes a statistical significance between the infected, sham-irradiated HUVEC group and the infected, irradiated HUVEC monolayers.

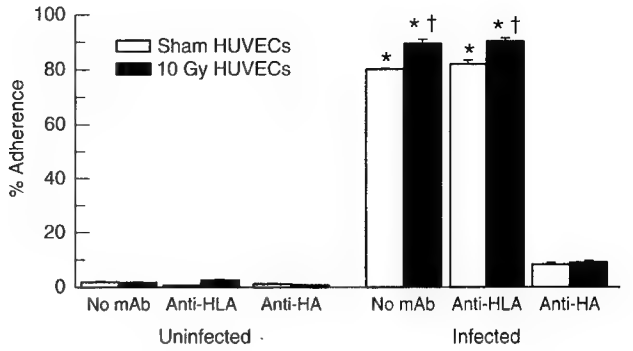

FIGURE 5. The effect of anti-HA on HL-60 cell adherence to sham (open bars) or 10 Gy-irradiated (filled bars), virus-infected (7 h) HUVEC monolayers was determined by incubating HUVECs with a saturating concentration (90 μg/ml) of anti-HA for 30 min at 37°C before and during the adhesion assay. To demonstrate specificity of the Ab block, the adhesion assay was performed in the presence of anti-HLA, a nonrelevant binding IgG Ab. Each point is the mean ± SEM of five replicates in a representative experiment of two separate experiments. * signifies a significant difference between the infected, sham-irradiated group and the corresponding control group ($p \leq 0.05$). † denotes a statistical difference between infected, irradiated HUVEC group and the corresponding infected, sham-irradiated HUVEC group.

Gamma radiation augments virus HA expression on influenza virus-infected HUVEC monolayers

Because HL-60 cell adherence to influenza virus-infected HUVEC monolayers is mediated by newly expressed HA on the surface of endothelial cells (15), we monitored HA expression on uninfected and virus-infected HUVEC monolayers exposed to varying doses of radiation. As expected, uninfected endothelial cells had insignificant levels of HA Ag (Fig. 4*A*, ○). In contrast, influenza virus infection of HUVECs for 7 h produced a 4.1-fold increase in surface HA expression (Fig. 4*A*, ●). At 48 h postirradiation, a dose-dependent increase in virus-induced HA Ag expression was observed with 10 Gy augmenting HA expression by 30.4% (Fig. 4*A*).

The time course of HA Ag expression in Figure 4*B* revealed a profile of enhancement similar to that noted in Figure 3 for virus-induced leukocyte adherence after irradiation. HA Ag increased in a time-dependent manner on HUVEC monolayers that were influenza virus-infected for 7 h (Fig. 4*B*). At 48 and 72 h postirradiation, HA Ag was increased significantly 1.5- and 2.2-fold, respectively. As was seen with the effect of radiation on virus-induced leukocyte adherence, the increased expression of HA did not saturate at 72 h postirradiation.

These results suggested that the augmented virus-induced adherence was the result of enhanced HA expression after irradiation. To directly demonstrate the role of surface HA in the radiation enhancement of the virus-induced adherence, influenza virus-infected (7 h) HUVEC monolayers were incubated with anti-HA (90 μg/ml) 30 min before and during the adhesion assay. As we have previously demonstrated, anti-HA inhibits HL-60 cell adherence to HUVEC monolayers that have been infected with a high influenza virus titer (10^6 pfu/ml) (Fig. 5) (Ref. 15). Virus-induced adherence to 10 Gy-irradiated HUVECs was completely blocked in the presence of anti-HA indicating that the radiation-induced increase in virus-induced adherence was mediated by an augmented expression of HA protein. A nonrelevant binding Ab, anti-HLA, had no effect on basal or virus-induced HL-60 cell adherence to sham- or 10 Gy- irradiated HUVEC monolayers.

Gamma radiation enhances HA mRNA levels in virus-infected HUVEC monolayers

To determine whether radiation affects mRNA levels of the viral HA gene, we performed Northern blot analysis with RNA isolated from irradiated and virus-infected HUVECs. HA mRNA levels in sham-irradiated, virus-infected HUVECs were slightly increased in one of two experiments performed. At 24 h after 10-Gy irradiation, cellular levels of HA mRNA from influenza virus-infected HUVECs was increased by 51% over mRNA levels observed in sham-irradiated HUVECs (Table III). HA gene expression increased by 70% at 48 h after irradiation (this was confirmed in a second experiment). As was seen with

Table III. *HA mRNA levels after γ-irradiation*[a]

Radiation Dose	Time Postirradiation	Relative mRNA[b]	
		− Influenza	+ Influenza
0 Gy		1.0	1.0
10 Gy	24 h	1.1	1.5
10 Gy	48 h	0.8	1.7
10 Gy	72 h	0.8	1.9

[a] At various times after sham or 10-Gy irradiation, HUVEC monolayers were infected with influenza virus for 24 h. As described in *Materials and Methods*, mRNA levels of HA were quantitated by using Northern blot analysis.

[b] HA mRNA levels in sham-irradiated HUVEC cultures was set at 1.0. All other values are expressed relative to that value.

HL-60 cell adherence and HA Ag expression (Figs. 3 and 4*B*), cellular levels of HA mRNA did not plateau by 72 h after 10-Gy irradiation with a 91% enhancement over levels in sham-irradiated HUVECs.

Gamma radiation increases production of influenza virus in HUVEC and monolayers

Virus progeny was harvested from infected HUVECs that had been sham or 10-Gy irradiated before infection. By using a HA assay to quantitate the virus progeny, we found that sham-irradiated HUVEC monolayers infected for 24 h yielded a virus titer of 10^7 pfu/ml. In contrast, there was a 2.3-fold increase in virus titer produced 48 h after 10-Gy irradiation of infected HUVEC monolayers. To determine whether radiation modulates influenza virus production in other cell types, we performed similar studies by using MDCK epithelial cells, a cell line that is well known to be susceptible to influenza virus (21). Virus progeny from sham-irradiated, MDCK cells that were virus infected for 24 h yielded a virus titer of 6.4×10^8 pfu/ml. Previous exposure to 10-Gy gamma radiation increased virus titer twofold in 24 h-infected MDCK monolayers.

Gamma radiation enhances influenza virus-induced cytotoxicity but not VSV-induced cytotoxicity

In our previous study (15) we demonstrated that HUVEC viability was unchanged 7 h after influenza virus infection, a time when influenza virus has undergone one replication cycle. However, after several replication cycles, cytopathic features such as cell rounding, detachment, and death occur (30). Therefore, we quantitated cell viability by using calcein-AM in sham or 10 Gy-irradiated HUVEC monolayers that were subsequently exposed to influenza virus for 24 h. HUVEC viability was not altered up to 72 h after exposure to a single 10-Gy dose of ionizing radiation (Fig. 6, filled bar). However, 24 h after HUVEC monolayers were infected with influenza virus alone, cell viability was decreased to 74.2 ± 4.5% ($n = 5$). Exposure of HUVEC monolayers to 10-Gy gamma irradiation increased influenza virus-induced cell killing by 21.2, 28.5, and 16.8% at 24, 48, and 72 h postirradiation, respectively

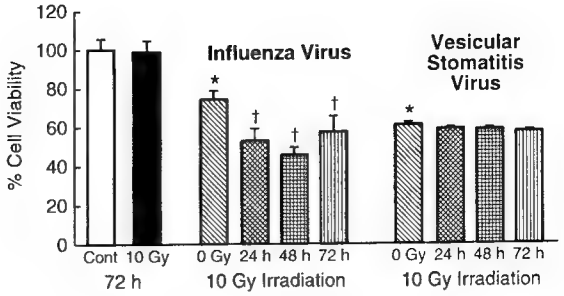

FIGURE 6. Effect of 10-Gy irradiation on HUVEC viability 24 h after virus infection and 48 h postirradiation. At various times after sham or 10-Gy irradiation, HUVEC monolayers were infected with influenza or VSV. Cell viability (described in the *Materials and Methods* section) was assessed at 24 h after virus infection. * denotes a significant difference between the infected, sham-irradiated group and the corresponding control group. † signifies a difference between the infected, irradiated HUVEC group and the corresponding infected, sham-irradiated HUVEC group. Each point is the mean ± SEM of five replicates in a representative experiment of three separate experiments.

(Fig. 6), suggesting that the enhanced killing may be a result of a synergism between the two challenges or that the killing may result from different mechanisms. Similarly, irradiated MDCK cells also were more susceptible to influenza virus-induced killing (data not shown).

Although influenza virus replication requires host RNA primer synthesized by cellular RNA polymerase II (31), other RNA viruses such as VSV require only cytoplasmic constituents to replicate (32). To explore the possibility that radiation is influencing viral replication through a nuclear mechanism and not a cytoplasmic mechanism, we compared the effect of radiation on influenza virus-induced HUVEC cytotoxicity with its effect on VSV-induced HUVEC cytotoxicity. A viability assay was performed with sham- or 10 Gy-irradiated HUVEC monolayers that were infected with VSV at various times after irradiation. Twenty-four hours after VSV infection, HUVEC viability was reduced by 40% (Fig. 6). Radiation did not significantly alter viability in VSV-infected HUVECs whether viability was measured at 1, 2, or 3 days after radiation exposure. Similarly, previous irradiation did not change the viability of VSV-infected MDCK epithelial cells (data not shown).

Discussion

At sites of infection and inflammation, the endothelial cell monolayer functions as an adhesive surface for leukocytes that diapedese out of the vasculature into injured underlying tissue. This study focuses on the effect of ionizing radiation on the ability of endothelial cell monolayers to bind leukocytes under quiescent conditions and in the face of a pathogen insult.

Our results demonstrate that although acute exposure of endothelial cell monolayers to gamma radiation does not

affect basal leukocyte adherence, it enhances influenza virus-induced adherence by increasing HA expression on the surface of endothelial cells. This lack of effect of ionizing radiation on basal leukocyte adherence contrasts with the findings of Dunn et al. (9) who found a 26% increase in human neutrophil adherence to bovine aortic endothelial cell monolayers 4 h after 5-Gy gamma irradiation. The discrepancy between our data on HL-60 cells binding to HUVECs and the findings of Dunn et al. cannot be explained by differences in cell types, because we also confirmed our observations by using BAECs and human neutrophils as well as cAMP-differentiated HL-60 cells. Unlike Dunn et al., who observed bovine endothelial cell damage within 4 h of irradiation, we did not detect a loss of endothelial cell viability up to 72 h after 10-Gy irradiation. Differences in the magnitude of endothelial cell damage induced by radiation may underlie the differences in leukocyte adhesion between our study and Dunn et al., because a preferential binding of leukocytes to injured or wounded bovine endothelial cells has been reported (33).

In our previous studies with the use of this in vitro model, influenza virus infection of endothelial cells increased leukocyte adherence by increasing HA surface Ag expression (15). In light of clinical findings demonstrating an increased risk of viral infections after radiation therapy (1–2, 5), the present study uses this in vitro model to characterize the effect of radiation on pathogen/endothelial interactions. We demonstrate that previous exposure of HUVEC monolayers to ionizing radiation promoted the interaction between leukocytes and influenza virus-infected endothelial cells. Furthermore, a direct relationship between surface HA protein expression and leukocyte adherence was confirmed by the following: 1) parallel increases in leukocyte adherence and viral HA Ag expression; and 2) anti-HA blocking virus-induced adherence in infected endothelial cells after irradiation.

Most importantly, radiation increased influenza virus production in endothelial cells as evidenced by increased mRNA HA levels and influenza virus titer yield. Comparable results were observed with the epithelial cell line, MDCK cells, often used in studying cellular processing of influenza virus (17). Thus, the increased susceptibility to influenza virus production resulting from exposure to ionizing radiation is not cell specific.

To better understand the mechanism underlying the increased virus production after irradiation, we compared the cytopathic ability of influenza virus to that of a rhabdovirus, VSV. Although synthesis of influenza virus mRNA requires a capped and methylated primer synthesized by cellular RNA polymerase II (31), VSV virion RNA is transcribed by a virus-associated RNA polymerase independent of host-cell nuclear functions (32). Our observations that previous exposure of both endothelial and epithelial cell lines to ionizing radiation did not alter the ability of VSV to kill cells, suggest that the increased influenza virus production may be related to this requirement for cellular RNA polymerase II enzyme activity. Thus, an increased rate of gene transcription may underlie the radiation effects we have described. Nuclear run-on experiments have illustrated a radiation-induced increase in the transcription rate of c-*jun*, an early-response gene (34), and TNF-α, a late-response gene, in human myeloid cells (35). Similar to our observations of radiation enhancement of influenza virus infectivity, Miller and Smith (36) demonstrated that ionizing radiation produces a 10 to 15% increase in infectivity of human fibroblasts by herpes simplex virus, which also requires cellular RNA polymerase II to replicate (37).

Alternatively, ionizing radiation may be working through other mechanisms such as enhancement of protein kinase C-dependent growth of influenza virus (38), since radiation increases protein kinase C mRNA levels and subsequent enzyme activity in some cell types (39–41). The increased susceptibility to influenza infection also may be related to the depressive effect of radiation on IFN production (42) in endothelial cells (43) leading to a decreased expression of Mx proteins which confer cellular resistance to influenza virus infection (44). However, this is unlikely because IFN also confers resistance to VSV infection (45), and we found no effect of radiation on VSV-induced endothelial cytotoxicity.

In summary, we have demonstrated that gamma radiation alone does not alter basal leukocyte adherence to endothelial cells but increases: 1) virus-induced leukocyte adherence, 2) influenza virus production in endothelial and epithelial cells, and 3) virus-induced endothelial and epithelial cell killing. If ionizing radiation induces similar effects in vivo, it would be expected to increase the risk of influenza virus infection in patients receiving radiotherapy. Moreover, a similar mechanism may underlie the increased susceptibility to infection by herpes simplex virus after radiation therapy, which has been well documented (1–4).

Acknowledgments

We thank Drs. Eva B. Cramer and Don R. Ratcliffe for critically reading the manuscript.

References

1. Fleming, P. 1991. Dental management of the pediatric oncology patient. *Curr. Opin. Dent. 1:577.*
2. Redding, S. W., E. B. Luce, and M. W. Boren. 1990. Oral herpes simplex virus infection in patients receiving head and neck radiation. *Oral Surg. Med. Oral Pathol. 69:578.*
3. Epstein, J. B. 1990. Infection prevention in bone marrow transplantation and radiation patients. *Natl. Cancer Inst. Monogr. 9:73.*
4. Woo, S., S. T. Sonis, and A. L. Sonis. 1990. The role of herpes simplex in the development of oral mucositis in bone marrow transplant recipients. *Cancer 66:2375.*
5. Sale, G. E., and C. D. Buckner. 1988. Pathology of bone marrow in transplant recipients. *Bone Marrow Examination 2:735.*
6. Sakata, K., Y. Aoki, N. Muta, A. Therahara, K. Karasawa, Y. Onogi, K. Nakagawa, K. Hasezawa, Y. Sasaki, and A. Akanuma. 1993.

Effect of human granulocyte colony-stimulating factor on neutropenia induced by radiotherapy and chemotherapy. *Oncology 50:238.*

7. Narayan, K., and W. J. Cliff. 1982. Morphology of irradiated microvasculature: a combined in-vivo and electron-microscopic study. *Am. J. Pathol. 106:47.*
8. Matzner, Y., M. Cohn, E. Hyam, E. Razin, Z. Fuks, M. R. Buchanan, T. A. Haas, I. Vlodavsky, and A. Eldor. 1988. Generation of lipid neutrophil chemoattractant by irradiated bovine aortic endothelial cells. *J. Immunol. 140:2681.*
9. Dunn, M. M., E. A. Drab, and D. B. Rubin. 1986. Effects of irradiation on endothelial cell-polymorphonuclear leukocyte interactions. *J. Appl. Physiol. 60:1932.*
10. Ratcliffe, D., G. Migliorisi, and E. Cramer. 1992. Translocation of influenza virus by migrating neutrophils. *Cell. Mol. Biol. 38:63.*
11. MacGregor, R. R., H. M. Friedman, E. J. Macarak, and N. A. Kefalides. 1980. Virus infection of endothelial cells increases granulocyte adherence. *J. Clin. Invest. 65:1469.*
12. Zajac, B. A., K. O'Neill, H. M. Friedman, and R. R. MacGregor. 1988. Increased adherence of human granulocytes to herpes simplex virus type 1-infected endothelial cells. *In Vitro Cell. Dev. Biol. 24: 321.*
13. Etingin, O. R., R. L. Silverstein, and D. P. Hajjar. 1991. Identification of a monocyte receptor on herpesvirus-infected endothelial cells. *Proc. Natl. Acad. Sci. USA 88:7200.*
14. Span, A. H. M., M. C. E. van Dam-Mieras, W. Mullers, J. Endert, A. D. Muller, and C. A. Bruggeman. 1991. The effect of virus infection on the adherence of leukocytes or platelets to endothelial cells. *Eur. J. Clin. Invest. 21:331.*
15. Colden-Stanfield, M., D. Ratcliffe, E. B. Cramer, and E. K. Gallin. 1993. Characterization of influenza virus-induced leukocyte adherence to human umbilical vein endothelial cell monolayers. *J. Immunol. 151:310.*
16. Chaplinski, T. J., and J. E. Niedel. 1982. Cyclic nucleotide-induced maturation of human promyelocytic leukemia cells. *J. Clin. Invest. 70:953.*
17. Matlin, K. S., H. Reggio, A. Helenius, and K. Simons. 1981. Infectious entry pathway of influenza virus in a canine kidney cell line. *J. Cell Biol. 91:601.*
18. Fuller, S., C.-H. von Bonsdorff, and K. Simons. 1984. Vesicular stomatitis virus infects and matures only through the basolateral surface of the polarized epithelial cell line, MDCK. *Cell 38:65.*
19. Carter, R. E., and D. M. Verrelli. 1973. AFRRI Cobalt whole-body irradiator. *Armed Forces Radiobiology Research Institute Technical Note 73–3.*
20. American Association of Physicists in Medicine, AAPM Task Group 21. 1983. A protocol for the determination of absorbed dose from high-energy photon and electron beams. *Med. Phys. 10:741.*
21. Rodriguez-Boulan, E. 1983. Polarized assembly of enveloped viruses from cultured epithelial cells. *Methods Enzymol. 98:486.*
22. Bailey, C. A., D. K. Miller, and J. Lenard. 1984. Effects of DEAE-dextran on infection and hemolysis by VSV: evidence that nonspecific electrostatic interactions mediate effective binding of VSV to cells. *Virology 133:111.*
23. Lefrancois, L., and D. S. Lyles. 1983. Antigenic determinants of vesicular stomatitis virus: analysis of antigenic variance. *J. Immunol. 130:394.*
24. Chomczynski, P., and N. Sacchi. 1987. Single step method of RNA isolation by acid guanidinium thiocyanate-phenol-chloroform extraction. *Anal. Biochem. 162:156.*
25. Kafatos, F. C., C. W. Jones, and A. Efstratiadis. 1979. Determination of nucleic acid sequence homologies and relative concentrations by a dot hybridization technique. *Nucleic Acids Res. 7:1541.*
26. Engler-Blum, G., M. Meier, J. Frank, and G. A. Muller. 1993. Reduction of background problems in nonradioactive Northern and Southern blot analyses enables higher sensitivity than ^{32}P-based hybridizations. *Anal. Biochem. 210:235.*
27. Kuchler, R. J. 1977. Isolation and identification of animal viruses. In *Biochemical Methods in Cell Culture and Virology.* Dowden, Hutchinson & Ross, Inc., Stroudsburg, PA, p. 144.
28. Pohlman, T. H., K. A. Stanness, P. G. Beatty, H. D. Ochs, and J. M. Harlan. 1986. An endothelial cell surface factor(s) induced in vitro by lipopolysaccharide, interleukin-1, and tumor necrosis factor-α increases neutrophil adherence by a CDw-18-dependent mechanism. *J. Immunol. 136:4548.*
29. Schleimer, R. P., and B. K. Rutledge. 1986. Cultured human vascular endothelial cells acquire adhesiveness for neutrophils after stimulation with interleukin-1, endotoxin, and tumor-promoting phorbol diesters. *J. Immunol. 136:649.*
30. Malherbe, H. H. 1985. Role of tissue culture systems. In *Laboratory Diagnosis of Viral Infections.* E. H. Lennette, ed. Marcel Dekker, Inc., New York, p. 47.
31. Kingsbury, D. W. 1990. Orthomyxoviridae and their replication. In *Virology.* B. N. Fields and D. M. Knipe, eds. Raven Press, Ltd., New York, p. 1075.
32. Wagner, R. R. 1990. Rhabdoviridae and their replication. In *Virology.* B. N. Fields and D. M. Knipe, eds. Raven Press, Ltd., New York, p. 867.
33. DiCorleto, P. E., and C. A. de la Motte. 1985. Characterization of the adhesion of the human monocytic cell line U937 to cultured endothelial cells. *J. Clin. Invest. 75:1153.*
34. Datta, R., D. E. Hallahan, S. M. Kharbanda, E. Rubin, M. L. Sherman, R. R. Weichselbaum, and D. W. Kufe. 1992. Involvement of reactive oxygen intermediates in the induction of c-*jun* gene transcription by ionizing radiation. *Biochemistry 31:8300.*
35. Sherman, M. L., R. Datta, D. E. Hallahan, R. R. Weichselbaum, and D. W. Kufe. 1991. Regulation of tumor necrosis factor gene expression by ionizing radiation in human myeloid leukemia cells and peripheral blood monocytes. *J. Clin. Invest. 87:1794.*
36. Miller, C. S., and K. O. Smith. 1991. Enhanced replication of herpes simplex virus type 1 in human cells. *J. Dent. Res. 70:111.*
37. Roizman, B., and A. E. Sears. 1990. Herpes simplex viruses and their replication. In *Virology,* 2nd Ed. B. N. Fields and D. M. Knipe, eds. Raven Press, Ltd., New York, p. 1795.
38. Kurokawa, M., H. Ochiai, K. Nakajima, and S. Niwayama. 1990. Inhibitory effect of protein kinase C inhibitor on the replication of influenza type A virus. *J. Gen. Virol. 71:2149.*
39. Woloschak, G. E., C.-M. Chang-Liu, and P. Shearin-Jones. 1990. Regulation of protein kinase C by ionizing radiation. *Cancer Res. 50:3963.*
40. Kim, C. Y., A. J. Giaccia, B. Strulovici, and J. M. Brown. 1992. Differential expression of protein kinase C epsilon protein in lung cancer cell lines by ionising radiation. *Br. J. Cancer 66:844.*
41. Hallahan, D. E., S. Virudachalam, D. Grdina, and R. R. Weichselbaum. 1992. The isoquinoline sulfonamide H7 attenuates radiation-mediated protein kinase C activation and delays the onset of x-ray-induced G2 arrest. *Int. J. Radiat. Oncol. Biol. Phys. 24:687.*
42. De Maeyer, E., P. Jullien, and J. De Maeyer-Guignard. 1967. Interferon synthesis in X-irradiated animals. II. Restoration by bone-marrow transplantation of circulating-interferon production in lethally-irradiated mice. *Int. J. Radiat. Biol. 13:417.*
43. Einhorn, S., A. Eldor, I. Vlodavsky, Z. Fuks, and A. Panet. 1985. Production and characterization of interferon from endothelial cells. *J. Cell. Physiol. 122:200.*
44. Aebi, M., J. Fah, N. Hurt, C. E. Samuel, D. Thomis, L. Bassigher, J. Pavlovic, O. Haller, and P. Staeheli. 1989. cDNA structures and regulation of two interferon-induced human Mx proteins. *Mol. Cell. Biol. 9:5062.*
45. Pavlovic, J., T. Zurcher, O. Haller, and P. Staeheli. 1990. Resistance to influenza virus and vesicular stomatitis virus conferred by expression of human MxA protein. *J. Virol. 64:3370.*

Therapeutic Efficacy of Recombinant Human Leukemia Inhibitory Factor in a Primate Model of Radiation-Induced Marrow Aplasia

By Ann M. Farese, Laurie A. Myers, and Thomas J. MacVittie

The therapeutic efficacy of recombinant human leukemia inhibitory factor (LIF) was examined in a nonhuman primate model of radiation-induced marrow aplasia. Rhesus monkeys received 450 cGy of total-body, 1:1 mixed neutron:gamma radiation. For 23 days thereafter, each monkey received a daily subcutaneous injection of LIF or human serum albumin (HSA) at a dose of 15 μg/kg body weight. Complete blood counts and white blood cell differentials were monitored for 60 days postirradiation. Administration of LIF significantly decreased ($P \leq .05$) the duration of thrombocytopenia (platelet count <30,000 or 20,000/μL), ie, 9.3 days or 6.3 days, respectively, versus the HSA-treated control monkeys, 12.2 days or 10.2 days, respectively. Treatment with LIF did not alter the duration of neutropenia (absolute neutrophil count <1,000/μL) as compared with the HSA-treated control monkeys. Cytokine administration did not exacerbate the radiation-induced anemia observed in the HSA-treated control monkeys.

THROMBOCYTOPENIA and neutropenia remain as dose-limiting consequences after high-dose irradiation or cytotoxic drug exposure. Cytokines such as recombinant human granulocyte and granulocyte-macrophage colony-stimulating factor have been effective in reducing the duration of neutropenia after radiation- or drug-induced marrow aplasia in preclinical[1-6] and clinical protocols.[7-9] Several cytokines have shown therapeutic efficacy in modulating the recovery of platelets after radiation-[6,10] or drug-induced marrow aplasia.[11-13] Interleukin-3 (IL-3) has shown a modest yet consistent efficacy in preclinical models of myelosuppression[6,11] but has demonstrated variable efficacy in modulating thrombocytopenia in the clinical situation.[14-18] More recently, IL-6 has displayed efficacy in reducing thrombocytopenia and enhancing recovery of platelets in murine,[14,19-22] canine,[23] and primate[24-26] models of either radiation-or drug-induced thrombocytopenia. Results from clinical trials with IL-6 have shown it to be efficacious in modulating drug-induced thrombocytopenia.[27,28] IL-11 has also been shown to enhance the recovery of platelets in several murine models of myelosuppression.[29-32]

Yet another cytokine, leukemia inhibitory factor (LIF), has recently been shown to promote megakaryocyte maturation in vitro[33,34] and to increase circulating levels of platelets in normal mice[35] and nonhuman primates.[36] The purpose of this study was to investigate the therapeutic efficacy of LIF in a high-dose, sublethal, primate model of radiation-induced marrow aplasia.

MATERIALS AND METHODS

Animals. Domestic male rhesus monkeys *(Macaca mulatta*; mean weight, 4.3 ± 0.59 kg) were housed in individual stainless steel cages in conventional holding rooms at the Armed Forces Radiobiology Research Institute (AFRRI) in a facility accredited by the American Association for Accreditation of Laboratory Animal Care. Monkeys were provided 10 air changes/h of 100% fresh air conditioned to 72°F ± 2°F with a relative humidity of 50% ± 20% and were maintained on a 12-hour light/dark full-spectrum light cycle with no twilight. Monkeys were provided with commercial primate chow, supplemented with fresh fruit and tap water ad libitum. Research was conducted according to the principles enunciated in the Guide for the Care and Use of Laboratory Animals.[36a]

Recombinant cytokine. The recombinant human LIF was provided by the Cytokine Development Unit of Sandoz Pharmaceuticals Corp (East Hanover, NJ). The nonglycosylated protein was extracted from *Escherichia coli* cells expressing the LIF cDNA from a plasmid vector. The in vitro biologic activity of the recombinant human LIF (rhLIF) was analyzed in a proliferation assay of the DA1 murine leukemia cell line and was approximately 13×10^6 U/mg protein. The units were calculated on the basis that 1 U of LIF was able to induce 50% of maximal proliferation. The endotoxin content was 10.6 EU/mg of LIF as determined by the Limulus assay[37] (Limulus amoebocyte lysate assay; Bio Whittaker, Inc, Walkersville, MD).

Irradiation. After a prehabituation period, each monkey was placed in an aluminum restraining chair and subjected to posterior-to-anterior total-body irradiation from the AFRRI Mark-F TRIGA nuclear reactor. The torso of each monkey was shielded from the intense gamma radiation emitted by placing a 2.5-cm lead shield between the core of the reactor and the exposure position. Each monkey received a pulse of 4.5 Gy (< 500 milliseconds) free-in-air total mixed neutrons and gamma rays with a precision of ±2.5% (%SD, n = 16) and a statistical accuracy of 10%. The neutron dose to the total dose (neutron + gamma) was 0.50% ± 2.3% (%SD, n = 17), with a statistical accuracy of 14%. All exposures were actively monitored by ionization chambers and passively monitored by sulfur activation tablets.

Study design. Each animal was irradiated on day 0 and randomly assigned to receive either LIF (n = 4) or human serum albumin (HSA; n = 5; Miles Inc, Cutter Biological, Elkhart, IN). LIF or HSA were administered as a single, subcutaneous injection at a dosage of 15 μg/kg/day. The dosage and administration route were based on results shown in normal rhesus primates by Mayer et al,[36] in which efficacy at platelet production without toxicity was evident at 10 μg/kg/d for 14 days.

Support. An antibiotic regimen was initiated prophylactically when the white blood cell count was less than 1,000/μL and continued daily until the white blood cell count was greater than 1,000/μL for 3 consecutive days. Gentamicin (Lyphomed, Deerfield, IL; 1.5 mg/kg, twice daily) and rocephin (Roche, Nutley, NJ; 100 mg/kg/d) were administered subcutaneously. Fresh, irradiated (1,500 cGy Co-60) whole blood from a random donor pool (monkeys

From Experimental Hematology, Armed Forces Radiobiology, Research Institute, Bethesda, MD; and the Cytokine Development Unit, Sandoz Pharmaceutical Corp, East Hanover, NJ.

Submitted March 5, 1994; accepted August 1, 1994.

Address reprint requests to Ann M. Farese, MS, Experimental Hematology, Armed Forces Radiobiology Research Institute, 8901 Wisconsin Ave, Bethesda, MD 20889-5603.

The publication costs of this article were defrayed in part by page charge payment. This article must therefore be hereby marked "advertisement" *in accordance with 18 U.S.C. section 1734 solely to indicate this fact.*

0006-4971/94/8411-0003$3.00/0

weighing >10 kg) was administered when the platelet count was less than 30,000/μL and the hematocrit was less than 20%. Whole blood transfusions and antibiotics were required to ensure 100% survival in all control HSA-treated animals (unpublished results).

Hematologic evaluations. Peripheral blood was obtained from the saphenous vein to assay complete blood (Model S Plus II; Coulter Electronics, Hialeah, FL) and differential counts (Wright-Giemsa stain; Ames Automated Slide Stainer, Elkhart, IN). Baseline levels were obtained before irradiation. These parameters were monitored for 60 days after irradiation and the degree of anemia and the durations of neutropenia (absolute neutrophil count <1,000/μL) and thrombocytopenia (platelet count either <30,000 or 20,000/μL) were assessed.

Statistical analysis. The Normal Scores Test was used to make pairwise comparisons of the durations of neutropenia and thrombocytopenia. The test was performed using the software package StatXact (Cytel Software Corp, Cambridge, MA) and exact P values were obtained. The Mann Whitney test was used to evaluate the statistical difference between the nadirs.

RESULTS

Platelet and neutrophil recovery. LIF administration induced recovery of circulating platelets to baseline values, without lessening the nadir, earlier than did HSA treatment (day 22 *v* day 32, respectively; Fig 1A). LIF administration, compared with HSA treatment, also significantly decreased the duration of thrombocytopenia either at a platelet count less than 30,000 or 20,000/μL ($P \leq .05$) to 9 days or 6.3 days *v* 12 days or 10.2 days, respectively (Fig 1A and Table 1). Although neither the duration of neutropenia nor the recovery of neutrophils in the LIF-treated monkeys differed from those in HSA-treated monkeys, the period of absolute neutropenia was modified by LIF administration (Fig 1B and Table 1).

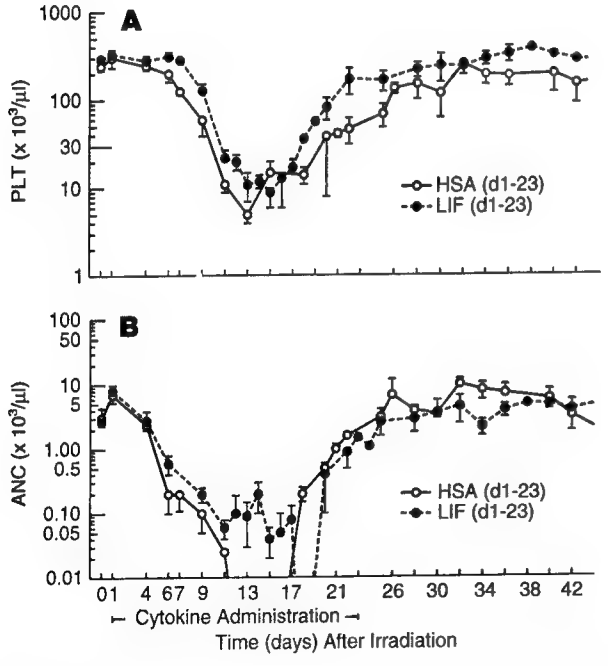

Fig 1. Regeneration of the circulating (A) platelets and (B) neutrophils after sublethal irradiation of rhesus monkeys treated with HSA or LIF. LIF or HSA were administered over a 23-day protocol by subcutaneous injections as described in Materials and Methods. Counts are mean ± SEM.

Table 1. Effect of LIF Therapy in Irradiated Monkeys: Duration and Mean Days of Cytopenia

Treatment	Thrombocytopenia (d) at a Platelet Count of 30,000/μL	Thrombocytopenia (d) at a Platelet Count of 20,000/μL	Neutropenia (d)
HSA	9-20 (12.2)	10-19 (10.2)	5-21 (17.2)
LIF	11-19 (9.25)*	12-17 (6.3)*	5.5-23 (18.5)

Monkeys receiving whole body irradiation with 450 cGy of mixed fission:neutron gamma radiation were treated with control protein (HSA) or LIF according to protocol. Neutropenia is an absolute neutrophil count of less than 1,000/μL. Thrombocytopenia is either a platelet count of less than 20,000 or 30,000/μL.

* $P \leq .05$.

Anemia. LIF did not exacerbate the radiation-induced anemia noted in HSA-treated monkeys (Fig 2). Mean hemoglobin (HGB) values were lower in the HSA-treated monkeys, although there was no significant difference in the respective HGB nadirs. The HGB values in the LIF-treated monkeys returned to within baseline levels more quickly (day 48) than in the HSA-treated monkeys (day 70). All animals did not require transfusions; the HSA-treated animals required an average of two transfusions per animal, whereas the LIF-treated animals received less than one transfusion per animal.

DISCUSSION

We have shown that the therapeutic administration of LIF, as compared with HSA, to sublethally irradiated monkeys can induce an earlier recovery of circulating platelets to normal levels and can signifiantly reduce the duration of thrombocytopenia. The return to normal circulating platelet levels is the result of the apparent increase in production rate of platelets during week 3 of LIF administration. This finding is concordant with results in normal primates receiving LIF[36] in which the onset of platelet production occurred at the end of a 14-day administration period. The number and size of megakaryocytes in the bone marrow of the normal primates did not change. However, recombinant murine LIF administered to normal mice increased both megakaryocyte and progenitor cells in marrow and spleen and resulted in an almost twofold increase in the circulating platelet count.[35]

Using the same radiation model as reported here, we recently described the therapeutic efficacy of IL-3 and IL-6 in promoting platelet and neutrophil production.[25] In our previous report, IL-3 and IL-6 reduced the duration of thrombocytopenia from 12 days in the controls to 6.6 days and 5 days, respectively.[25] IL-3 and IL-6 were used at the same dose (15 μg/kg/d) and protocol as reported here.

The therapeutic efficacy of LIF was suggested by data showing the shared gp130 signal transducing component

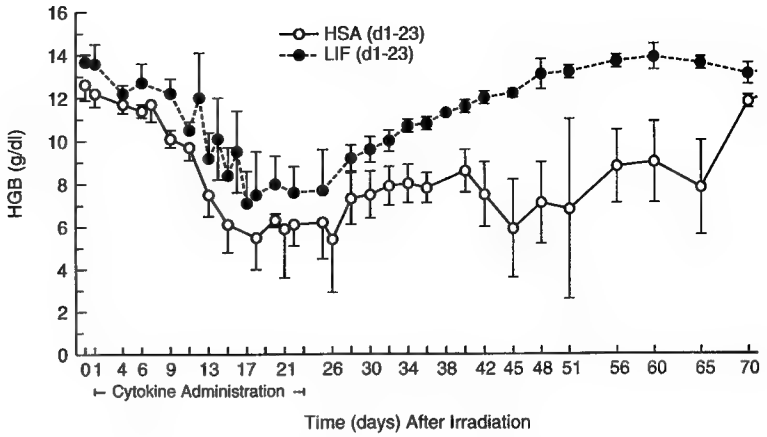

Fig 2. Hemoglobin values in grams per deciliter (mean ± SEM) for rhesus monkeys treated with HSA or LIF. LIF or HSA were administered for 23 consecutive days after sublethal irradiation as described in Materials and Methods.

with IL-6, IL-11, and Oncostatin-M,[38] in addition to in vitro studies with murine and human bone marrow cell cultures.[34,35] Metcalf et al[35] showed that LIF increased megakaryocyte colony formation and megakaryocytes when used in combination with IL-3. LIF alone had no demonstrable direct effect on these parameters despite the presence of LIF receptors on both immature and mature murine megakayocytes. Burstein et al[34] compared LIF with IL-6 and IL-11 and found that LIF promoted megakaryocyte maturation in both liquid murine and human marrow cultures but did not induce an increase in megakaryocyte number in the absence of IL-3. This LIF-induced response did not appear to be facilitated through IL-6 action because the presence of an anti–IL-6 antibody had no influence on the LIF-induced increase in ploidy. However, LIF has been shown to induce synthesis and release of biologically active IL-6 from monocytes.[39] Leary et al[40] also showed that LIF in combination with IL-3 enhanced human marrow-derived blast-cell colony formation.

The lack of an LIF-induced production of neutrophils noted in this model of radiation-induced marrow aplasia agrees with that observed in normal animals. Daily injections of LIF into normal mice[35] or primates[36] had no influence on total and differential leukocyte counts. In a previous study of radiation-induced marrow aplasia in the primate, we showed that neither IL-6 nor IL-3 significantly altered the duration of neutropenia or the recovery of neutrophils but, as currently shown with LIF, did modify the neutropenic nadir, relative to HSA-treated controls.[25]

These results show that LIF may be effective in the treatment of radiation-induced thrombocytopenia. This effect may be mediated in part through the concomitant presence of endogenous IL-3, IL-6, or other complementary cytokines in the postirradiation marrow environment.

ACKNOWLEDGMENT

The authors thank Richard T. Brandenburg, David R. Matlick, and Eloise K. Seams for their superb technical assistance and William Jackson for assistance with statistical analysis.

REFERENCES

1. Kobayashi Y, Okabe T, Urabe A, Suzuki N, Takaku F: Human granulocyte colony-stimulating factor produced by *Escherichia coli* shortens the period of granulocytopenia induced by irradiation in mice. Jpn J Cancer Res 78:763, 1987

2. Monroy RL, Skelly RR, Taylor P, Dubois A, Donahue RE, MacVittie TJ: Recovery from severe hematopoietic suppression using recombinant human granulocyte-macrophage colony-stimulating factor. Exp Hematol 16:344, 1988

3. Tanikawa S, Nakao I, Tsuneoka K, Nara N: Effects of recombinant granulocyte colony-stimulating factor (rG-CSF) and recombinant granulocyte-macrophage colony-stimulating factor (rGM-CSF) on acute radiation hematopoietic injury in mice. Exp Hematol 17:883, 1989

4. MacVittie TJ, Monroy RL, Patchen ML, Souza LM: Therapeutic use of recombinant human G-CSF (rhG-CSF) in a canine model of sublethal and lethal whole-body irradiation. Int J Radiat Biol 57:723, 1990

5. Patchen ML, MacVittie TJ, Solberg B, Souza LM: Therapeutic administration of recombinant human granulocyte colony-stimulating factor accelerates hemopoietic regeneration and enhances survival in a murine model of radiation-induced myelosuppression. Int J Cell Cloning 8:107, 1990

6. Farese AM, Williams DE, Seiler FR, MacVittie TJ: Combination protocols of cytokine therapy with interleukin-3 and granulocyte macrophage-colony stimulating factor in a primate model of radiation-induced marrow aplasia. Blood 82:3012, 1993

7. Brochud MH, Scarffe JH, Thatcher N, Crowther D, Souza LM, Alton NK, Testa NG, Dexter TM: Phase I/II study of recombinant human granulocyte colony-stimulating factor in patients receiving intensive chemotherapy for small cell lung cancer. Br J Cancer 56:809, 1987

8. Antman KS, Griffen JD, Elias A, Socinski MA, Ryan L, Cannistra SA, Oette D, Whitley M, Frie E III, Schnipper LE: Effect of recombinat human granulocyte-macrophage colony-stimulating factor on chemotherapy-induced myelosuppression. N Engl J Med 319:593, 1988

9. Crawford J, Ozer H, Stoller R, Johnson D, Lyman G, Tabbara I, Kris M, Grous J, Picozzi V, Rausch G, Smith R, Gradishar W, Yahanda A, Vincent M, Stewart M, Glaspy J: Reduction by granulocyte colony-stimulating factor of fever and neutropenia induced by chemotherapy in patients with small-cell lung cancer. N Engl J Med 325:164, 1991

10. Williams DE, Dunn JT, Park LS, Frieden EA, Seiler FR, Farese AM, MacVittie TJ: A GM-CSF/IL-3 fusion protein promotes neutrophil and platelet recovery in sublethally irradiated rhesus monkeys. Biotechnol Ther 4:17, 1993

11. Gillio AP, Gasparetto C, Laver J, Abboud M, Bonilla MA, Garnick MB, O'Reilly RJ: Effects of interleukin-3 on hemtopoietic

recovery after 5-fluorouracil or cyclophosphamide treatment of cynomolgus primates. J Clin Invest 85:1560, 1990

12. Winton EF, Srinivasiah J, Kim BK, Hillyer CD, Strobert EA, Orkin JL, Swenson RB, McClure HM, Myers LA, Saral R: Effect of recombinant human interleukin-6 (rhIL-6) and rhIL-3 on hematopoietic regeneration as demonstrated in a nonhuman primate chemotherapy model. Blood 84:65, 1994

13. Gonter PW, Hillyer CD, Strobert EA, Orkin JL, Swenson RB, McClure HM, Myers LA, Winton EF: The effect of varying ratios of administered rhIL-3 and rhGM-CSF on post-chemotherapy marrow regeneration in a nonhuman primate model. Blood 82:365a, 1993 (abstr, suppl 1)

14. Ganser A, Seiplet G, Lindemann A, Ottmann OG, Falk S, Eder M, Herrmann F, Becher R, Höffken K, Büchner T, Klausmann M, Frisch J, Schulz G, Mertelsmann R, Hoelzer D: Effects of recombinant human interleukin-3 in patients with myelodysplastic syndromes. Blood 76:455, 1990

15. Nemunaitis J, Buckner CD, Appelbaum FR, Lilleby K, Wolff S, Bierman P, Kessinger A, Resta D, Campion M, Young DC, Zeigler Z, Rosenfeld C, Shadduck RK, Singer JW: Phase I trial with recombinant human interleukin-3 (rhIL-3) in patients with lymphoid cancer undergoing autologous bone marrow transplantation (ABMT). Blood 80:85a, 1992 (abstr, suppl 1)

16. Biesma B, Pax HB, Willemse PH, Mulder NH, Sleijfer DT, Gietema JA, Mull R, Limburg PC, Bouma J, Vellenga E, de Vries EG: Effects of interleukin-3 after chemotherapy for advanced ovarian cancer. Blood 80:1141, 1992

17. Gerhartz HH, Walther J, Bunica O, Klener P, Visani G, Peschl C, Huber C, Wilmanns W, Mull R, Sklenar I: Clinical-hematological-and cytokine-response to interleukin-3 (IL-3) supported chemotherapy in resistant lymphomas: A phase II study. Proc Am Soc Clin Oncol 11:329, 1992 (abstr)

18. Fibbe WE, Raemaekers J, Verdonck LF, Schouten HC, van Imhof G, Tromp B, Willemze R, van Bree J, Hessels JA, Vellenga E: Human recombinat interleukin-3 after autologous bone marrow transplantation for maligant lymphoma. Ann Oncol 3:163, 1992 (abstr)

19. Laterveer L, van Damme J, Willemze R, Fibbe WE: Continuous infusion of interleukin-6 in sublethally irradiated mice accelerates platelet reconstitution and the recovery of myeloid but not of megakarocytic progenitor cells in bone marrow. Exp Hematol 21:1621, 1993

20. Patchen ML, Fischer R, MacVittie TJ: Effects of combined administration of interleukin-6 and granulocyte colony stimulating factor on recovery from radiation-induced hemopoietic aplasia. Exp Hematol 21:338, 1993

21. Patchen ML, MacVittie TJ, Williams JL, Schwartz GN, Souza LM: Administration of interleukin-6 stimulates multilineage hematopoiesis and accelerates recovery from radiation-induced hematopoietic depression. Blood 77:472, 1991

22. Ishibashi T, Asano S: IL6 and thrombocytopoiesis. Res Immunol 143:752, 1992

23. Burstein SA, Downs T, Friese P, Lynam S, Anderson S, Henthorn J, Epstein RB, Savage K: Thrombocytopoiesis in normal and sublethally irradiated dogs: Response to human interleukin-6. Blood 80:420, 1992

24. Herodin F, Mestries JC, Janodet D, Martin S, Mathieu J, Gascon MP, Pernin MO, Ythier A: Recombinant glycosylated human interluekin-6 accelerates peripheral blood platelet count recovery in radiation-induced bone marrow depression in baboons. Blood 80:688, 1992

25. MacVittie TJ, Farese AM, Patchen ML, Myers LA: Therapeutic efficacy of recombinant interleukin-6 alone and combined with recombinant human interleukin-3 in a nonhuman primate model of high-dose, sublethal, radiation-induced marrow aplasia. Blood 84:2515, 1994

26. Zeidler C, Kanz, L, Hurkuck, F, Rittmann KL, Wildfang I, Kadoya T, Mikayama T, Souza L, Welte K: In vivo effects of interleukin-6 on thrombopoiesis in healthy and irradiated primates. Blood 80:2740, 1992

27. Weber J, Yang JC, Topalian SL, Parkinson DR, Schwartzentruber DS, Ettinghausen SE, Gunn H, Mixon A, Kim H, Cole D, Levin R, Rosenberg SA: Phase I trial of subscutaneous interleukin-6 in patients with advanced malignancies. J Clin Oncol 11:499, 1993

28. Demetri GD, Samuels B, Gordon M, Merica EA, Mazanet R, Antman KH, Hoffman R, Young DC, Samuel S, Bukowski R: Recombinant human interleukin-6 (IL-6) increases circulating platelet counts and C-reactive protein levels in vivo: Initial results of a phase I trial in sarcoma patients with normal hemopoiesis. Blood 80:88a, 1992 (abstr, suppl 1)

29. Leonard JP, Neben TY, Quinto C, Goldman SJ: Recombinant human interleukin-11 (rhIL-11) accelerates pheripheral platelet and RBC recovery following combined sublethal irradiation and carboplatin treatment in mice. Blood 80:91a, 1992 (abstr, suppl 1)

30. Du XX, Neben S, Goldman S, Williams DA: Effects of recombinant interleukin-11 on hematopoietic reconstitution in transplant mice: Acceleration of recovery of peripheral blood neutrophils and platelets. Blood 81:27, 1993

31. Hangoc G, Yin T, Copper S, Schendel P, Yang YC, Broxmeyer HE: In vivo effects of recombinant interleukin-11 on myelopoiesis in mice. Blood 81:965, 1993

32. Neben TY, Loebelenz J, Hayes L, McCarthy K, Stoudemire J, Schaub R, Goldman SJ: Recombinant human interleukin-11 stimulates megakayocytopoiesis and increases peripheral platelets in normal and splenectomized mice. Blood 81:901, 1993

33. Metcalf D, Hilton D, Nicola NA: Leukemia inhibitory factor can potentiate murine megakaryocyte production in vitro. Blood 77:2150, 1991

34. Burstein SA, Mei RL, Henthorn J, Friese P, Turner K: Leukemia inhibitory factor and interleukin-11 promote maturation of murine and human megakaryocytes in vitro. J Cell Physiol 153:305, 1992

35. Metcalf D, Nicola NA, Gearing DP: Effects of injected leukemia inhibitory factor on hemopoietic and other tissues in mice. Blood 76:50, 1990

36. Mayer P, Geissler K, Ward M, Metcalf D: Recombinant human leukemia inhibitory factor induces acute phase proteins and raises the blood platelet counts in nonhuman primates. Blood 81:3226, 1993

36a. The Institute of Laboratory Animal Resources, National Research Council: Guide for the Care and Use of Laboratory Animals. Washington DC, National Institutes of Health publication no. 86-23

37. Levin J, Bang FB: Clottable protein in limulus: Its localization and kinetics of its coagulation by endotoxin. Thromb Diath Haemorrh 19:186, 1968

38. Taga T, Kishimoto T: Cytokine receptors and signal transduction. FASEB J 6:3387, 1992

39. Villiger PM, Geng Y, Lotz M: Induction of cytokine expression by leukemia inhibitory factor. J Clin Invest 91:1575, 1993

40. Leary AG, Wong GG, Clark SC, Smith AG, Ogawa M: Leukemia inhibitory factor differentiation-inhibiting activity/human interleukin for DA cells augments proliferation of human hematopoietic stem cells. Blood 75:1960, 1990

Reprinted from The Neurobiology of NO• and •OH
Volume 738 of the *Annals of the New York Academy of Sciences*
November 17, 1994

Role of Nitric Oxide Synthase, Superoxide Dismutase, and Glutathione Peroxidase in Radiation-Induced Decrease in Norepinephrine Release

S. B. KANDASAMY

Behavioral Sciences Department
Armed Forces Radiobiology Research Institute
Bethesda, Maryland 20889-5603

INTRODUCTION

Although the central nervous system (CNS) is considered to be relatively resistant to the direct effects of ionizing radiation, the dose and the time elapsed after radiation exposure can have a complex effect on the CNS. The hippocampus is important in critical functions such as learning, memory, and motor performance, and these functions are impaired after exposure to ionizing radiation.[1] Noradrenergic systems are important in mediating arousal, food intake, and to some extent motor functions. Histofluorescence and immunohistochemical techniques have shown noradrenergic pathways in the hippocampus.[2] Several factors can contribute to acute nervous system damage *in vivo*: (1) reduced systemic blood pressure following exposure to 25–100 Gy of γ radiation,[3–5] (2) decreased cerebral blood flow in various regions of the brain, including the hippocampus,[3–5] (3) ischemia produced by the decreased blood flow, which is likely to affect neuronal activity;[6] (4) free radical generation with resulting oxygen radicals implicated in cell damage following ischemia; (5) brain ischemia-induced release of an excessive amount of glutamate in the hippocampus, which acts on nitric oxide (NO) synthase to form NO through *N*-methyl-D-aspartate (NMDA) receptors, causing toxic effects.[6]

Antioxidant enzymes, such as superoxide dismutase (SOD), glutathione peroxidase (GSHPx), and catalase, offer protection against ionizing radiation-induced oxidants.[7] Pretreatment with recombinant human interleukin-1α or β (rhIL-1α or β) protects mice from the lethal effects of radiation, and it has been reported that the radioprotectant effect of rhIL-1α or β may involve induction of endogenous manganese SOD (MnSOD).[8] SOD might be a naturally occurring compound with a radioprotective effect[9] because intravenous administration of SOD provoked an increase in SOD level in various tissues of experimental animals and led to enhanced resistance to ionizing radiation.[10,11] Involvement of SOD and GSHPx in the attenuation of radiation-induced hyperthermia by rhIL-1α has also been reported.[12]

Experiments were conducted *in vitro* to determine the effect of exposure to ionizing radiation on hippocampal norepinephrine (NE) release, stimulated by KCl at 0.5, 24, 48, and 72 h after irradiation/sham-irradiation, the role of NO synthase in the radiation-induced decrease in NE release, and the effect of the cyclooxygenase inhibitor indomethacin on radiation-decreased hippocampal NE release. In addition, the effect of rh1L-1β on the levels of GSHPx, the effect of SOD in the hippocampus 48 h after rhIL-1β pretreatment, and the effect of rhIL-1β, SOD, and

GSHPx on decreases in hippocampal NE release 48 h after radiation exposure were determined. This paper reviews work being done in this laboratory.[13,14]

METHODS

Male Sprague-Dawley rats, weighing 200–300 g, were euthanized by decapitation, and the brains were removed. The hippocampus was dissected using the methods of Glowinski and Iversen.[15] NE was measured by high-performance liquid chromatography coupled with electrochemical detection. Hippocampal prostaglandin E_2 (PGE_2) levels were measured by radioimmunoassay. Release of hippocampal NE *in vitro* was stimulated by KCl, and irradiation procedures were carried out as described previously.[16] Rats were exposed bilaterally to varying doses of γ rays, using a ^{60}Co source at a dose rate of 10 Gy/min. SOD and GSHPx in the hippocampus was measured as described by Kandasamy *et al.*[12] Statistical analysis was performed using

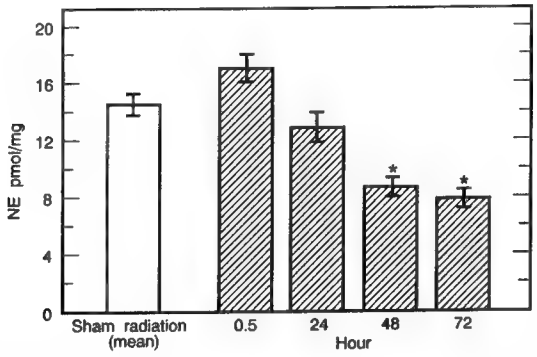

FIGURE 1. NE release 0.5, 24, 48, and 72 hr after exposure to 10 Gy gamma rays. Values are means ± SEM of three separate experiments. *significantly different from sham radiation; $p < 0.05$.

Student's *t*-test. Multiple comparisons with sham-irradiated/irradiated values were done by analysis of variance and Dunnett's test. Data were identified as significant if $P < 0.05$.

RESULTS

There was no significant difference in NE release between irradiated and sham-irradiated rats when the hippocampal NE concentration was determined 0.5 h after radiation exposure (5–30 Gy at 10 Gy/min). However, there were significant decreases in hippocampal NE release 48 and 72 h after exposure to 5 (data not shown) and 10 Gy (FIG. 1) and 24, 48, and 72 h after exposure to 30 Gy of γ rays (FIG. 2). Based on the above data, a postirradiation time period of 48 h and a γ-radiation dose of 10 Gy at 10 Gy/min were chosen for further studies with the NO synthase inhibitor ^{6}N-nitro-L-arginine (NO_2-arg) and the cyclooxygenase inhibitor indomethacin. Pretreating rats with 1 mg/kg of NO_2-arg administered i.p. 1 h before irradiation

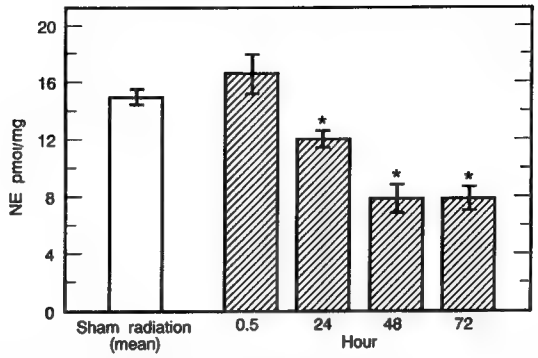

FIGURE 2. NE release 0.5, 24, 48, and 72 hr after exposure to 30 Gy gamma rays. Values are means ± SEM of three separate experiments. *Significantly different from sham radiation; $p < 0.05$.

or sham-irradiation had no effect on the radiation-decreased NE release (data not shown). However, 3 mg/kg of NO_2-arg prevented the radiation-decreased NE release (FIG. 3); 5 mg/kg (FIG. 4) and 10 mg/kg (data not shown) NO_2-arg not only prevented the decrease in NE release in irradiated rats but also enhanced NE release in sham-irradiated rats (FIG. 4). Pretreatment with 1–3 mg/kg of indomethacin i.p. 1 h before irradiation or sham-irradiation did not prevent radiation-decreased NE release and had no effect on sham-irradiated NE release (data not shown). In addition, i.p. pretreatment with 5–20 mg/kg of NO_2-arg did not inhibit rhIL-1β-induced PGE_2 levels (data not shown).

When 10 μg/kg of rhIL-1β was administered i.p. 48 h before sham irradiation, it increased hippocampal levels of total and selenium-dependent GSHPx (FIG. 5) and had no effect on SOD (FIG. 6) and NE release (FIG. 7). Radiation exposure decreased hippocampal NE release (FIGS. 5, 8, and 9), decreased hippocampal levels of total and selenium-dependent GSHPx (FIG. 6), and had no effect on hippocampal SOD (FIG. 7). However, rhIL-1β pretreatment prevented radiation-decreased NE

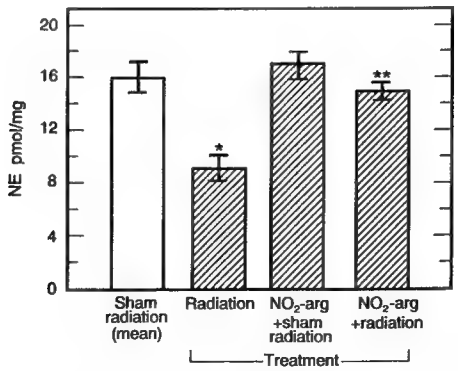

FIGURE 3. Effect of pretreatment with 3 mg/kg NO_2-arg i.p. 1 hr before radiation (10 Gy). Values are means ± SEM of three separate experiments. *Significantly different from sham radiation; $p < 0.05$. **Significantly different from radiation; $p < 0.05$.

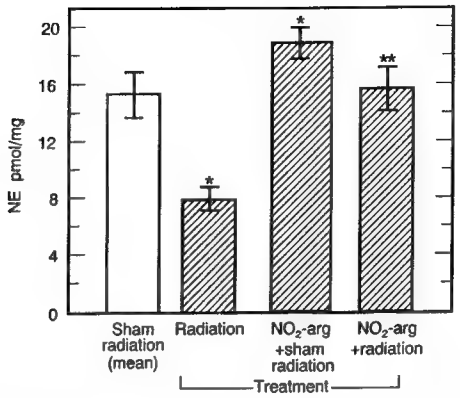

FIGURE 4. Effect of pretreatment with 5 mg/kg NO_2-arg i.p. 1 hr before irradiation (10 Gy). Values are means ± SEM of three separate experiments. *Significantly different from sham radiation; $p < 0.05$. **Significantly different from radiation; $p < 0.05$.

release (FIG. 5), increased hippocampal SOD (FIG. 7), and prevented the fall in total and selenium-dependent GSHPx (FIG. 6). In addition, *in vitro* administration of 10 or 30 μg of SOD and 1 or 3 units of GSHPx prevented the radiation-decreased NE release (FIGS. 8 and 9).

DISCUSSION

These experiments demonstrate that radiation had no effect on hippocampal NE release 0.5 h after exposure but decreased NE release 24, 48, and 72 h after exposure, depending on the radiation dose. At the present time we have no data to explain the

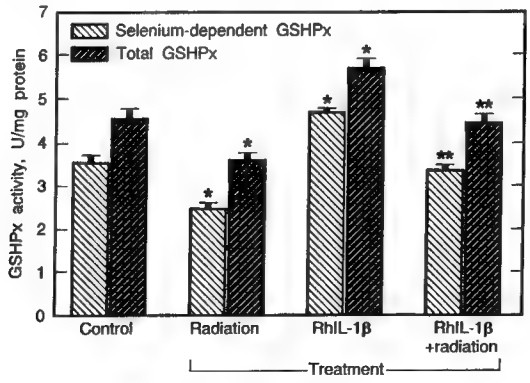

FIGURE 5. Effects of 48-h pretreatment with 10 μg/kg of rhIL-1β alone, in combination with 10 Gy of radiation, and radiation alone on hippocampal selenium-dependent and total GSHPx levels. *Significantly different from control value; $p < 0.05$. **Significantly different from irradiated value; $p < 0.05$.

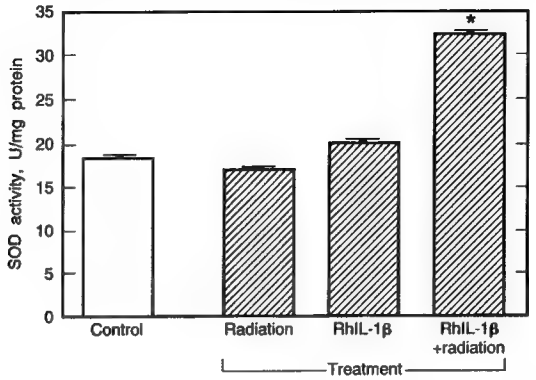

FIGURE 6. Effects of 48-h pretreatment with 10 μg/kg of rhIL-1β alone, in combination with 10 Gy of radiation, and radiation alone on hippocampal SOD levels. *Significantly different from irradiated value; $p < 0.05$.

differences in NE release at postirradiation time intervals. However, it has been suggested that the blood–brain barrier could be disrupted by ionizing radiation[17] and would allow radiation-released neurotransmitters, such as prostaglandins (PGs), histamine, serotonin, and other circulating factors, (abnormal) access to neurons that modulate hippocampal NE release.[18] It has been shown that prostaglandins of the E series inhibit the release of NE from sympathetic nerves in the CNS and in the periphery; conversely, inhibition of prostaglandin synthesis leads to an increase in NE release.[19] The failure of indomethacin to prevent radiation-decreased hippocampal NE release and the failure of NO_2-arg to inhibit rhIL-1β-induced PGE_2 levels suggest that the enhancement of NE release by NO_2-arg in the hippocampus is not due to inhibition of PGE_2 synthesis.

Immunochemical localization of NO synthase has been demonstrated in most areas of the rat brain, including the hippocampus. NO synthase forms NO from

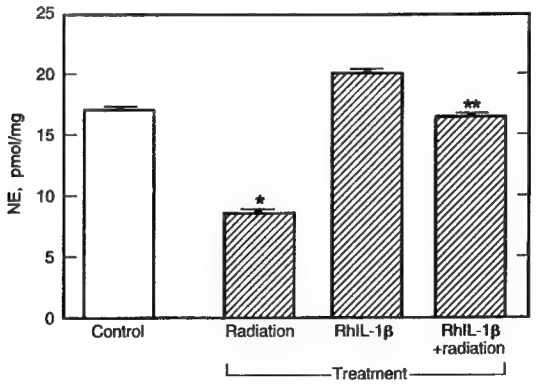

FIGURE 7. Effects of 48-h pretreatment with 10 μg/kg of rhIL-1β alone, in combination with 10 Gy of radiation, and radiation alone on NE release in the hippocampus. *Significantly different from control value; $p < 0.05$. **Significantly different from irradiated value; $p < 0.05$.

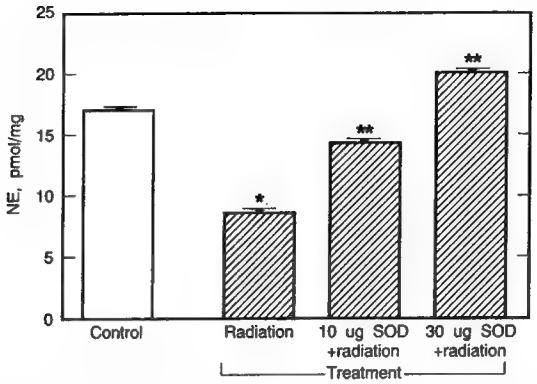

FIGURE 8. Effects of *in vitro* administration of SOD on radiation-decreased NE 48 h after exposure to 10 Gy of radiation. *Significantly different from control value; $p < 0.05$. **Significantly different from irradiated value; $p < 0.05$.

l-arginine.[6] Potential functions of NO have been elucidated using NOS inhibitors, which are derivatives of arginine. Many studies have used L-N^G-monomethyl arginine (Me-arg), which is converted into arginine in several tissues and confounds interpretations. NO_2-arg is more potent than Me-arg and does not appear to undergo extensive metabolism.[20] NO_2-arg is a competitive inhibitor of NOS, and it inhibits NOS activity irreversibly in the brain after systemic administration.[21] Pretreatment with NO_2-arg reversed the radiation-decreased NE release, suggesting that NO synthase is involved in this phenomenon. Pretreatment with NO_2-arg also enhanced NE release in sham-irradiated rats, suggesting that NO is involved in the regulation of NE under normal conditions.

As one of a special class of hormones called cytokines, rhIL-1β is a polypeptide of approximately 17.5 kDa. This polypeptide is synthesized and released by activated monocytes and macrophages to produce a number of effects, including stimulating

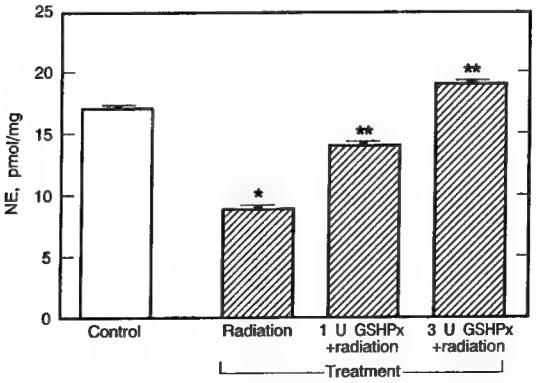

FIGURE 9. Effects of *in vitro* administration of GSHPx on radiation-decreased NE release 48 h after exposure to 10 Gy of radiation. *Significantly different from control value; $p < 0.05$. **Significantly different from irradiated value; $p < 0.05$.

hepatocytes to elaborate acute phase proteins, secreting interleukin-2 (IL-2) and other lymphokines from T-cells, and producing fever by affecting thermosensitive neurons within the hypothalamic preoptic nucleus.[22] In addition, after systemic or intracerebroventricular administration, rhIL-1β has shown a number of other central actions, including stimulating corticotropin-releasing hormone secretion,[23] suppressing food intake,[24] inducing slow wave sleep,[25] inducing analgesia,[26] and acting as an astroglial growth factor. Using immunocytochemical techniques, Lechan *et al.*[27] have demonstrated the use of rhIL-1β in regions of the rat CNS involved with hypophysiotropic, autonomic, limbic, and extrapyramidal functions. A radioligand binding study has shown that rhIL-1β receptors are widely distributed throughout the brain, especially in neuron-rich sites such as the granule cell layer of the dentate gyrus, the pyramidal cell layer of the hippocampus, and the granule cell layer of the cerebellum, as well as in the hypothalamus.[28] Although rhIL-1β cannot penetrate the blood–brain barrier, it exerts its central effects by entering the brain through the organum vasculosum of lamina terminalis,[29] a hypothalamic area that lacks the blood–brain barrier.

Considering the role of free radicals in radiation injury, it is apparent that mechanisms of protection involve detoxification of radicals produced by radiation.[30] Protectors of this type include xenobiotic scavengers of free radicals and inducible endogenous antioxidant defense mechanisms such as antioxidant enzymes.[31,32] Cell damage induced by superoxide radicals and related oxygen species, such as singlet oxygen and hydroxyl radicals, has recently been tentatively connected with the etiology of a number of pathological conditions in the brain.[33–36] Enzymatic defense against activated oxygen species involves a cooperative action of several enzymes. The major defense against toxicity of superoxide radicals is conferred by SOD. This enzyme catalyzes the dismutation of superoxide radicals to hydrogen peroxide and oxygen. Although the resulting hydrogen peroxide is relatively less toxic (scavenged by catalase and GSHPx), a highly toxic hydroxyl radical is produced when hydrogen peroxide reacts with superoxide or with transition metals such as iron or copper. Therefore, catalase and GSHPx, which scavenge hydrogen peroxide, act in concert with SOD.[37]

Lipton *et al.*[38] reported that congeners of NO are either neuroprotective or neurodestructive. NO can exist in distinct oxidation-reduction states that have very different biological actions. Indeed, the designation "nitric oxide" should be restricted to the reduced NO· form of the molecule, the parent NO should be called "nitrogen monoxide," and the oxidized form NO^+, "nitrosonium ion." Lipton *et al.*[38] present evidence that the neurotoxic action of NO· derived from the NO form of the molecule, which reacts with superoxide anion to form peroxynitrite, is probably the final neurotoxic agent. On the other hand, NO in the form of the NO^+ reacts with the thiol group of the NMDA receptor to block glutamate neurotransmission. In other words, conditions favoring NO· give rise to neurotoxicity, whereas neuroprotective effects occur in the presence of NO^+.

These studies demonstrate that rhIL-1β and irradiation together increased the hippocampal SOD level and prevented the fall in the GSHPx level. In addition, with rhIL-1β pretreatment, SOD and GSHPx prevented the radiation-decreased NE release. Induction of MnSOD messenger RNA by IL-1α, IL-1β, lipopolysaccharide, and tumor necrosis factor have been reported.[39–41] Although no results are currently available on the measurement of glutamate release in the hippocampus following exposure to radiation, our results support the hypothesis that toxic overstimulation of glutamate receptors by radiation or excitotoxicity contributes to overproduction of NO that can be toxic to neurons. NO freely diffuses to adjacent target neurons where it combines with the superoxide anion (O_{2-}) produced by radiation to yield the

peroxynitrite anion ($ONOO^-$), which may cause cell death.[42] It has been reported that SOD attenuates $ONOO^-$-induced neurotoxicity.[43] Although the mechanisms involved in prevention of radiation-decreased NE release in the hippocampus by rhIL-1β is unknown at the present time, it has been suggested that some of the mechanisms may be (a) increased production of antioxidant enzymes by rhIL-1β that scavenge free radicals generated by radiation, and (b) prevention of the formation of NO while enhancing the formation of NO^+. Work is in progress to determine the effect of the corticotropin-releasing hormone, which is stimulated by rhIL-1β, on radiation-decreased NE release and antioxidant enzyme levels.

CONCLUSION

These results suggest that ionizing radiation decreased hippocampal NE release 24, 48, and 72 h after exposure, and NO synthase is implicated in this radiation-decreased NE release. In addition, the prevention of radiation-decreased NE release in the hippocampus by rhIL-1β involves SOD and GSHPx.

REFERENCES

1. KIMELDORF, D. J. & E. L. HUNT. 1965. Neurophysiological effects of ionizing radiation. *In* Ionizing Radiation: Neural Function and Behavior, D. J. Kimeldorf and E. L. Hunt, Eds.: 59–108. Academic Press. New York.
2. HEAL, D. J. 1990. The effects of drugs on behavioural models of central noradrenergic function. *In* The Pharmacology of Noradrenaline in the Central Nervous System, D. J. Heal and C. A. Marsden, Eds.: 266–315. Oxford Univ. Press. New York.
3. CHAPMAN, P. H. & R. J. YOUNG. 1968. Effect of cobalt-60 gamma irradiation on blood pressure and cerebral blood flow in the *Macaca mulatta*. Radiat. Res. **35:** 78–85.
4. COCKERHAM, L. G., T. J. CERVENY & J. D. HAMPTON. 1986. Postradiation regional cerebral blood flow in primates. Aviat. Space Environ. Med. **57:** 578–582.
5. COCKERHAM, L. G., T. F. DOYLE, M. A. DONLON & E. A. HELGESON. 1984. Canine postradiation histamine levels and subsequent response to Compound 48/80. Aviat. Space Environ. Med. **55:** 1041–1045.
6. SNYDER, S. H. & D. S. BREDT. 1991. Nitric oxide as a neuronal messenger. Trends Pharmacol. Sci. **12:** 125–128.
7. HALL, E. J. 1988. The physics and chemistry of radiation absorption. *In* Radiobiology for the Radiologist, 3rd ed., E. J. Hall, Ed.: 1–16. Lippinocott. Philadelphia.
8. KUMAR, K. S., Y. N. VAISHNAV, C. SMITH & E. P. CLARK. 1992. Radiation injury and antioxidant mechanisms of protection. *In* Eicosanoids and Other Bioactive Lipids in Cancer, Inflammation and Radiation Injury, S. Nigam, K. V. Honn, L. J. Marnett, and T. L. Walden, Jr., Eds.: 333–339. Kluwer. Boston.
9. BARTOSZ, G., W. LEYKO & R. FRIED. 1979. Is superoxide dismutase a physiological radioprotector? Experientia **35:** 1194.
10. PETKAU, A. 1978. Radiation protection by superoxide dismutase. Photochem. Photobiol. **28:** 765–774.
11. PETKAU, A., S. CHELACK & S. D. PLESKACH. 1978. Protection by superoxide dismutase of white blood cells in x-irradiated mice. Life Sci. **22:** 867–882.
12. KANDASAMY, S. B., K. S. KUMAR & A. H. HARRIS. 1992. Involvement of superoxide dismutase and glutathione peroxidase in attenuation of radiation-induced hyperthermia by interleukin-1α in rats. Brain Res. **606:** 106–110.
13. KANDASAMY, S. B., S. A. STEVENS-BLAKELY, T. K. DALTON & A. H. HARRIS. 1992. Implication of nitric oxide synthase in radiation-induced decrease in hippocampal noradrenaline release in rats. *In* The Biology of Nitric Oxide, S. Moncada, M. A. Marletta, J. B. Hibbs, Jr., and E. A. Higgs, Eds.: 252–254. Portland Press. London.

14. KANDASAMY, S. B., T. K. DALTON & A. H. HARRIS. 1993. Effect of interleukin-1β on nitric oxide synthase-mediated decreases in hippocampal norepinephrine release in rats. Proceedings of the Third International Meeting on the Biology of Nitric Oxide (Cologne, Germany, Oct. 2–Oct. 5, 1993). In press.
15. GLOWINSKI, J. & L. L. IVERSEN. 1966. Regional studies of catecholamines in the rat brain. Int. J. Neurochem. **13:** 655–669.
16. JOSEPH, J. A., S. B. KANDASAMY, W. A. HUNT, T. K. DALTON & S. STEVENS. 1987. Radiation-induced increases in sensitivity of cataleptic behavior to haloperidol: Possible involvement of prostaglandins. Pharmacol. Biochem. Behav. **29:** 335–341.
17. NAIR, V. & L. J. ROTH. 1964. Effect of x-irradiation and certain other treatments on blood brain barrier permeability. Radiat. Res. **23:** 249–264.
18. KANDASAMY, S. B. & W. A. HUNT. 1990. Involvement of prostaglandins and histamine in radiation-induced temperature responses in rats. Radiat. Res. **121:** 8490.
19. BERGSTROM, S., L. O. FARNEBO & K. FUXE. 1973. Effect of prostaglandin E_2 on central and peripheral catecholamine neurons. Eur. J. Pharmacol. **21:** 362–368.
20. HECKER, M., J. A. MITCHELL, H. J. HARRIS, M. KATSURA, C. THIEMERMANN & J. R. VANE. 1990. Endothelial cells metabolize N^G-monomethyl-L-arginine to L-citruline and subsequently to L-arginine. Biochem. Biophys. Res. Commun. **167:** 1037–1043.
21. DWYER, M. A., D. S. BREDT & S. H. SNYDER. 1991. Nitric oxide synthase: Irreversible inhibition by L-N^G-nitroarginine in brain *in vitro* and *in vivo*. Biochem. Biophys. Res. Commun. **176:** 1136–1141.
22. COCEANI, F., J. LEES & C. A. DINARELLO. 1988. Occurrence of interleukin-1 in cerebrospinal fluid of the conscious cat. Brain Res. **446:** 245–250.
23. BERKENBOSCH, F., J. VAN OERS, A. DEL REY, F. TILDERS & H. BESEDOVSKY. 1987. Corticotropin-releasing factor-producing neurons in the rat activated by interleukin-1. Science **128:** 524–526.
24. PLATA-SALAMAN, C. R., Y. OOMURA & Y. KAI. 1988. Tumor necrosis factor and interleukin-1β: Suppression of food intake by direct action in the central nervous system. Brain Res. **448:** 106–114.
25. KRUEGER, J. M., J. WALTER, C. A. DINARELLO, S. M. WOLFF & L. CHEDID. 1984. Sleep promoting effects of endogenous pyrogen (interleukin-1). Am. J. Physiol. **246**: R994–R999.
26. NAKAMURA, H., K. NAKANISHI, A. KITA & T. KADOKAWA. 1988. Interleukin-1 induces analgesia in mice by a central action. Eur. J. Pharmacol. **149:** 49–54.
27. LECHAN, R. M., R. TONI, B. D. CLARK, J. G. CANNON, A. R. SHAW, C. A. DINARELLO & S. REICHLIN. 1990. Immunoreactive interleukin-1β localization in the rat forebrain. Brain Res. **514:** 135–140.
28. FARRAR, W. L., J. M. HILL, A. HAREL-BELLAN & M. VINOCOUR. 1987. The immunological brain. Immunol. Rev. **100:** 361–378.
29. KATSUURA, G., A. ARIMURA, K. KOVES & P. E. GOTTSCHALL. 1990. Involvement of organum vasculosum of lamina terminalis and preoptic area in interleukin-1β-induced ACTH release. Am. J. Physiol. **258:** E163–E171.
30. KUMAR, K. S., Y. N. VAISHNAV & J. F. WEISS. 1988. Radioprotection by antioxidant enzymes and enzyme mimetics. Pharmacol. Ther. **39:** 301–309.
31. BIAGLOW, J. E., M. E. VARNES, E. R. EPP, E. P. CLARK & M. ASTOR. 1986. Redox enzymes and thiol radicals. *In* Oxygen and Sulfur Radicals in Chemistry and Medicine, A. Breccia, M. A. J. Rodgers, and G. Semerano, Eds.: 89–102. Lo Scarabeo. Italy.
32. CHAPMAN, J. D., A. P. REUVERS, J. BORSA & C. L. GREENSTOCK. 1973. Chemical radioprotection and radiosensitization of mammalian cells growing in vitro. Radiat. Res. **56:** 291–306.
33. CADET, J. B., J. B. LOHR & D. V. JESTE. 1986. Free radicals and tardive dyskinesia. Trends Neurosci. **9:** 108–109.
34. DEXTER, D. T., C. J. CARTER, F. R. WELLS, F. JAVOY-AGID, Y. AGID, A. LEES, P. JENNER & C. D. MARSDEN. 1991. Basal lipid peroxidation in substantia nigra is increased in Parkinson's disease. J. Neurochem. **52:** 381–389.
35. HALLWELL, B. & J. M. GUTTERIDGE. 1985. Oxygen radicals and the nervous system. Trends Neurosci. **5:** 22–26.

36. SAGGU, H., J. COOKSEY, D. DEXTER, F. R. WELLS, A. LEES, P. JENNER & C. D. MARSDEN. 1989. A selective increase in particulate superoxide dismutase activity in parkinsonian substantia nigra. J. Neurochem. **53:** 692–697.
37. WEISS, J. F. & K. S. KUMAR. 1988. Antioxidant mechanisms in radiation injury and radioprotection. *In* Cellular Antioxidant Defense Mechanisms, Vol II, C. K. Chow, Ed.: 163–189. CRC Press. Boca Raton, Fla.
38. LIPTON, S. A., Y. CHOL, Z. PAN, S. Z. LEL, H. V. CHEN, N. J. SUCHER, J. LOSCALZO, D. J. SINGEL & J. S. STAMLER. 1993. A redox-based mechanism for the neuroprotective and neurodestructive effects of nitric oxide and related nitroso-compounds. Nature **364:** 626–632.
39. WONG, G. H. W. & D. V. GOEDDEL. 1988. Induction of manganese superoxide dismutase by tumor necrosis factor: Possible protective mechanism. Science **242:** 941–944.
40. MASUDA, A., D. L. LONGO, Y. KOBAYASHI, E. APPELLA, J. J. OPPENHEIM & K. MATSUSHIMA. 1988. Induction of mitochondrial manganese superoxide dismutase by interleukin 1. FASEB. **2:** 3087–3091.
41. VISNER, G. A., W. C. DOUGALL, J. M. WILSON, I. A. BURR & H. S. NICK. 1989. Regulation of manganese superoxide dismutase by lipopolysaccharide, interleukin-1 and tumor necrosis factor. J. Biol. Chem. **265:** 2856–2864.
42. BECKMAN, J. S., T. W. BECKMAN, J. CHEN, P. A. MARSHALL & B. A. FREEMAN. 1990. Apparent hydroxyl radical production by peroxynitrite: Implications for endothelial injury from nitric oxide and superoxide. Proc. Natl. Acad. Sci. U.S.A. **87:** 1620–1624.
43. RADI, R., J. S. BECKMAN, K. M. BUSH & B. A. FREEMAN. 1991. Peroxynitrite oxidation of sulfhydryls. The cytotoxic potential of superoxide and nitric oxide. J. Biol. Chem. **266:** 4244–4250.

IL-12 Protects Bone Marrow from and Sensitizes Intestinal Tract to Ionizing Radiation[1]

Ruth Neta,[2]* Steve M. Stiefel,* Fred Finkelman,† Steven Herrmann,‡ and Nasima Ali*

*Department of Experimental Hematology, Armed Forces Radiobiology Research Institute, Bethesda, MD 20889; †Department of Medicine, Uniformed Services University for Health Sciences, Bethesda, MD 20889; and ‡Cellular Immunology, Genetics Institute, Cambridge, MA 02140

IL-12, a potent stimulator of hemopoietic progenitor cells, was evaluated as a potential protector against ^{60}Co-gamma radiation-induced lethal hemopoietic syndrome in mice. Administration of IL-12 before lethal irradiation of genetically distinct strains of mice, B6D2F$_1$ and C3H/HeJ, protected a significant fraction of both strains of mice from death. Radioprotection was associated with a fivefold increase in the number of bone marrow cells at 6 days after irradiation. Even at supralethal doses of radiation (1200 cGy), the number of c-*kit*$^+$ bone marrow cells 3 days after irradiation was twofold greater in IL-12-treated mice than in saline-treated mice. However, mice that received IL-12 and 1200 cGy (B6D2F$_1$) or 900 cGy (C3H/HeJ) died of the gastrointestinal syndrome, as was evident by gross necroscopy and histologic evaluation, within 4 to 6 days after irradiation. Induction of the gastrointestinal syndrome in mice not treated with IL-12 required radiation doses of 1500 cGy or greater in both strains. Thus, at doses of radiation at which IL-12 still protects c-*kit*$^+$ hemopoietic cells, it sensitizes the intestinal tract to damage. Radioprotection with IL-12 was abrogated by anti-IL-1R or anti-stem cell factor Ab. Anti-IFN-γ Ab did not affect IL-12-induced hemopoietic radioprotection, but abrogated sensitization of the intestinal tract by IL-12. The sensitizing effect of IL-12 may be related to its ability to prime mice to subsequent inflammatory challenge, as demonstrated by an almost 100-fold increase in circulating TNF and IL-6 levels in normal B6D2F$_1$ mice challenged with IL-12 and LPS. This priming effect of IL-12 also was abrogated by anti-IFN-γ Ab. *The Journal of Immunology,* 1994, 153: 4230.

Exposure to ionizing radiation can lead to three distinct modes of death, depending on the magnitude of the dose of radiation. At very high doses, in excess of 100 Gy, death that results from neurologic and cardiovascular breakdown occurs within 1 h and is referred to as the cerebrovascular syndrome (1, 2). At intermediate doses of radiation in mice, usually exceeding 15 Gy, death occurs in a matter of days (4 to 6), is associated with the destruction of gastrointestinal (GI)[3] tissue, and is referred to as the GI syndrome (1, 2). At lower doses of radiation, ranging from 7 to 15 Gy (depending on the strain of mice), death occurs within 1 to 4 wk, is ascribed to hemopoietic failure, and, therefore, is referred to as the hemopoietic syndrome (3).

Administration of the cytokines IL-1, stem cell factor (SCF), and TNF before irradiation protects mice from death as a result of the hemopoietic syndrome (4–6). Abs to any one of these three cytokines abrogate LPS-induced radioprotection and render untreated mice more sensitive to radiation lethality (7–9). This finding indicates that endogenous production of these three cytokines in untreated mice and in mice that are radioprotected with LPS is the basis for radioprotection. Furthermore, radioprotection with IL-1 is abrogated by anti-SCF Ab, and radioprotection with SCF is reduced by anti-IL-1R Ab, which suggests that radioprotection with either cytokine requires interaction with the other (10, 11). Consistent with this

Received for publication May 24, 1994. Accepted for publication August 4, 1994.

The costs of publication of this article were defrayed in part by the payment of page charges. This article must therefore be hereby marked *advertisement* in accordance with 18 U.S.C. Section 1734 solely to indicate this fact.

[1] This work was supported by the Armed Forces Radiobiology Research Institute, Defense Nuclear Agency, under Research Work Unit 00129 and by the Office of the Naval Research and Development Contract N000759WR00024. The opinions contained herein are the private views of the author; no endorsement by the Defense Nuclear Agency has been given or should be inferred. The research was conducted according to the principles enunciated in the "Guide for the Care and Use of Laboratory Animals" prepared by the Institute of Laboratory Animal Resources, National Research Council.

[2] Address correspondence and reprint requests to Dr. Ruth Neta, Department of Experimental Hematology, Armed Forces Radiobiology Research Institute (AFRRI), Building 42, 8901 Wisconsin Avenue, Bethesda, MD 20889 -5603.

[3] Abbreviations used in this paper: GI, gastrointestinal; BM, bone marrow; BMC, bone marrow cells; SCF, stem cell factor; PE, phycoerythrin.

0022-1767/94/$02.00

requirement for interaction of IL-1, SCF, and TNF in radioprotection, combined administration of IL-1 and TNF or IL-1 and SCF results in synergistic radioprotection (5, 10, 11).

IL-12 is a newly identified cytokine produced by monocytes/macrophages and lymphocytes after challenge with bacteria or their products (12). Originally identified as NK cell stimulatory factor (13, 14), IL-12 has been recognized to play a role in the generation of Th1 cells from Th0 cells (14–16). More recently, IL-12 has been implicated as a hemopoietic cytokine on the basis of its ability to synergize with hemopoietic growth factors to increase the number and the size of hemopoietic colonies (17–19). Because of the ability of IL-12 to promote the growth of hemopoietic progenitor cells, we have evaluated IL-12 for its ability to protect from lethal irradiation.

Materials and Methods

Mice

$B6D2F_1$ and C3H/HeJ female mice, 8 to 10 wks old, were purchased from The Jackson Laboratory (Bar Harbor, ME). Mice were handled as described previously (5). All animal use protocols were approved by the Institutional Animal Use and Care Committee, Armed Forces Radiobiology Research Institute (AFRRI).

Abs

Rat monoclonal IgG1 anti-murine IL-1R Ab (35F5) and anti-murine IL-6 (20F3) were generous gifts from Dr. Richard Chizzonite (Hoffmann-La Roche, Nutley, NJ) and Dr. John Abrams (DNAX, Palo Alto, CA), respectively (20, 21). A rat IgG1 mAb to β-galactosidase (GL113) was used as a control. Anti-murine TNF (TN3.19.12.) was a generous gift from Dr. Robert Schreiber (Washington University, St. Louis, MO) (22). Rat IgG1 anti-IFN-γ mAb (XMG-6) was purified from ascites by $(NH_4)_2SO_4$ precipitation and DE-52 ion-exchange chromatography. A polyclonal rabbit anti-murine SCF Ab was generously provided by Dr. Douglas Williams (Immunex, Seattle, WA), along with rabbit preimmune control serum. Chromatographically purified rat IgG (Sigma Chemical Co., St. Louis, MO) was used as an additional control. R-phycoerythrin (R-PE)-conjugated rat anti-mouse c-*kit* mAb 3C1 (IgG2b) and PE-conjugated rat IgG2b (control) were purchased from PharMingen (San Diego, CA).

Treatment

Murine rIL-12 (batch MRB 021693–1.2, bioactivity of 5.6×10^6 U/mg) was provided by Genetics Institute (Cambridge, MA) and human IL-1 (rhuIL-1α 117–271 Ro 24–5008 lot IL 1 2/88, activity 3×10^8 U/mg) was kindly provided by Dr. Peter Lomedico, (Hoffmann-La Roche). The Abs and recombinant cytokines were diluted in pyrogen-free saline on the day of injection. Abs or control Ig were given i.p. 6 to 20 h before i.p. injection of cytokines. In experiments in which TNF and IL-6 in the serum were assessed, mice were challenged with 5 μg/mouse of LPS.

Irradiation

Mice were randomized, placed in ventilated Plexiglass containers, and bilaterally irradiated by using the AFRRI ^{60}Co whole body irradiator as described (11). The number of surviving mice was recorded daily for 30 day.

FACS analysis

Bone marrow cells (BMC) were obtained by flushing femurs into RPMI medium that contained 5% FCS. After being washed, cells were counted and resuspended in Dulbecco's PBS with 2% FCS at the concentration of 2×10^6/ml. Cells were stained for 30 min with 10 μg/ml of either PE-conjugated, anti-murine c-*kit* Ab (3C1) or PE-conjugated, control IgG2b. The cells were washed twice and resuspended in 1 ml of 2% FCS and Dulbecco's PBS. The percentage of c-*kit*$^+$ cells was calculated by subtracting the percentage of cells stained with control Ab from the percentage of cells stained with c-*kit* Ab.

Immunofluorescence analysis was performed with an EPICS ELITE flow cytometer (Coulter Electronics, Miami, FL) by using logarithmic amplification. RBCs, platelets, and debris were excluded from the analysis on the basis of light scatter criteria. Twenty-five thousand cells were counted for each histogram.

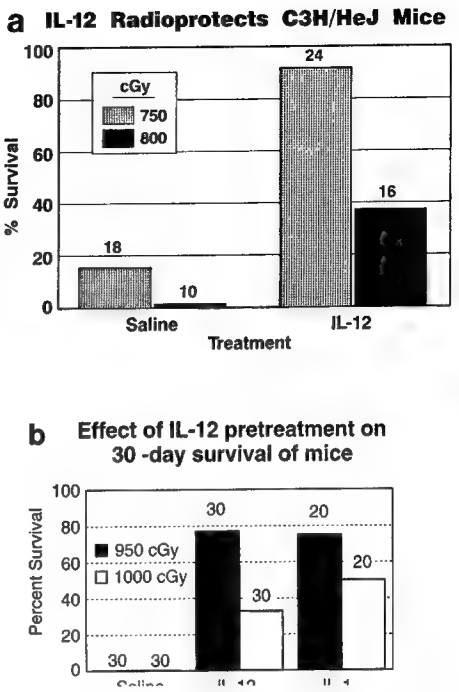

FIGURE 1. Radioprotective effect of IL-12 in mice. C3H/HeJ (*a*) and $B6D2F_1$ (*b*) mice received 1 μg/mouse of IL-12, IL-1, or saline injections and, 18 h later, were irradiated with the indicated doses. The results are presented as the percentage of survival 30 days after irradiation. The numbers above the bars represent the total number of mice in each experimental group.

TNF and IL-6 assays

TNF cytotoxicity in the sera was assessed on L-929 fibroblasts plated in 96-well, flat-bottom microtiter plates. After 24-h incubation of 4×10^4 L cells/well to establish confluent monolayers, twofold serial dilutions (in duplicates) of each test serum were added to wells in the presence of actinomycin D (1 μg/ml). That the cytotoxic effect was indeed caused by TNF was confirmed by simultaneous addition of anti-TNF Ab (TN3, 12.19) to serum samples. After 20-h incubation, the plates were washed and stained with 0.05% crystal violet in 20% ethanol. The standard, human rTNF (kindly provided by Dr. Grace Wong, Genentech, San Francisco, CA), was included in each assay, with 1 U being equivalent to a concentration lysing 50% of the cells and ranging from 1.9 to 3.8 pg/U in different assays. IL-6 was quantified by using a murine IL-6 ELISA from Endogen (Boston, MA).

Statistical analysis

Statistical evaluation of the results was conducted by using χ^2 analysis.

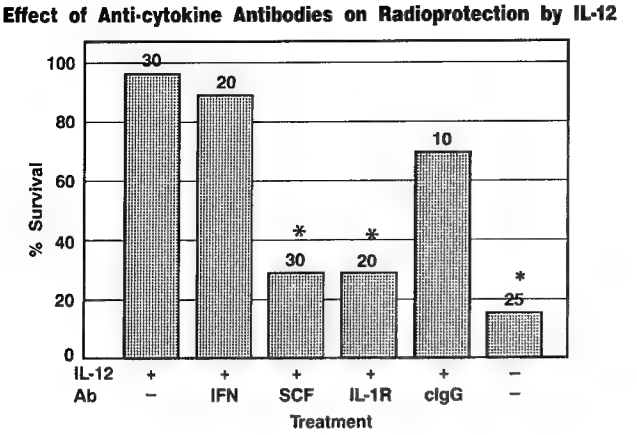

FIGURE 2. Effect of anti-IL-1R, anti-SCF, and anti-IFN-γ Abs on radioprotection with IL-12. $B6D2F_1$ mice received i.p. 100 μg/mouse of anti-IFN-γ, anti-IL-1R, GL113 (control IgG2b), or 1:20 dilution of anti-SCF serum and, 5 h later, 1 μg/mouse of IL-12. Twenty hours later, the mice were exposed to 950-cGy ^{60}Co whole body radiation. The survival was recorded daily for 30 days. * $p < 0.001$ different from IL-12-radioprotected mice.

Results

Radioprotection by IL-12 administered before irradiation

The stimulatory effect of IL-12 on hemopoietic progenitors (17–19), similar to those reported for SCF and IL-1 (23), inspired us to undertake experiments to compare IL-12 with IL-1 as a potential radioprotector. A single dose of 1 μg/mouse of IL-12 given i.p. 18 to 24 h before a ^{60}Co-gamma whole body lethal irradiation protected a significant fraction of C3H/HeJ and $B6D2F_1$ mice from death (Fig. 1, *a* and *b*). The radioprotective effect of IL-12 was comparable with that of IL-1 (Fig. 1*b*). The mice treated with IL-12 had increased numbers of nucleated BMC (8.4×10^5/femur in IL-12-treated mice vs 1.8×10^5/femur in control mice) at 6 days after 950-cGy radiation.

The effect of anti-IL-1R, anti-SCF, and anti-IFN-γ Ab on IL-12-induced radioprotection

Our previous work showed that SCF and IL-1 are interdependent radioprotectors (10, 11). Although there is no evidence that IL-12 induces SCF or IL-1, IL-12 is an inducer of IFN-γ, and a number of its effects are attributed to IFN-γ. As shown in Figure 2, Ab to IFN-γ did not affect IL-12 radioprotection (although the same amount of this Ab was effective in other assays; see below), whereas Abs to IL-1R and SCF abrogated IL-12 radioprotection, which indicates that the radioprotective effect of IL-12 is not mediated by IFN-γ, but does require IL-1 and SCF cooperation.

Table I. *Effect of IL-12 dosage on radiosensitization*[a]

Treatment	Mean Survival Time (days)		
	$B6D2F_1$		C3H/HeJ
	Before	After	Before
IL-12, 1.0 μg	4.0 ± 0.0	4.0 ± 0.0	3.9 ± 1.6
IL-12, 0.2 μg	4.7 ± 0.9	4.3 ± 0.7	8.9 ± 1.3
IL-12, 0.04 μg	6.2 ± 1.0	5.6 ± 0.8	11.8 ± 1.2
Saline	9.6 ± 1.2		12.1 ± 1.0

[a] Mice (n = 20 for each experimental group) received i.p. injections of IL-12 either 18 h before or 1 h after irradiation with 1200 cGy ($B6D2F_1$) or 900 cGy (C3H/HeJ).

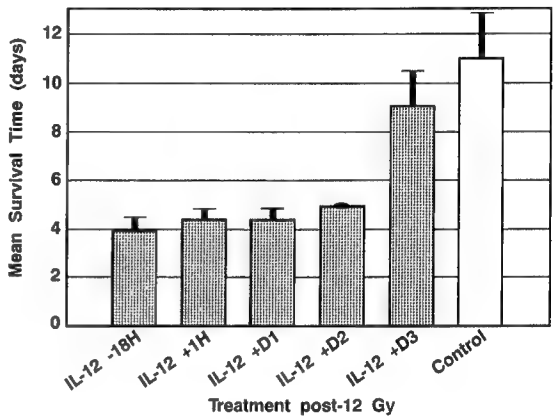

FIGURE 3. Time dependence of the radiosensitizing effect of IL-12. $B6D2F_1$ mice received 1 μg/mouse of IL-12 at the indicated times, before or after 1200-cGy irradiation. The number of mice in each experimental group ranged from 18 to 30.

IL-12 sensitizes mice to the lethal effect of radiation

IL-1 and SCF given in combination are synergistic in protecting mice from lethal radiation (10, 11). In these studies, the $LD_{50/30}$ were as follow: 866 cGy for saline-treated mice; and 1009 cGy for IL-1-treated and 1106 cGy for SCF-treated mice, whereas the treatment with the combination of the two cytokines resulted in $LD_{50/30}$ of 1273 cGy. Because IL-12, like IL-1 and SCF, has a costimulatory effect on BM progenitor cell growth and, as shown above, also is radioprotective by itself, we tested the possibility that IL-12 may enhance radioprotection by SCF or IL-1. Unexpectedly, combined administration of SCF and IL-12, as well as administration of IL-12 alone, resulted in accelerated death of mice exposed to 1200 cGy (Table I). Both $B6D2F_1$ and C3H/HeJ mice that received 1 μg/mouse of IL-12 succumbed within 4 days to radiation-induced death, which is consistent with death as a result of GI injury. This apparent sensitizing effect was dependent on the dose of IL-12 and the strain of mouse. One hundred percent of C3H/HeJ mice (which are more susceptible to radiation ($LD_{100/30}$ = 750 cGy) than are $B6D2F_1$ mice

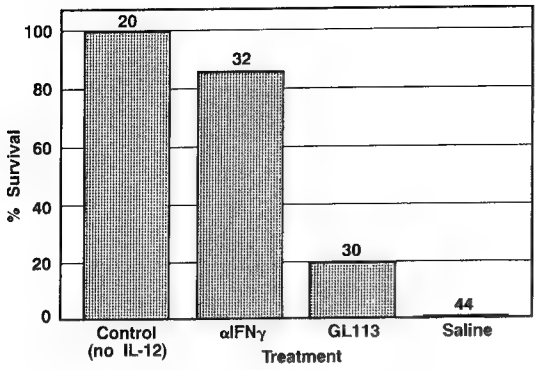

FIGURE 4. The protective effect of anti-IFN-γ Ab on sensitization of mice to GI death by IL-12. $B6D2F_1$ mice received 100 μg/mouse anti-IFN-γ Ab, an isotype-matched IgG (GL113), or saline then 200 ng of IL-12 either 18 h before or 1 h after irradiation with 1200-cGy whole body ^{60}Co gamma. The results present survival at 6 days. The numbers above the bars represent the number of mice in each experimental group.

($LD_{100/30}$ = 950 cGy)) were dead within 4 days after 900 cGy, and $B6D2F_1$ mice died within 4 days after 1200 cGy. In the absence of IL-12 treatment, the C3H/HeJ died within 6 days after 1500 cGy, and $B6D2F_1$ mice required doses greater than 1600 cGy. Similar sensitization of $B6D2F_1$ mice also was induced when IL-12 was given 18 h before or within 2, but not 3, days after irradiation (Fig. 3). The sensitizing effect of IL-12 was abrogated by 100 μg/mouse of anti-IFN-γ Ab, thus, indicating that IFN-γ was an essential mediator contributing to accelerated death (Fig. 4).

Three days after irradiation with 1200 cGy, mice treated with IL-12 had twofold higher numbers of nucleated BMC/femur that expressed c-*kit*$^+$, a phenotypic marker characteristic of BM progenitor cells, than did control mice (Table II and Fig. 5). This result indicates that even at doses of radiation at which it causes GI damage and death, IL-12 still radioprotects hemopoietic cells.

Table II. *The radioprotective effect of IL-12 on BMC of mice irradiated with 1200 cGy*[a]

Treatment	BMC/Femur	Percentage of c-*kit*$^+$	c-*kit*$^+$/Femur
RX + IL-12	3.4×10^4	9.7	3,298
RX control	2.8×10^4	5.4	1,512

[a] $B6D2F_1$ mice (10 mice/group) received 1 μg/mouse of IL-12 18 h before whole-body ^{60}Co irradiation. Three days after irradiation, BMC from 10 femurs/group were analyzed as described in *Materials and Methods*.

Gross necropsy 3 days after 1200-cGy radiation of mice treated with IL-12 revealed that the lumen of the small intestine was moderately distended with fluid ingests, which suggests the disruption in the absorption process. In mice treated with IL-12 and anti-IFN-γ Ab, the gut seemed to be normal. As determined microscopically, treating 1200-cGy-irradiated mice with IL-12 greatly exacerbated the histologically observed damage to the gut induced by radiation alone, with a much greater decrease occurring in the number of crypts (Fig. 6, *b* vs *d*). The extent of damage caused by IL-12 and 1200 cGy was greater than that caused by 1600-cGy irradiation (Fig. 6*c*), a dose that results in death of $B6D2F_1$ mice within 6 days. Treating the 1200-cGy-irradiated, IL-12-treated mice with anti-IFN-γ Ab markedly reversed the damage (Fig. 6*e*). In contrast, megakaryocytes were absent from the spleens of 1200-cGy-irradiated mice, but still were found in the spleens of irradiated mice that received IL-12, as well as those that received IL-12 plus anti-IFN-γ Ab, further

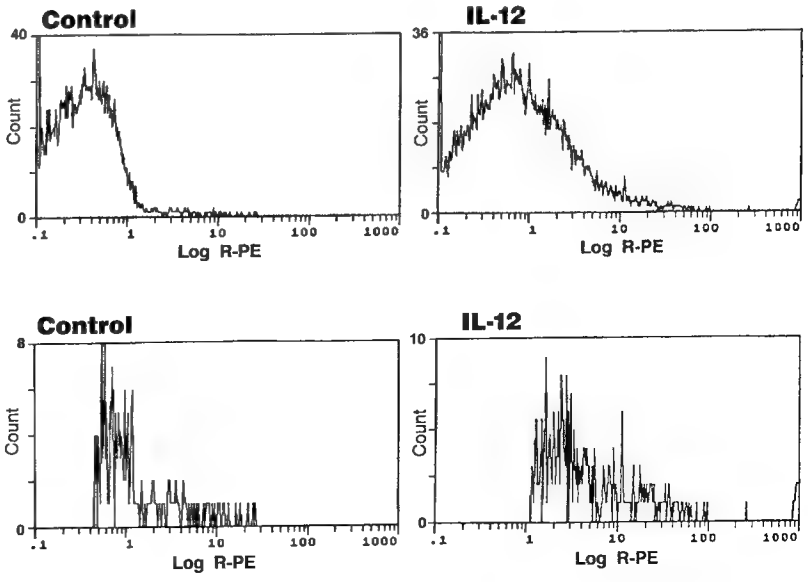

FIGURE 5. Flow cytometric profiles of BMC obtained 3 days after 1200-cGy irradiation, with and without IL-12 treatment, and stained with anti-c-*kit* Ab. The *upper panels* represent total BMC stained for c-*kit*, and the *lower panels* represent the cells that remained after cells that stained for IgG had been subtracted (see also Table II).

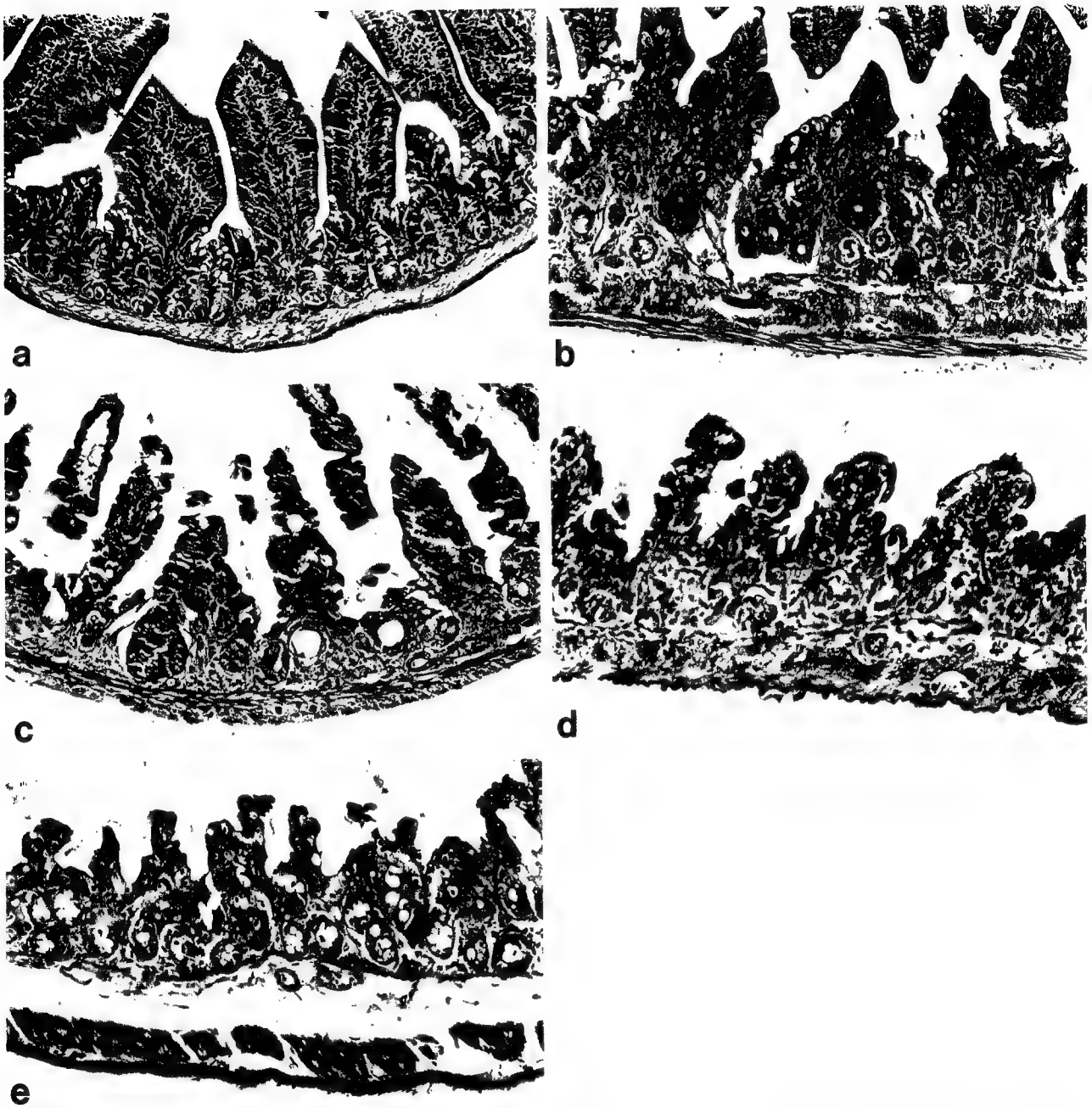

FIGURE 6. Photomicrographs of jejunal sections from normal B6D2F$_1$ mice (*a*), and from 1200-cGy-irradiated mice (*b*, *d*, and *e*), and 1600-cGy-irradiated mice (*c*) 3 days after radiation. *Panel a*) normal B6D2F$_1$ mice exhibit normal appearance, shape, number, and length of the mucosal villi, along with organized appearance of the deep crypt layer. *Panel b*) in 1200-cGy-irradiated mice, moderate damage to the mucosa is observed, villi exhibit a moderate shortening in length and decrease in number, the layer containing the deep crypt area displays a decrease in crypt number, and occasional crypts contain necrotic epithelial cells sloughed from the basement membrane. *Panel c*) 1600-cGy-irradiated mice show moderate to severe damage to the mucosa, and some viable crypts are still evident in the deep mucosa, but a majority have lost cellularity. Some crypts contain only a few viable epithelial cells; villi are shortened and, in some areas, fused. *Panel d*) IL-12 treatment and 1200-cGy irradiation result in severe mucosal damage, evidenced by a marked shortening of villi and evidence of villi fusion; remaining epithelial cells lining the villi tips exhibit pleomorphism; and most deep crypt areas have lost epithelial lining cells, causing many to collapse. *Panel e*) in mice that received anti-IFN-γ Ab, IL-12, and 1200 cGy, mucosal villi also are shortened and fewer in number, but less severe damage to the mucosal layer is visible than in *c* or *d*; there is a moderate decrease in the number of deep crypt areas; but remaining crypts are lined by viable epithelial cells, are similar in size and shape, and maintain a more ordered appearance in this layer.

Table III. *The effect of dose of IL-12 on LPS induction of TNF and IL-6*[a]

IL-12	LPS	TNF (ng/ml)	IL-6 (ng/ml)
1000 ng	+	16.8 ± 4.6	78.8
100 ng	+	14.8 ± 4.9	80.0
20 ng	+	8.5 ± 2.3	26.5
None	+	0.1 ± 0.05	1.69

[a] $B6D2F_1$ mice received IL-12 in indicated doses and, 18 h later, 5 μg/mouse of LPS. Groups of mice (three to five/group) were bled 90 min and 4 h later for TNF and IL-6 assays, respectively. Control mice that received the priming and challenging injections of 1 μg/mouse of IL-12 had no detectable TNF or IL-6.

Table IV. *Time dependence of IL-12 priming for LPS induction of TNF and IL-6*[a]

Interval Between IL-12 and LPS (h)	TNF (pg/ml)	IL-6 (pg/ml)
0	250	1,975
4	8,000	32,600
18	64,000	84,800
48	32,000	85,200
72	32,000	47,300
96	4,000	ND
120	2,000	ND

[a] $B6D2F_1$ mice received i.p. 200 ng/mouse of IL-12 and, at indicated time intervals, were administered i.p. 5 μg/mouse of LPS. Mice were bled at 60 to 90 min for TNF and at 4 h for IL-6 determinations. The results are the mean values of five separate experiments having three mice/group. TNF levels at individual time points did not vary by more than twofold to fourfold in individual experiments.

confirming that hemopoietic components were protected by IL-12.

Effect of IL-12 on LPS-induced TNF and IL-6 production

It is possible that, in addition to inducing IFN-γ, IL-12 treatment of mice results in additional systemic effects that, in turn, may contribute to the observed exacerbation of radiation-induced damage to the gut. One such possibility may involve excessive production of proinflammatory cytokines. To assess this possibility, normal mice received IL-12 and subsequently were challenged with LPS. Such combined treatment greatly enhanced the levels of the proinflammatory cytokines TNF and IL-6. Priming for LPS induction of IL-6 and TNF was observed at doses of IL-12 as low as 20 ng/mouse (Table III), was detectable within 4 h after IL-12 administration, peaked at 18 to 72 h, and still was present at 5 days after IL-12 administration (Table IV). As in the case of sensitization by IL-12 to GI injury caused by irradiation, the priming was abrogated by anti-IFN-γ Ab (Table V).

Discussion

The results of our study demonstrate that treating mice with IL-12 has opposite effects on the response of hemopoietic and intestinal tissue to ionizing radiation. The increased survival of IL-12-treated mice given lethal irradiation (which causes death from hemopoietic failure) is associated with increased numbers of nucleated BMC in IL-12-treated vs control, saline-treated mice. Moreover, greater numbers of c-*kit*$^+$ BMC were detected in IL-12-treated mice compared with control mice 3 days after radiation with 1200 cGy, although IL-12-treated, but not control mice, succumbed to GI death 1 day later.

Table V. *Anti-IFN-γ Ab abrogates IL-12 priming for LPS-induced TNF and IL-6*[a]

Treatment			TNF	IL-6
Ab	IL-12	LPS	(pg/ml)	(pg/ml)
–	–	+	125	2,600
anti-IFN-γ	+	+	250	4,590
IgG	+	+	4,000	82,100

[a] Groups of $B6D2F_1$ mice (three to six/group) were administered 100 μg/mouse of anti-IFN-γ or IgG control and, 5 h later, 1 μg/mouse of IL-12. After an additional 18 h, mice received 5 μg/mouse of LPS. Blood was obtained 90 min and 4 h later for TNF and IL-6 measurements, respectively.

The radioprotective effect of IL-12 on BMC may be related to its ability to stimulate hemopoiesis. Although IL-12 by itself does not support the growth of progenitor cell colonies, it acts synergistically together with SCF and IL-1 to promote the growth of primitive hemopoietic stem cells (17–19). Indeed, radioprotection with IL-12 requires the presence of IL-1 and SCF, as was indicated by abrogation of the radioprotection by anti-IL-1R and anti-SCF Ab (Fig. 2). This mutual interdependence of IL-12, IL-1, and SCF extends our previous findings on co-dependence of IL-1 and SCF in radioprotection (10, 11). Unlike many other effects of IL-12, its induction of radioprotection is IFN-γ independent, because it is not abrogated by anti-IFN-γ Ab. This is consistent with the finding that IL-12 acts directly to stimulate proliferation of primitive stem cells (17).

The identification of IL-12, IL-1, and SCF as protectors of hemopoiesis from radiation poses a question of whether and how their synergistic, costimulatory effects on hemopoiesis contribute to radioprotection. We hypothesize that radioprotection, in part, may be on the basis of the ability of these cytokines to induce and/or promote cycling of early hemopoietic progenitors to reach a more radioresistant phase of the cell cycle. Both IL-1 and SCF in vivo stimulate expansion of early hemopoietic progenitor cells (24–27). Within 18 h after administration of IL-1 progenitor, BMC were much more sensitive to hydroxyurea, which is selectively toxic to cells in the S phase, and had an increased proportion of cells in the $S+G_2+M$ phase of cell cycle (24, 25). Moreover, the lag period (greater than 4 h but less than 48 h) that is required for optimal radioprotection with IL-1 (4), SCF (11), and IL-12 (data not shown) further suggests that entry into a specific phase of the cell cycle, rather than mere expansion of hemopoietic progenitors, may be critical for radioprotection. Studies

with synchronized cultures of numerous mammalian cell lines have established that the late S phase of the cell cycle is most radioresistant (28). Similarly, in vivo synchronization of rapidly dividing crypt cells in mouse jejunum by 5 i.p. injections of hydroxyurea followed by exposure at time intervals thereafter to 1100 cGy of gamma rays indicated that crypt cells irradiated during late S phase were 100-fold more resistant than were the cells in G_1/S phase (29). These observations lead us to predict that driving stem and progenitor cells to late S phase may contribute to myeloprotection.

The finding that a single dose of IL-12, even as low as 40 ng/mouse, renders irradiated mice more sensitive to death as a result of GI damage was unexpected. The dose of radiation that was lethal within 4 to 6 days to 100% of IL-12-treated mice was lower by 600 cGy for C3H/HeJ mice (900 cGy instead of 1500 cGy) and by 400 cGy in $B6D2F_1$ mice (1200 cGy instead of 1600 cGy). Histologically, the damage to crypt cells observed in jejunal sections obtained 3 days after combined treatment with IL-12 and 1200 cGy from $B6D2F_1$ mice was even more extensive than was the damage caused by 1600 cGy. Because anti-IFN-γ Ab abrogates this sensitizing effect of IL-12, IFN-γ is an important mediator for such sensitization. The finding that IL-12 primes mice to LPS challenge and enhances production of TNF and IL-6 may be relevant to increased gut sensitivity to radiation. The gut may be an important target tissue in which priming by IL-12 to subsequent inflammatory stimuli occurs. Because probably only a small fraction of the 5-μg dose of LPS reaches the gut, we presume that our experimental system reflects conditions under which IL-12 exacerbates damage caused by agents such as LPS or ionizing radiation. This priming by IL-12 for the induction of TNF and IL-6 by LPS may be associated with the ability of IL-12 to prime mice for the lethal Shwartzman reaction (30). Although our attempts to measure TNF in the sera of mice 3 days after 1200-cGy radiation did not show evidence of high levels of TNF in circulation (results not shown), IL-12 has been reported to enhance TNF gene expression (31). Consequently, it is possible that TNF is increased and bound to cells in tissues and may promote apoptotic death via the TNFR-1 (32–34).

Acknowledgments

We thank Dr. Bill McBride for discussions, Drs. G. D. Ledney and T. J. MacVittie for critical reading of the manuscript, Lillie Heman-Ackah for preparing intestinal sections, and Mark Moorman for flow cytometry analysis of BMC.

References

1. Hall, E. J. 1988. *Radiobiology for the Radiologist.* Lippincott Co., Philadelphia.
2. Bond, V. P., T. M. Fliedner, and J. O. Archambeau. 1965. *Mammalian Radiation Lethality: A Disturbance in Cellular Kinetics*, Academic Press, New York.
3. Lorenz, E., D. Uphoff, T. R. Reid, and E. Shelton. 1951. Modification of irradiation injury in mice and guinea pigs by bone marrow injections. *J. Natl. Cancer Inst. 12:197.*
4. Neta R., S. D. Douches, and J. J. Oppenheim. 1986. IL-1 is a radioprotector. *J. Immunol. 136:2483.*
5. Neta, R., J. J. Oppenheim, and S. D. Douches. 1988. Interdependence of the radioprotective effects of human recombinant IL-1, tumor necrosis factor, granulocyte colony-stimulating factor, and murine recombinant granulocyte-macrophage colony-stimulating factor. *J. Immunol. 140:108.*
6. Zsebo, K. M., K. A. Smith, C. A. Hartley, M. Greenblatt, K. Cooke, W. Rich, and I. K. McNiece. 1992. Radioprotection of mice by recombinant stem cell factor. *Proc. Natl. Acad. Sci. USA 89:9464.*
7. Neta, R., J. J. Oppenheim, R. D. Schreiber, R. Chizzonite, G. D. Ledney, and T. J. MacVittie. 1991. Role of cytokines (interleukin 1, tumor necrosis factor, and transforming growth factor β) in natural and lipopolysaccharide-enhanced radioresistance. *J. Exp. Med. 173: 1177.*
8. Neta, R., R. Perlstein, S. N. Vogel, G. D. Ledney, and J. Abrams. 1992. Role of IL 6 in protection from lethal irradiation and in endocrine responses to IL 1 and TNF. *J. Exp. Med. 175:689.*
9. Neta, R., D. Williams, F. Selzer, and J. Abrams. 1993. Inhibition of c-*kit* ligand/steel factor by antibodies reduces survival of lethally-irradiated mice. *Blood 81:324.*
10. Neta, R., J. M. Wang, J. J. Oppenheim, N. Davis, and C. M. Dubois. 1994. Cytokine interactions in protection from lethal irradiation: synergy of IL-1 and *kit* ligand. In *The Negative Regulation of Hematopoiesis: From Fundamental Aspects to Clinical Applications.* M. Guigon, F. Lemoine, N. Dainiak, A. Schechter, and A. Najman, eds. John Libbey Eurotext, Montrouge, France. In press.
11. Neta, R., J. J. Oppenheim, J. M. Wang, C. M. Snapper, M. A. Moorman, and C. M. Dubois. 1994. Synergy of IL-1 and stem cell factor in radioprotection of mice is associated with IL-1 up-regulation of mRNA and protein expression for c-*kit* on bone marrow cells. *J. Immunol. 153:1536.*
12. Trincheri, G. 1993. Interleukin-12 and its role in the generation of Th1 cells. *Immunol. Today 14:335.*
13. Kobayashi, M., L. Fritz, M. Ryan, R. M. Hewick, S. C. Clark, S. Chan, R. Loudon, F. Sherman, B. Perussia, and G. Trincheri 1989. Identification and purification of natural killer cell stimulatory factor (NKSF), a cytokine with multiple biologic effects on human lymphocytes. *J. Exp. Med. 170:827.*
14. Stern, A. S., F. J. Podlaski, J. D. Hulmes, Y.-C. E. Pan, P. M. Quinn, A. G. Wolitzky, P. C. Familletti, D. L. Stremlo, T. Truitt, R. Chizzonite, and M. K. Gately. 1990. Purification to homogeneity and partial characterization of cytotoxic lymphocyte maturation factor from human B-lymphoblastoid cells. *Proc. Natl. Acad. Sci. USA 87:6808.*
15. Heinzel, F. P., D. S. Schoenhaut, R. M. Rerko, L. E. Rosser, and M. K. Gately. 1993. Recombinant IL-12 cures mice infected with *Leishmania major. J. Exp. Med. 177:1505.*
16. Locksley, R. M. 1993. Interleukin 12 in host defense against microbial pathogens. *Proc. Natl. Acad. Sci. USA 90:5879.*
17. Jacobsen, S. E. W., O. P. Veiby, and E. B. Smeland. 1993. Cytotoxic lymphocyte maturation factor (interleukin 12) is a synergistic growth factor for hematopoietic stem cells. *J. Exp. Med. 178:413.*
18. Ploemacher, R. E., P. L. van Soest, H. Voorvinden, and A. Boudewijn. 1993. Interleukin-12 synergizes with interleukin-3 and steel factor to enhance recovery of murine hematopoietic stem cells in liquid culture. *Leukemia 7:1381.*
19. Hirayama, F., N. Katayama, S. Neben, D. Donaldson, E. B. Nickbarg, S. C. Clark, and M. Ogawa. 1994. Synergistic interaction between interleukin-12 and steel factor in support of proliferation of murine lymphohematopoietic progenitors in culture. *Blood 83:92.*
20. Chizzonite, R., T. Truitt, P. L. Kilian, A. S. Stern, P. Nunes, K. P. Parker, K. L. Kaffka, A. O. Chua, D. K. Lugg, and U. Gubler. 1989. Two high-affinity interleukin-1 receptors represent separate gene products. *Proc. Natl. Acad. Sci. USA 86:8029.*
21. Starnes, H. F., M. K. Pearce, A. Tewari, J. H. Yim, J. C. Zou, and J. S. Abrams. 1990. Anti-IL-6 monoclonal antibodies protect against lethal *Escherichia coli* infection and lethal TNF: a challenge in mice. *J. Immunol. 145:4185.*

22. Sheehan, K. C. F., N. H. Ruddle, and R. D. Schriber. 1989. Generation of hamster monoclonal antibodies that neutralize tumor necrosis factors. *J. Immunol. 142:3884.*
23. Muench, M. O., J. G. Schneider, and M. A. S. Moore. 1991. Interactions among colony-stimulating factors, IL-1β, IL-6, and *kit*-ligand in the regulation of primitive murine hematopoietic cells. *Exp. Hematol. 20:339.*
24. Neta, R., M. B. Sztein, J. J. Oppenheim, S. Gillis, and S. D. Douches. 1987. In vivo effects of IL-1. I. Bone marrow cells are induced to cycle following administration of IL-1. *J. Immunol. 139:1861.*
25. Schwartz, G. N., T. J. MacVittie, R. M. Vigneulle, M. L. Patchen, S. D. Douches, J. J. Oppenheim, and R. Neta. 1987. Enhanced hematopoietic recovery in irradiated mice pretreated with interleukin-1 (IL-1). *Immunopharmacol. Immunotoxicol. 9:371.*
26. Johnson, C. S., D. J. Keckler, and M. I. Topper. 1989. In vivo hematopoietic effects of recombinant interleukin 1α in mice: stimulation of granulocytic, monocytic, megakaryocytic and early erythroid progenitors; suppression of late stage erythropoiesis, and reversal of erythroid suppression with erythropoietin. *Blood 73:678.*
27. Fleming, W. H., E. J. Alpern, N. Uchida, K. Ikuta, and I. L. Weissman. 1993. Steel factor influences the distribution and activity of murine hematopoietic stem cells in vivo. *Proc. Natl. Acad. Sci. USA 90:3760.*
28. Sinclair, W. K., and R. A. Morton. 1966. X-ray sensitivity during the cell generation cycle of cultured Chinese hamster cells. *Radiat. Res. 29:450.*
29. Withers, H. R., K. Mason, B. O. Reid, N. Dubraysky, H. T. Barkley, B. W. Brown, and J. B. Smathers. 1974. Response of mouse intestine to neutrons and gamma rays in relation to dose fractionation and cell cycle. *Cancer 34:39.*
30. Ozmen, L., M. Pericin, M. K. Gately, R. Chizzonite, D. Heumann, and G. Garotta. 1993. IFNγ and IL-12 in the Shwartzman reaction (Abs). *Lymphokine Cytokine Res. 12:376.*
31. Morris S. C., K. B. Madden, J. J. Adamowicz, W. C. Gause, B. R. Hubbard, M. K. Gately, and F. D. Finkelman. 1994. Effects of IL-12 on in vivo cytokine gene expression and Ig isotype selection. *J. Immunol. 152:1048.*
32. Greenblatt, M. S., and L. Elias. 1992. The type B receptor for tumor necrosis factor-α mediates DNA fragmentation in HL-60 and U937 cells and differentiation in HL-60 cells. *Blood 80:1339.*
33. Tartaglia, L. A., T. M. Ayers, G. H. W. Wong, and D. V. Goeddel. 1993. A novel domain within 55-kd TNF receptor signals cell death. *Cell 74:845.*
34. Wong, G. H. W., and D. V. Goeddel. 1994. Fas antigen and p55 TNF receptor signal apoptosis through distinct pathways. *J. Immunol. 152:1751.*

Neuroendocrinology
Editor-in-Chief: C. Kordon, Paris

Reprint
Publisher: S. Karger AG, Basel
Printed in Switzerland

Corticotropins and Neuroimmune Interactions

Neuroendocrinology 1994;60:418–425

Systemically Administered Histamine H_1 and H_2 Receptor Antagonists Do Not Block the ACTH Response to Bacterial Lipopolysaccharide and Interleukin-1

Robert S. Perlstein[a]
Neerav R. Mehta[a]
Edward H. Mougey[c]
Ruth Neta[a]
Mark H. Whitnall[b]

Departments of
[a] Experimental Hematology and
[b] Physiology, Armed Forces Radiobiology, Research Institute, Bethesda, Md.,
[c] Neuroendocrinology and Neurochemistry Branch, Department of Medical Neurosciences, Walter Reed Army Institute of Research, Washington, D.C., USA

Key Words
Histamine
Histamine receptors
Histamine antagonists
Lipopolysaccharide
Interleukin-1
Adrenocorticotropic hormone
Corticotropin

Abstract
The administration of lipopolysaccharide (LPS) results in the activation of the hypothalamic-pituitary-adrenal axis (HPAA). We recently reported that the participation and interaction of LPS-induced proinflammatory cytokines were obligatory for the stimulation of adrenocorticotropic hormone (ACTH) release by LPS. LPS and LPS-derived cytokines also stimulate the release of histamine (HA). HA is a known hypothalamic neurotransmitter and activates the HPAA. Therefore, to elucidate the role of HA in LPS- and cytokine-induced ACTH release, we evaluated the effects of several HA H_1 and H_2 receptor antagonists on the ACTH response to LPS, recombinant human interleukin-1α (rhIL-1α) and HA in mice. Although all 3 of the H_1 receptor antagonists administered (mepyramine (MEP), diphenhydramine (DPH) or promethazine (PMZ)) were able to block the 10-min ACTH response to HA, only PMZ (a less selective H_1 receptor antagonist than MEP) was able to reduce the LPS- or rhIL-1α-induced ACTH responses. Ranitidine, a powerful and selective H_2 receptor antagonist, had little effect on the LPS- and rhIL-1α-induced ACTH responses, while metiamide (MET), a much less potent first-generation H_2 receptor antagonist, substantially diminished ACTH release. The greater effectiveness of PMZ, in contrast to MEP or DPH, probably relates to the ability of phenothiazine derivatives to inhibit non-HA-dependent pathways involved in the stimulation of the HPAA by cytokines; the same may be true of MET. Our results suggest that, in contrast to the essential role of HA in the activation of the HPAA by noninflammatory stressors, the stimulation of ACTH release by LPS and rhIL-1α is not as dependent on the participation of either the H_1 or the H_2 receptor.

Introduction

We previously reported that the activation of the hypothalamic-pituitary-adrenal axis (HPAA) by lipopolysaccharide (LPS) requires the participation and interaction of the LPS-induced proinflammatory cytokines, interleukin (IL)-1, IL-6 and tumor necrosis factor (TNF), and that the relative importance of these three cytokines varies at different time points after LPS challenge [1–4]. Histamine (HA) production is also stimulated by LPS [5, 6] as

Received:
February 3, 1994
Accepted after revision:
May 24, 1994

Robert S. Perlstein, MD, FACP
Colonel USAF MC
EXH/AFRRI
Bethesda, MD 20889-5603 (USA)

well as LPS-derived cytokines [7–9], and HA, in turn, can induce the production and potentiate the action of inflammatory cytokines [10–12]. HA acts as a hypothalamic neurotransmitter [13–16] and is involved in the neuroendocrine control of pituitary hormone secretion [17, 18], including the stimulation of the HPAA [17–28].

Recently, the presumed hypothalamic site of action of HA was confirmed. Ohgo et al. [29] observed that HA elicited a significant increase in corticotropin-releasing hormone (CRH) from superfused rat hypothalamic explants and Kjær et al. [27] reported that the central administration of both HA H_1 and H_2 agonists significantly increased the CRH concentration in pituitary portal blood. The same group also noted that the plasma adrenocorticotropic hormone (ACTH) responses to centrally administered HA were significantly attenuated by the preadministration of specific antisera to CRH or vasopressin (VP) suggesting that CRH and VP mediate the ACTH response to HA [28].

Both centrally and systemically administered H_1 and H_2 receptor antagonists diminish the plasma ACTH response to HA in experimental animals further suggesting the participation of both H_1 and H_2 receptors in HA-induced ACTH release [17, 19, 21–25]. Recently, an essential role for both the H_1 and H_2 receptor in the activation of the HPAA by various noninflammatory stressors has also been demonstrated [30, 31].

These studies suggested the possibility that HA may be a mediator of LPS- and cytokine-induced ACTH release. In the only report to date involving antihistamines and an inflammatory stressor, i.e. LPS, Suzuki and co-workers [5, 6] partially blocked the corticosterone response to LPS in rats by preinjecting the H_1 receptor antagonist, promethazine (PMZ), and concluded that the H_1 receptor plays an important role in LPS-induced HPAA activation. On the other hand, Ohgo et al. [29] observed that rhIL-1β-induced CRH release from superfused rat hypothalamo-neurohypophyseal complexes was not affected by a combination of H_1 and H_2 receptor antagonists. We therefore decided to further evaluate the role of HA in the activation of the HPAA by LPS and IL-1 by assessing the effects of various H_1 and H_2 receptor antagonists in mice.

Materials and Methods

Animals and Experimental Procedures

Female C3H/HeN mice were purchased from the Animal Genetics and Production Branch, NCI (Frederick, Md., USA). Mice were handled as previously described [3]. All research procedures were approved by an Institutional Animal Care and Use Committee.

In the first set of experiments, groups of 5 mice were injected intraperitoneally (i.p.) with vehicle (0.5 ml pyrogen-free normal saline), LPS, one of five different antihistamines alone or LPS mixed with one of the five different antihistamines at 08:00 h. Either 2 or 4 h later, unanesthetized mice were decapitated (model 130 Rodent Decapitator; Harvard Apparatus, South Natick, Mass., USA) with minimal stress to obtain plasma samples for ACTH. In the second set of experiments, the procedure was identical except that recombinant human IL-1α (rhIL-1α) was substituted for LPS and plasma ACTH samples were obtained only 2 h after the injections.

In the third set of experiments, groups of 5 mice were injected i.p. with vehicle or one of five different antihistamines at 07:30 h. Thirty minutes later, HA was administered i.p. to all of the pretreated groups, and HA or vehicle was administered to groups that had not received any pretreatment as well. Plasma samples were acquired 10 min after HA or vehicle injections.

LPS, rhIL-α, Histamine, Antihistamines

rhIL-1α (117–271 Ro 24-5008, lot IL-1 2/88; specific activity 3×10^8 U/mg) was generously provided by Dr. Peter Lomedico, Hoffmann-La Roche (Nutley, N.J., USA). LPS (protein-free; prepared from *Escherichia coli* K235 by the phenol-water extraction method) was kindly provided by Dr. Stefanie Vogel, Uniformed Services University of the Health Sciences (Bethesda, Md., USA).

HA dihydrochloride was obtained from Sigma (St. Louis, Mo., USA). The H_1 receptor antagonists used were mepyramine (MEP; Sigma), diphenhydramine (DPH; Parke Davis, Morris Plains, N.J., USA) and PMZ (Wyeth, Philadelphia, Pa., USA). The H_2 receptor antagonists used were ranitidine (RAN; Glaxo, Research Triangle Park, N.C., USA) and metiamide (MET; SmithKline Beecham, King of Prussia, Pa., USA).

All amounts of LPS, rhIL-1α, HA and all of the antihistamines except MET were diluted in 0.5 ml pyrogen-free saline just prior to injection. MET was dissolved in 1.0 *N* HCl, adjusted to pH 4–6 with 0.1 *N* NaOH, and then diluted with saline.

Measurement of Plasma ACTH

ACTH was assayed in plasma obtained from decapitated mice using an ^{125}I RIA kit (Incstar Corp., Stillwater, Minn., USA) as previously described [3]. The ACTH antibody used in this assay is derived from rabbits immunized against $ACTH_{1-24}$, a region that is identical in human and murine ACTH. The threshold sensitivity of this assay was 8 pg/ml.

Statistical Analysis

In figures 1–4, evaluation of the results was carried out using analysis of variance, followed by Fisher's protected least significant difference test.

Results

Effects of H_1 Receptor Antagonists, MEP or DPH, or H_2 Receptor Antagonist, RAN, on the Plasma Level of ACTH 2 h after Challenge with LPS or rhIL-1α

Figure 1a demonstrates the effect of the H_1 receptor antagonists, MEP or DPH, or the H_2 receptor antagonist, RAN, on the 2 h ACTH response to 1 μg of LPS. We chose 1 μg of LPS because, in our earlier work, it was the

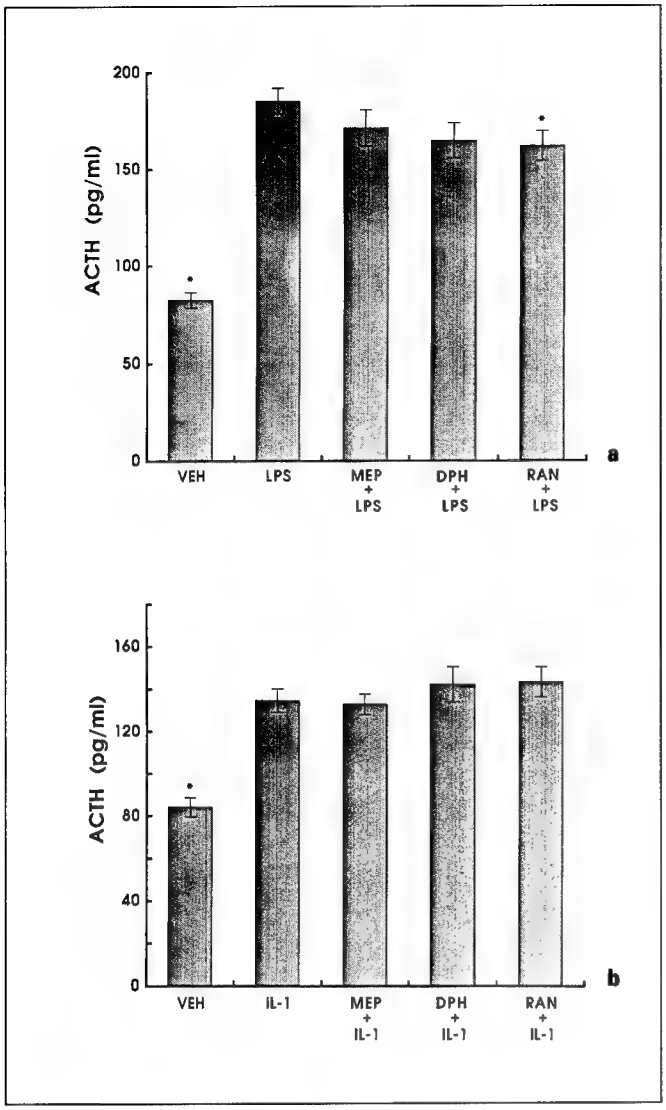

Fig. 1. Effects of H_1 receptor antagonists, MEP or DPH, or H_2 receptor antagonist, RAN, on the plasma level of ACTH 2 h after challenge with LPS (**a**) or rhIL-1α (**b**). C3H/HeN mice received i.p. injection of MEP (30 mg/kg), DPH (5 mg/kg) or RAN (30 mg/kg) mixed with 1 μg of LPS (**a**) or 100 ng of rhIL-1α (**b**). Other mice were administered vehicle, or 1 μg of LPS (**a**), or 100 ng of rhIL-1α (**b**) only. Blood samples were obtained 2 h after all injections. Each bar represents the mean ± SEM for 9–35 animals. * $p < 0.05$ (vs. LPS alone (**a**) or rhIL-1α alone (**b**)).

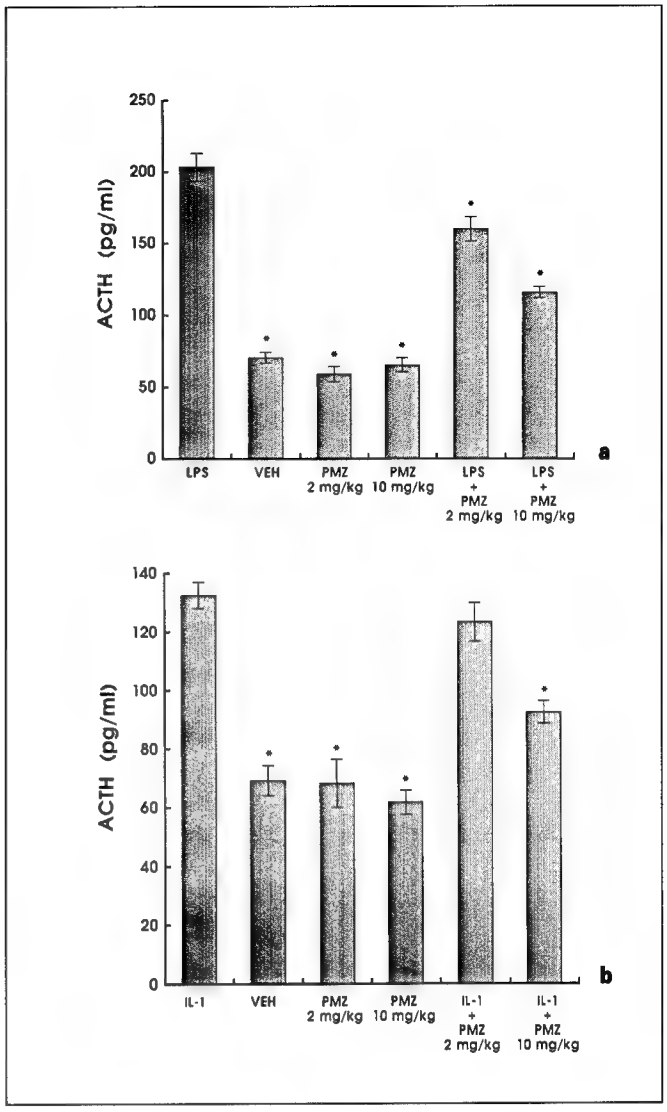

Fig. 2. Effects of H_1 receptor antagonist, PMZ, on the plasma level of ACTH 2 h after challenge with LPS (**a**) or rhIL-1α (**b**). C3H/HeN mice received i.p. injection of PMZ (2 or 10 mg/kg) mixed with 1 μg of LPS (**a**) or 100 ng of rhIL-1α (**b**). Other mice were administered vehicle, or PMZ (2 or 10 mg/kg), or 1 μg of LPS (**a**), or 100 ng rhIL-1α (**b**) only. Blood samples were obtained 2 h after all injections. Each bar represents the mean ± SEM for 9–25 animals. * $p < 0.05$ (vs. LPS alone (**a**) or rhIL-1α alone (**b**)).

smallest dose of LPS which produced a maximal ACTH response at 2 h [1]. The doses of MEP (10 and 30 mg/kg), DPH (2 and 5 mg/kg) and RAN (10 and 30 mg/kg) chosen inhibit HA-induced ACTH release when administered systemically to rats [19, 22, 23]. Only data for the larger doses of antihistamine are shown. Neither MEP nor DPH attenuated the LPS-induced ACTH response. RAN produced a significant, but very small, decrease in LPS-induced ACTH release. Neither MEP, DPH nor RAN had an effect on the 4 h ACTH response to 5 μg of LPS [data not shown].

Figure 1b demonstrates the effect of the same doses of MEP, DPH or RAN on the 2 h ACTH response to 100 ng of rhIL-1α. In our mice, the administration of 100 ng

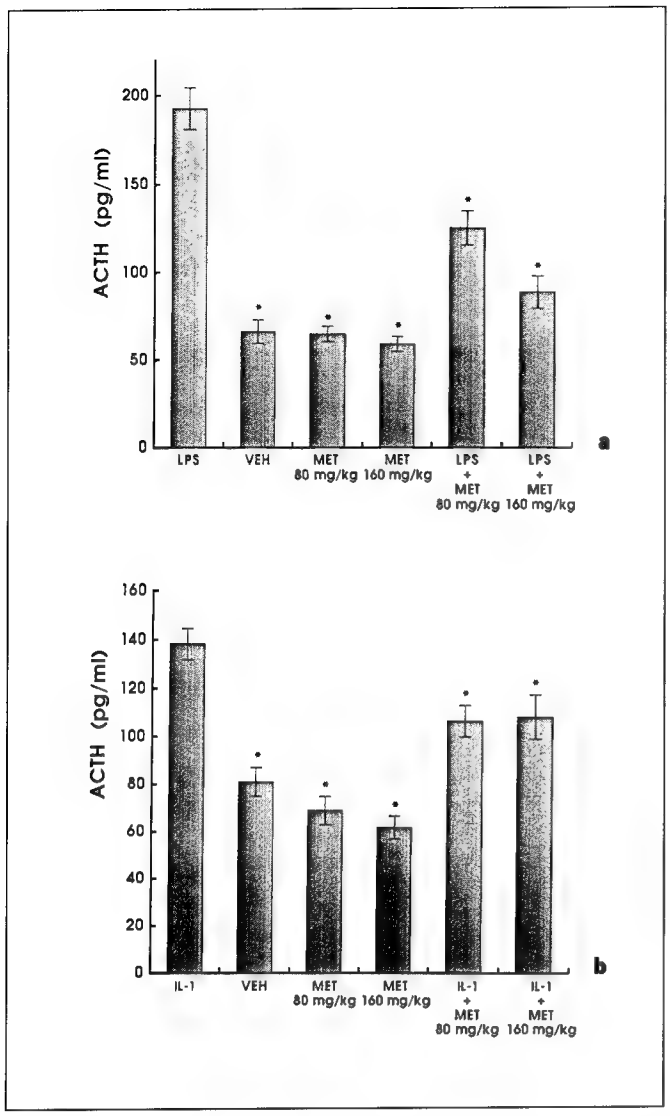

Fig. 3. Effects of H_2 receptor antagonist, MET, on the plasma level of ACTH 2 h after challenge with LPS (**a**) or rhIL-1α (**b**). C3H/HeN mice received i.p. injection of MET (80 or 160 mg/kg) mixed with 1 μg of LPS (**a**) or 100 ng of rhIL-1α (**b**). Other mice were administered vehicle, or MET (80 or 160 mg/kg), or 1 μg of LPS (**a**), or 100 ng rhIL-1α (**b**) only. Blood samples were obtained 2 h after all injections. Each bar represents the mean ± SEM for 9–15 animals. * $p < 0.05$ (vs. LPS alone (**a**) or rhIL-1α alone (**b**)).

of rhIL-1α results in a reproducible, submaximal 2 h ACTH response [1–4]. Again, only data for the larger doses of antihistamine are shown. MEP, DPH or RAN had no effect on the rhIL-1α-induced ACTH response.

The 2 or 4 h ACTH responses to the antihistamines administered alone were negligible [data not shown], and no different from the ACTH response to vehicle alone.

Effects of H_1 Receptor Antagonist, PMZ, on the Plasma Level of ACTH 2 h after Challenge with LPS or rhIL-1α

Figure 2a demonstrates the effect of the H_1 receptor antagonist, PMZ, on the 2 h ACTH response to 1 μg of LPS. The doses of PMZ (2 and 10 mg/kg) chosen diminish HA-induced ACTH release [22, 23], and HA- or LPS-induced corticosterone release [5] when administered systemically to rats. Either 2 or 10 mg/kg of PMZ significantly diminished the ACTH response to 1 μg of LPS in a dose-dependent fashion. These doses had a similar effect on the 4 h ACTH response to 5 μg of LPS [data not shown].

Figure 2b demonstrates the effect of the same doses of PMZ on the 2 h ACTH response to 100 ng of rhIL-1α. The 10 mg/kg dose of PMZ significantly attenuated the rhIL-1α-induced ACTH response.

The 2 or 4 h ACTH responses to either dose of PMZ administered alone were negligible and no different from the ACTH response to vehicle alone.

Effects of H_2 Receptor Antagonist, MET, on the Plasma Level of ACTH 2 h after Challenge with LPS or rhIL-1α

Figure 3a demonstrates the effect of the H_2 receptor antagonist, MET, on the 2 h ACTH response to 1 μg of LPS. The doses of MET (80 and 160 mg/kg) chosen diminish HA-induced ACTH release when administered systemically to rats [22, 23]. Either 80 or 160 mg/kg of MET significantly inhibited the ACTH response to 1 μg of LPS in a dose-dependent fashion. These doses had a similar effect on the 4 h ACTH response to 5 μg of LPS [data not shown].

Figure 3b demonstrates the effect of the same doses of MET on the 2 h ACTH response to 100 ng of rhIL-1α. Either dose of MET partially blocked the rhIL-1α-induced ACTH response.

The 2 or 4 h ACTH responses to either dose of MET administered alone were negligible and no different from the ACTH response to vehicle alone.

Effects of Pretreatment with the H_1 Receptor Antagonists, MEP, DPH or PMZ, or the H_2 Receptor Antagonists, RAN or MET, on the Plasma Level of ACTH Ten Minutes after Challenge with HA

Figure 4 demonstrates the effect of pretreatment with the H_1 receptor antagonists, MEP (30 mg/kg), DPH (5 mg/kg) or PMZ (10 mg/kg), or the H_2 receptor antagonists, RAN (30 mg/kg) or MET (160 mg/kg), on the 10-min ACTH response to 10 mg/kg of HA. The amount of

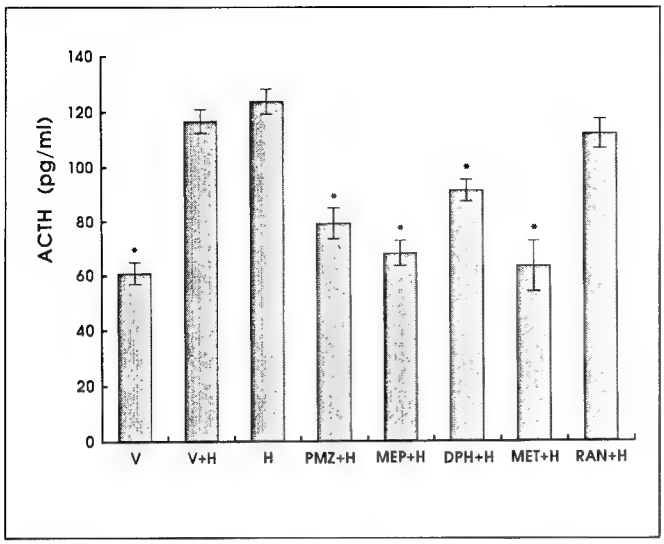

Fig. 4. Effects of pretreatment with the H_1 receptor antagonists, MEP, DPH or PMZ, or the H_2 receptor antagonists, RAN or MET, on the plasma level of ACTH 10 min after challenge with HA. C3H/HeN mice received i.p. injection of MEP (30 mg/kg), DPH (5 mg/kg), PMZ (10 mg/kg), RAN (30 mg/kg), MET (160 mg/kg) or vehicle 30 min before i.p. challenge with HA (10 mg/kg). Other mice were administered vehicle or HA (10 mg/kg) without antihistamine pretreatment. Blood samples were obtained 10 min after HA or vehicle injections. Each bar represents the mean ± SEM for 9–20 animals. * $p < 0.05$ (vs. HA with vehicle pretreatment or HA without any pretreatment).

HA chosen effectively stimulates the HPAA when administered systemically to rats [5, 22, 23]. The doses of antihistamines chosen inhibit HA-induced ACTH [19, 22, 23] and corticosterone [5] release when administered systemically to rats and were identical to the amounts which were mixed with LPS or rhIL-1α in the experiments described above. Pretreatment with MEP, DPH, PMZ or MET significantly blunted HA-induced ACTH release which was unaffected by the preadministration of vehicle alone. On the other hand, pretreatment with RAN had no effect on the ACTH response to HA.

Discussion

Our results suggest that, in contrast to the essential role of HA in the activation of the HPAA by noninflammatory stressors [30, 31], the stimulation of ACTH release by LPS and rhIL-1α is not as dependent on the participation of either the H_1 or the H_2 receptor.

We were not able to reduce the LPS- or rhIL-1α-induced ACTH responses with the very potent and selective H_1 receptor antagonists, MEP or DPH [32, 33]. On the other hand, the H_1 receptor antagonist, PMZ (a phenothiazine derivative with less selectivity than MEP for the H_1 receptor [33]), completely abrogated the ACTH response to LPS (at 2 and 4 h) as well as the 2 h ACTH response to rhIL-1α. In support of these findings, Suzuki et al. [5] reported that PMZ partially diminished the LPS-induced corticosterone response in rats; however, no other H_1 receptor antagonists were administered. Although only PMZ blocked the LPS- and rhIL-1α-induced ACTH responses, all of the H_1 receptor antagonists employed were able to significantly diminish the 10-min ACTH response to HA, as previously reported [17, 19, 22, 23].

The reason only PMZ, among all the H_1 receptor antagonists employed, was capable of blocking LPS- and rhIL-1α-induced ACTH release is not clear. The explanation may be based in part on the well-known ability of phenothiazine derivatives, i.e. PMZ (as opposed to MEP and DPH), to substantially inhibit phospholipase A_2 (PLA_2) and therefore prostaglandin generation in vivo [34, 35] and in vitro [36]. Prostaglandins are intimately involved in the inflammatory response [37–40] and mediate many of the effects of IL-1, IL-6 and TNF [35, 39–43] – including their activation of the HPAA [44–47]. Not surprisingly, chlorpromazine, the prototype antipsychotic phenothiazine, inhibits LPS, TNF or IL-1 stimulation of corticosterone production [48]. It also possesses significant anti-inflammatory effects in rodents including protection against LPS- and IL-1β-induced lethality [35, 49, 50] and blockade of LPS induction of TNF [50].

Phenothiazine derivatives can impact on other transduction processes as well, i.e. calmodulin antagonism [51], impaired synthesis of diacylglycerol and phosphatidylcholine [52, 53]. Therefore, PMZ may have interfered with non-PLA_2-dependent mechanisms necessary for IL-1 message transduction [54] and cytokine activation of the HPAA.

Our data suggest that the H_2 receptor, as well as the H_1 receptor, is not an important mediator of LPS- or rhIL-1α-induced ACTH release. RAN, a powerful and highly selective later generation H_2 receptor antagonist [33, 55, 56], did not affect the rhIL-1α-induced ACTH response and only slightly decreased ACTH release after LPS administration. The largest dose of RAN administered (30 mg/kg) was severalfold greater than the amount of intra-arterial RAN previously observed to be very effective in blocking HA-induced ACTH release in rats [19]. In contrast, MET, a much less potent first-generation H_2

receptor antagonist [33, 55, 56], substantially diminished the ACTH response to LPS and rhIL-1α. Suzuki et al. [5] were not able to inhibit the LPS-induced corticosterone response with MET, but these authors did not measure ACTH levels which may well have been diminished in spite of a persistent corticosterone response [57]. It is possible that MET possesses multiple effects like PMZ and therefore inhibits non-HA-dependent pathways involved in the stimulation of the HPAA by cytokines. For example, MET can block α-adrenergic receptors [58].

In our study, MET, but not RAN, blocked HA-induced ACTH release. Previous reports are contradictory on this issue. Several investigators have observed that H_2 receptor antagonists, as compared with H_1 receptor antagonists, are relatively inefficient in attenuating the stimulation of ACTH release by HA [22–25]; in contrast, other authors have reported that H_2 receptor antagonists administered centrally or systemically are very effective in diminishing HA-induced ACTH release [19, 21]. The reasons for these discrepant findings are not readily apparent.

In conclusion, our data indicate that the H_1 receptor is not involved in LPS- or rhIL-1α-induced ACTH release. The present results also do not support an important role for the H_2 receptor in these responses. We and others have established that IL-1 is an essential mediator of the stimulation of the HPAA by LPS [1, 59]. Therefore, our findings are consistent with the observations of Ohgo et al. [29] who showed that a combination of H_1 and H_2 receptor antagonists failed to interfere with rhIL-1β-induced CRH release from superfused rat hypothalamic explants. In addition, our results cast doubt on the conclusions of Suzuki and co-workers [5, 6] who suggested a more significant role for the H_1 receptor in LPS-induced HPAA stimulation.

As noted earlier, experiments involving the intracerebroventricular (i.c.v.) administration of antihistamines to rats indicated that both the H_1 and H_2 receptor play essential roles in the ACTH response to noninflammatory stressors [30, 31]; the H_2 receptor was found to be somewhat more important after restraint or ether stress [30] and the H_1 receptor more consequential after insulin-induced hypoglycemia [31]. Our observation that H_1 and H_2 receptors are not important mediators of LPS- or rhIL-1α-induced ACTH release contrasts with these findings and suggests that inflammatory and noninflammatory stressors activate the HPAA by different pathways. This hypothesis is concordant with our previous demonstration in rats that IL-1 and LPS activate both VP-containing and VP-deficient CRH axons in the external zone of the median eminence of the hypothalamus [60–62], while noninflammatory stressors selectively activate only the VP-containing CRH axons [60, 63].

It is also possible that the different routes of antihistamine administration (i.p. vs. i.c.v.) account for these contrasting observations. Although antihistamines administered i.p. cross the blood-brain barrier (H_1 receptor antagonists much better than H_2 receptor antagonists) [33, 64, 65], they may not access histaminergic receptors in the central nervous system (CNS)/hypothalamus in the same concentration as i.c.v. injected antihistamines. However, in an earlier study, the intra-arterial and i.c.v. administration of H_1 or H_2 receptor antagonists resulted in comparable blockade of HA-induced ACTH release [19], indicating that the systemic administration of both types of antihistamines (even the more hydrophilic H_2 receptor antagonists) can result in effective access to the CNS/hypothalamus.

Acknowledgments

We thank Drs. T.J. MacVittie and G.D. Ledney for critically reviewing the manuscript; Dr. P. Lomedico, Dr. S. Vogel and SmithKline Beecham for graciously providing us with rhIL-1α, LPS and MET respectively, and Petty Officer Sam Tom for his technical assistance.

Supported by the Armed Forces Radiobiology Research Institute, Defense Nuclear Agency, under work units 00129 and 00105. Views presented in this paper are those of the authors; no endorsement by the Defense Nuclear Agency or the Department of Defense has been given or should be inferred. Research was conducted according to the principles enunciated in the *Guide for the Care and Use of Laboratory Animals* prepared by the Institute of Laboratory Animal Resources, National Research Council.

References

1 Perlstein RS, Whitnall MH, Abrams JS, Mougey EH, Neta R: Synergistic roles of interleukin-6, interleukin-1 and tumor necrosis factor in the ACTH response to bacterial lipopolysaccharide in vivo. Endocrinology 1993;132:946–952.

2 Neta R, Perlstein R, Vogel SN, Ledney GD, Abrams J: Role of interleukin-6 in protection from lethal irradiation and in endocrine responses to interleukin-1 and tumor necrosis factor. J Exp Med 1992;175:689–694.

3 Perlstein RS, Mougey EH, Jackson WE, Neta R: Interleukin-1 and interleukin-6 act synergistically to stimulate the release of adrenocorticotropic hormone in vivo. Lymphokine Cytokine Res 1991;10:141–146.

4 Neta R, Abrams JS, Perlstein RS, Rokita H, Sipe JD, Vogel SN, Whitnall MH: Interactions of the cytokines IL-1, TNF, and IL-6 in in vivo host responses; in Rovel M (ed): IL-6: Physiopathology and Clinical Potentials. New York, Serono Symposia Publications/Raven Press, 1992, vol 88, pp 195–202.

5 Suzuki S, Nakano K: Suppression of endotoxin-induced corticosterone secretion in rats by H_1-antihistamine. Am J Physiol 1985;248: E26–E30.

6 Nakano K, Suzuki S, Oh C: Significance of increased secretion of glucocorticoids in mice and rats injected with bacterial endotoxin. Brain Behav Immun 1987;1:159–172.

7 Endo Y: Induction of histidine and ornithine decarboxylase activities in mouse tissues by recombinant interleukin-1 and tumor necrosis factor. Biochem Pharmacol 1989;38:1287–1292.

8 Piquet-Pellorce C, Homo-Delarche F, Dy M: Interleukin-1 and/or tumor necrosis factor-α synergize with granulocyte-macrophage colony-stimulating factor to enhance histamine synthesis in hematopoietic cells: Role of prostaglandin E_2. Eur J Immunol 1989;19:1999–2003.

9 Subramanian N, Bray MA: Interleukin-1 releases histamine from human basophils and mast cells in vitro. J Immunol 1987;138:271–275.

10 Okamoto H, Oh C, Nakano K: Possible involvement of adenosine 3′,5′-cyclic monophosphate and extracellular calcium ions in histamine stimulation of interleukin-1 release from macrophage-like P388D1 cells. Immunology 1990;70:186–190.

11 Vannier E, Dinarello CA: Histamine enhances interleukin (IL)-1-induced gene expression and protein synthesis via H_2 receptors in peripheral blood mononuclear cells: Comparison with IL-1 receptor antagonist. J Clin Invest 1993;92: 281–287.

12 Meretey K, Falus A, Taga T, Kishimoto T: Histamine influences the expression of the interleukin-6 receptor on human lymphoid, monocytoid and hepatoma cell lines. Agents Actions 1991;33:189–191.

13 Schwartz J, Arrang J, Garbarg M, Pollard H, Ruat M: Histaminergic transmission in the mammalian brain. Physiol Rev 1991;71:1–51.

14 Prell GD, Green JP: Histamine as a neuroregulator. Annu Rev Neurosci 1986;9:209–254.

15 Watanabe T, Taguchi Y, Shiosaka S, Tanaka J, Kubota H, Terano Y, Tohyama M, Wada H: Distribution of the histaminergic neuron system in the central nervous system of rats: A fluorescent immunohistochemical analysis with histidine decarboxylase as a marker. Brain Res 1984;295:13–25.

16 Inagaki Y, Yamatodani A, Ando-Yamamoto M, Tohyama M, Watanabe T, Wada H: Organization of histaminergic fibers in the rat brain. J Comp Neurol 1988;273:283–300.

17 Knigge U, Warberg J: The role of histamine in the neuroendocrine regulation of pituitary hormone secretion. Acta Endocrinol (Copenh) 1991;24:609–619.

18 Weiner RI, Ganong WF: Role of monoamines and histamine in regulation of anterior pituitary secretion. Physiol Rev 1978;58:905–976.

19 Knigge U, Bach FW, Matzen S, Bang P, Warberg J: Effect of histamine on the secretion of pro-opiomelanocortin-derived peptides in rats. Acta Endocrinol (Copenh) 1988;119:312–319.

20 Knigge U, Wollesen F, Dejgaard A, Larsen K, Christiansen PM: The effect of histamine stimulation and H_2-receptor inhibition on the pituitary prolactin and ACTH release and on cortisol secretion in human males. Horm Metab Res 1983;15:89–91.

21 Bugajski J, Gadek A: Central H_1- and H_2-histaminergic stimulation of pituitary-adrenocortical response under stress in rats. Neuroendocrinology 1983;36:424–430.

22 Reilly MA, Sigg EB: Suppression of histamine-induced adrenocorticotropic hormone release by antihistamines and antidepressants. J Pharmacol Exp Ther 1982;222:583–588.

23 Morita Y, Koyama K: Histamine-induced ACTH secretion and inhibitory effect of antihistaminic drugs. Jpn J Pharmacol 1979;29: 59–65.

24 Tsujimoto S, Okumura Y, Kamei C, Tasaka K: Effects of intracerebroventricular injection of histamine and related compounds on corticosterone release in rats. Br J Pharmacol 1993; 109:807–813.

25 Tsujimoto S, Kamei C, Yoshida T, Tasaka K: Changes in plasma adrenocorticotropic hormone and cortisol levels induced by intracerebroventricular injection of histamine and its related compounds in dogs. Pharmacology 1993;47:73–83.

26 Rudolph C, Richards GE, Kaplan S, Ganong WF: Effect of intraventricular histamine on hormone secretion in dogs. Neuroendocrinology 1979;29:169–177.

27 Kjær A, Knigge U, Plotsky PM, Bach FW, Warberg J: Histamine H_1 and H_2 receptor activation stimulates ACTH and β-endorphin secretion by increasing corticotropin-releasing hormone in the hypophyseal portal blood. Neuroendocrinology 1992;56:851–855.

28 Kjær A, Knigge U, Bach FW, Warberg J: Histamine- and stress-induced secretion of ACTH and β-endorphin: Involvement of corticotropin-releasing hormone and vasopressin. Neuroendocrinology 1992;56:419–428.

29 Ohgo S, Nakatsuru K, Ishikawa E, Matsukura S: Interleukin-1 stimulates the release of corticotropin-releasing factor from superfused rat hypothalamo-neurohypophyseal complexes independently of the histaminergic mechanism. Brain Res 1991;558:217–223.

30 Knigge U, Matzen S, Bach FW, Bang P, Warberg J: Involvement of histaminergic neurons in the stress-induced release of pro-opiomelanocortin-derived peptides in rats. Acta Endocrinol (Copenh) 1989;120:533–539.

31 Kjær A, Knigge U, Langer Madsen E, Soe-Jensen P, Bach FW, Warberg J: Insulin/hypoglycemia-induced adrenocorticotropin and β-endorphin release: Involvement of hypothalamic histaminergic neurons. Endocrinology 1993;132: 2213–2220.

32 Garrison JC: Histamine, bradykinin, 5-hydroxytryptamine, and their antagonists; in Gilman AG, Rall TW, Nies AS, Taylor P (eds): Goodman and Gilman's The Pharmacological Basis of Therapeutics. New York, Pergamon Press, 1990, pp 575–599.

33 Hill SJ: Distribution, properties and functional characteristics of three classes of histamine receptor. Pharmacol Rev 1990;42:45–83.

34 Vadas P, Stefanski E, Pruzanski W: Potential therapeutic efficacy of inhibitors of human phospholipase A_2 in septic shock. Agents Actions 1986;19:194–202.

35 Boraschi D, Villa L, Ghiara P, Tagliabue A, Mengozzi M, Solito E, Parente L, Silvestri S, Van Damme J, Ghezzi P: Mechanism of acute toxicity of IL-1β in mice. Eur Cytokine Netw 1991;2:61–67.

36 Blackwell G, Flower R: Inhibition of phospholipase. Br Med Bull 1983;39:260–264.

37 Bone RC: The pathogenesis of sepsis. Ann Intern Med 1991;115:457–469.

38 Vadas P, Hay JB: Involvement of circulating phospholipase A_2 in the pathogenesis of the hemodynamic changes in endotoxin shock in rabbits. Can J Physiol Pharmacol 1983;61: 561–566.

39 Dinarello CA: Interleukin-1 and interleukin-1 antagonism. Blood 1991;77:1627–1652.

40 Dinarello CA, Wolff SM: The role of interleukin-1 in disease. N Engl J Med 1993;328:106–113.

41 Spangelo BL, Jarvis WD, Judd AM, MacLeod RM: Induction of interleukin-6 release by interleukin-1 in rat anterior pituitary cells in vitro: Evidence for an eicosanoid-dependent mechanism. Endocrinology 1991;129:2886–2894.

42 Neta R, Sayers TJ, Oppenheim JJ: Relationship of TNF to interleukins; in Aggarwal BB, Vilcek J (eds): Tumor Necrosis Factors: Structure, Function, and Mechanism of Action. New York, Dekker, 1992, pp 499–566.

43 Kettelhut IC, Fiers W, Goldberg AL: The toxic effects of tumor necrosis factor in vivo and their prevention by cyclooxygenase inhibitors. Proc Natl Acad Sci USA 1987;84:4273–4277.
44 Rivier C, Vale W: Stimulatory effect of interleukin-1 on adrenocorticotropin secretion in the rat: Is it modulated by prostaglandins? Endocrinology 1991;129:384–388.
45 Navarra P, Tsagarakis S, Faria MS, Rees LH, Besser GM, Grossman AB: Interleukins-1 and -6 stimulate the release of corticotropin-releasing hormone-41 from rat hypothalamus in vitro via the eicosanoid cyclooxygenase pathway. Endocrinology 1991;128:37–44.
46 Navarra P, Pozzoli G, Brunetti L, Ragazzoni E, Besser M, Grossman A: Interleukin-1β and interleukin-6 specifically increase the release of prostaglandin E_2 from rat hypothalamic explants in vitro. Neuroendocrinology 1992;56: 61–68.
47 Sharp BM, Matta SG: Prostaglandins mediate the adrenocorticotropin response to tumor necrosis factor in rats. Endocrinology 1993;132: 269–274.
48 Bertini R, Mengozzi M, Bianchi M, Sipe JD, Ghezzi P: Chlorpromazine protection against interleukin-1 and tumor necrosis factor-mediated activities in vivo. Int J Immunopharmacol 1991;13:1085–1090.
49 Bertini R, Bianchi M, Mengozzi M, Ghezzi P: Protective effect of chlorpromazine against the lethality of interleukin-1 in adrenalectomized or actinomycin D-sensitized mice. Biochem Biophys Res Commun 1989;165:942–946.
50 Gadina M, Bertini R, Mengozzi M, Zandalasini M, Mantovani A, Ghezzi P: Protective effect of chlorpromazine on endotoxin toxicity and TNF production in glucocorticoid-sensitive and glucocorticoid-resistant models of endotoxic shock. J Exp Med 1991;173:1305–1310.
51 Rainteau D, Wolf C, Bereziat G, Polonovski J: Binding of a spin-labelled chlorpromazine analogue to calmodulin. Biochem J 1984;221:659–663.
52 Graham A, Bennett AJ, McLean AAM, Zammit VA, Brindley DN: Factors regulating the secretion of lysophosphatidylcholine by rat hepatocytes compared with the synthesis and secretion of phosphatidylcholine and triacylglycerol. Effects of albumin, cyclohexamide, verapamil, EGTA and chlorpromazine. Biochem J 1988;253:687–692.
53 Martin A, Hopewell R, Martin-Sanz P, Morgan JE, Brindley DN: Relationship between the displacement of phosphatidate phosphohydrolase from the membrane-associated compartment by chlorpromazine and the inhibition of the synthesis of triacylglycerol and phosphatidylcholine in rat hepatocytes. Biochim Biophys Acta 1986;876:581–591.
54 Rosoff PM, Savage N, Dinarello CA: Interleukin-1 stimulates diacylglycerol production in T lymphocytes by a novel mechanism. Cell 1988; 54:73–81.
55 Brogden RN, Carmine AA, Heel RC, Speight TM, Avery GS: Ranitidine: A review of its pharmacology and therapeutic use in peptic ulcer disease and other allied diseases. Drugs 1982;24:267–303.
56 Brimblecombe RW, Duncan WAM, Durant GJ, Emmett JC, Ganellin CR, Leslie GB, Parsons ME: Characterization and development of cimetidine as a histamine H_2-receptor antagonist. Gastroenterology 1978;74:339–347.
57 Papaikonomou E: Rat adrenocortical dynamics. J Physiol (Lond) 1977;265:119–131.
58 Griffith OR, Marshall I, Nasmyth PA: Blockade of pre-synaptic α-adrenoceptors by metiamide. Br J Pharmacol 1978;64:416P.
59 Rivier C, Chizzonite R, Vale W: In the mouse, the activation of the hypothalamic-pituitary-adrenal axis by a lipopolysaccharide (endotoxin) is mediated through interleukin-1. Endocrinology 1989;125:2800–2805.
60 Whitnall MH: Regulation of the hypothalamic corticotropin-releasing hormone neurosecretory system. Prog Neurobiol 1993;40:573–629.
61 Whitnall MH, Perlstein RS, Mougey EH, Neta R: Effects of interleukin-1 on the stress-responsive and -nonresponsive subtypes of corticotropin-releasing hormone neurosecretory axons. Endocrinology 1992;131:37–44.
62 Whitnall MH, Perlstein RS, Mougey EH, Neta R: The hypothalamo-pituitary-adrenal axis in rodents: Corticotropin-releasing hormone/vasopressin coexistence and cytokine effects; in Kvetnansky R, McCarty R, Axelrod J (eds): Stress: Neuroendocrine and Molecular Approaches. New York, Gordon & Breach Science Publishers, 1992, pp 449–456.
63 Whitnall MH: Stress selectively activates the vasopressin-containing subset of corticotropin-releasing hormone neurosecretory cells. Neuroendocrinology 1989;50:702–707.
64 Sorkin EM, Heel RC: Terfenadine: A review of its pharmacodynamic properties and therapeutic efficacy. Drugs 1985;29:34–56.
65 Walt RP, Labrooy SJ, Avgerinos A, Oehr T, Riley A, Misiewicz JJ: Investigations on the penetration of ranitidine into the cerebrospinal fluid and a comparison of the effects of ranitidine and cimetidine on male sex hormones. Scand J Gastroenterol 1981;16(suppl 60):19–24.

DISTRIBUTION LIST

DEPARTMENT OF DEFENSE

ARMED FORCES INSTITUTE OF PATHOLOGY
ATTN: RADIOLOGIC PATHOLOGY DEPARTMENT

ARMED FORCES RADIOBIOLOGY RESEARCH INSTITUTE
ATTN: PUBLICATIONS DIVISION
ATTN: LIBRARY

ARMY/AIR FORCE JOINT MEDICAL LIBRARY
ATTN: DASG-AAFJML

ASSISTANT TO SECRETARY OF DEFENSE
ATTN: AE
ATTN: HA(IA)

DEFENSE NUCLEAR AGENCY
ATTN: TITL
ATTN: DDIR
ATTN: RARP
ATTN: MID

DEFENSE TECHNICAL INFORMATION CENTER
ATTN: DTIC-DDAC
ATTN: DTIC-FDAC

FIELD COMMAND DEFENSE NUCLEAR AGENCY
ATTN: FCIEO

INTERSERVICE NUCLEAR WEAPONS SCHOOL
ATTN: TCHTS/RH

LAWRENCE LIVERMORE NATIONAL LABORATORY
ATTN: LIBRARY

UNDER SECRETARY OF DEFENSE (ACQUISITION)
ATTN: OUSD(A)/R&AT

UNIFORMED SERVICES UNIVERSITY OF THE HEALTH SCIENCES
ATTN: LIBRARY

DEPARTMENT OF THE ARMY

AMEDD CENTER AND SCHOOL
ATTN: HSMC-FCM

HARRY DIAMOND LABORATORIES
ATTN: SLCHD-NW
ATTN: SLCSM-SE

SURGEON GENERAL OF THE ARMY
ATTN: MEDDH-N

U.S. ARMY AEROMEDICAL RESEARCH LABORATORY
ATTN: SCIENTIFIC INFORMATION CENTER

U.S. ARMY CHEMICAL RESEARCH, DEVELOPMENT, AND ENGINEERING CENTER
ATTN: SMCCR-RST

U.S. ARMY INSTITUTE OF SURGICAL RESEARCH
ATTN: DIRECTOR OF RESEARCH

U.S. ARMY MEDICAL RESEARCH INSTITUTE OF CHEMICAL DEFENSE
ATTN: SGRD-UV-R

U.S. ARMY NUCLEAR AND CHEMICAL AGENCY
ATTN: MONA-NU

U.S. ARMY RESEARCH INSTITUTE OF ENVIRONMENTAL MEDICINE
ATTN: SGRD-UE-RPP

U.S. ARMY RESEARCH OFFICE
ATTN: BIOLOGICAL SCIENCES PROGRAM

WALTER REED ARMY INSTITUTE OF RESEARCH
ATTN: DIVISION OF EXPERIMENTAL THERAPEUTICS

DEPARTMENT OF THE NAVY

NAVAL AEROSPACE MEDICAL RESEARCH LABORATORY
ATTN: COMMANDING OFFICER

NAVAL MEDICAL COMMAND
ATTN: MEDCOM-21

NAVAL MEDICAL RESEARCH AND DEVELOPMENT COMMAND
ATTN: CODE 40C

NAVAL MEDICAL RESEARCH INSTITUTE
ATTN: LIBRARY

NAVAL RESEARCH LABORATORY
ATTN: LIBRARY

OFFICE OF NAVAL RESEARCH
ATTN: BIOLOGICAL SCIENCES DIVISION

DEPARTMENT OF THE AIR FORCE

BOLLING AIR FORCE BASE
ATTN: AFOSR

BROOKS AIR FORCE BASE
ATTN: AL/OEBSC
ATTN: USAFSAM/RZ
ATTN: OEHL/RZ

OFFICE OF AEROSPACE STUDIES
ATTN: OAS/XRS

SURGEON GENERAL OF THE AIR FORCE
ATTN: HQ USAF/SGPT
ATTN: HQ USAF/SGES

U.S. AIR FORCE ACADEMY
ATTN: HQ USAFA/DFBL

OTHER FEDERAL GOVERNMENT

ARGONNE NATIONAL LABORATORY
ATTN: ACQUISITIONS

BROOKHAVEN NATIONAL LABORATORY
ATTN: RESEARCH LIBRARY, REPORTS SECTION

CENTER FOR DEVICES AND RADIOLOGICAL HEALTH
ATTN: HFZ-110

GOVERNMENT PRINTING OFFICE
ATTN: DEPOSITORY RECEIVING SECTION
ATTN: CONSIGNED BRANCH

LIBRARY OF CONGRESS
ATTN: UNIT X

LOS ALAMOS NATIONAL LABORATORY
ATTN: REPORT LIBRARY/P364

NATIONAL AERONAUTICS AND SPACE ADMINISTRATION
ATTN: RADLAB

NATIONAL AERONAUTICS AND SPACE ADMINISTRATION
GODDARD SPACE FLIGHT CENTER
ATTN: LIBRARY

NATIONAL CANCER INSTITUTE
ATTN: RADIATION RESEARCH PROGRAM

NATIONAL DEFENSE UNIVERSITY
ATTN: LIBRARY

U.S. DEPARTMENT OF ENERGY
ATTN: LIBRARY

U.S. FOOD AND DRUG ADMINISTRATION
ATTN: WINCHESTER ENGINEERING AND ANALYTICAL CENTER

U.S. NUCLEAR REGULATORY COMMISSION
ATTN: LIBRARY

RESEARCH AND OTHER ORGANIZATIONS

AUSTRALIAN DEFENCE FORCE
ATTN: SURGEON GENERAL

BRITISH LIBRARY (SERIAL ACQUISITIONS)
ATTN: DOCUMENT SUPPLY CENTRE

CENTRE DE RECHERCHES DU SERVICE DE SANTE DES ARMEES
ATTN: DIRECTOR

INHALATION TOXICOLOGY RESEARCH INSTITUTE
ATTN: LIBRARY

INSTITUTE OF RADIOBIOLOGY
ARMED FORCES MEDICAL ACADEMY
ATTN: DIRECTOR

KAMAN SCIENCES CORPORATION
ATTN: DASIAC

NBC DEFENSE RESEARCH AND DEVELOPMENT CENTER OF THE FEDERAL ARMED FORCES
ATTN: WWDBW ABC-SCHUTZ

NCTR-ASSOCIATED UNIVERSITIES
ATTN: EXECUTIVE DIRECTOR

RUTGERS UNIVERSITY
ATTN: LIBRARY OF SCIENCE AND MEDICINE

UNIVERSITY OF CALIFORNIA
ATTN: LABORATORY FOR ENERGY-RELATED HEALTH RESEARCH
ATTN: LAWRENCE BERKELEY LABORATORY

UNIVERSITY OF CINCINNATI
ATTN: UNIVERSITY HOSPITAL, RADIOISOTOPE LABORATORY

XAVIER UNIVERSITY OF LOUISIANA
ATTN: COLLEGE OF PHARMACY